THE IDENTIFICATION AND VALIDATION OF GRIN2D AS A NOVEL ENDOTHELIAL TARGET IN COLORECTAL CANCER, AND THE INVESTIGATION OF ITS EFFECTS AS A THERAPEUTIC TUMOUR VACCINE

by

HENRY JOHN MURRAY FERGUSON

MBBCh (Hons.) MRCS

A thesis submitted to The University of Birmingham for the degree of

DOCTOR OF MEDICINE

Molecular Angiogenesis Group

School of Immunity and Infection and Cancer Studies

College of Medical and Dental Sciences

The University of Birmingham

March 2015

UNIVERSITY OF
BIRMINGHAM

University of Birmingham Research Archive

e-theses repository

This unpublished thesis/dissertation is copyright of the author and/or third parties. The intellectual property rights of the author or third parties in respect of this work are as defined by The Copyright Designs and Patents Act 1988 or as modified by any successor legislation.

Any use made of information contained in this thesis/dissertation must be in accordance with that legislation and must be properly acknowledged. Further distribution or reproduction in any format is prohibited without the permission of the copyright holder.

Abstract

A shortlist of candidate tumour endothelial markers was generated by Microarray comparison of differential gene expression between multiple patient-matched colorectal cancer and normal colon samples. This list was narrowed through a process of literature review, real-time quantitative polymerase chain reaction and immunohistochemistry. GRIN2D, a subunit of a glutamate dependent, ionotropic NMDA receptor, and facilitator of cellular calcium influx, previously found in neuronal tissues, was identified as the most promising target from this shortlist.

Through siRNA knockdown and analysis in *in vitro* models of angiogenesis, it has been demonstrated that a decrease in GRIN2D expression significantly decreases cellular migration, communication and chemotaxis, without adversely affecting cell viability or proliferation in HUVEC.

Vaccination with a murine GRIN2D-Fc fusion protein in combination with Freund's adjuvant stimulated a specific immune response to this self-antigen, by breaking immune tolerance. The resulting increase in specific IgG1 antibody titers, indicative of Th2 T-cell response, resulted in a significant reduction in physiological angiogenesis in the subcutaneous sponge assay, and a significant decrease in colorectal tumour growth in a murine subcutaneous CT26 tumour model.

GRIN2D represents a novel tumour endothelial marker in colorectal cancer. A hypothesised mechanism for the observed effects is an inhibition of endothelial calcium influx, leading to decreased angiogenic potential in tumour endothelial cells.

Dedication

For My Family

Acknowledgments

My first thanks go to my supervisors. Professor Roy Bicknell has supported me through my initiation into the world of ‘real’ science, and guided me, as an initial novice, through this complex project. He has enthusiastically supported my work, and absorbed the cost of my laboratory consumables, even when funding bodies failed to see the potential of this project. Mr Tariq Ismail has been a true surgical mentor throughout my MD studies, and always been available for advice and guidance. He has facilitated opportunities to both further my research exposure, and attend learned meetings to present my work, without which the impact of this research would have been severely limited.

Next, I would like to thank the members of the Bicknell Laboratory for working with me so supportively, especially in my early months, when I needed it most. I have never felt out of place, despite the laboratory being so far from my usual comfort zone. A special mention goes to Joseph Wragg, who oversaw my first few months’ work, and ensured that I learned many precise experimental methods, which ensured this work is of high calibre. Latterly, Kabir Khan has also been of particular support, both with his expertise in molecular biology, and also as a selfless proofreader!

Finally, without the support of my wife, Claire, I would not have been able to focus on my research in the way I have. Her strength as a mother, and in managing the rigours of a clinical career are a source of great pride to me, but the support she has offered me, even when recently post-partum, has shown me that there is always time to get things done! I thank her from the bottom of my heart.

Table of Contents

Chapter One **Introduction** **1**

1.1 Colorectal Cancer 2

1.1.1 Histology of Colorectal Cancer 3

1.1.2 The Adenoma – Carcinoma Sequence 3

1.1.3 Staging and Prognosis of Colorectal Cancer 4

1.1.4 Treatment of Colorectal Cancer 5

1.2 Angiogenesis 9

1.2.1 Physiological Angiogenesis 9

1.2.2 Tumour Angiogenesis 11

1.2.3 Anti-angiogenic Therapies 13

1.2.4 Vascular Targeting Therapies 13

1.3 Vascular Endothelium 15

1.3.1 Isolation of Endothelial Cells 15

1.3.2 Tumour Endothelial Markers (TEMs) 16

1.3.3 GRIN2D 16

1.4 Vaccination 19

1.4.1 Vaccine Design 19

1.4.2 The Immune Response to Vaccination 20

1.4.3 Therapeutic Vaccination In Colorectal Cancer 24

1.5 Hypothesis, Aims and Objectives 26

Chapter Two **Materials and Methods** **28**

2.1 Materials 29
2.1.1 Equipment 29
2.1.2 Consumables, Chemicals and Reagents 31
2.1.3 Oligonucleotides 32
2.1.4 Antibodies 33
2.1.5 siRNA Duplexes 34
2.1.6 DNA Vectors and Plasmids 35
2.1.7 Cell Lines 35
2.1.8 Cell Culture Media 35
2.1.9 Biological Materials and Solutions 36
2.1.10 Buffers and Solutions 36

2.2 Methods 37
2.2.1 Molecular Biology 37
2.2.2 Cell Biology 43
2.2.3 Protein Analysis 53
2.2.4 Protein Production 55
2.2.5 Animal Models 58
2.2.6 Bioinformatic Websites 61
2.2.7 Statistical Methods 62

Chapter Three **Identification and Validation of Novel Tumour Endothelial Markers in Colorectal Cancer** **63**

3.1 Identification of Novel TEMs in Colorectal Cancer 64
3.1.1 Isolation of Endothelial Cells from Fresh Colorectal Resection Specimens 64
3.1.2 Microarray Identification of Gene Candidates 65
3.1.3 Narrowing the Shortlist 66

3.2 Validation of Novel TEMs in Colorectal Cancer 71
3.2.1 Real-time Quantitative PCR Validation of Gene Shortlist 71
3.2.2 Immunohistochemical Validation 77

3.3 Functional Characterisation of GRIN2D 79
3.3.1 siRNA Knockdown of GRIN2D in HUVEC 79
3.3.2 Scratch Wound Assay 80
3.3.3 Matrigel Cellular Interaction Assay 82
3.3.4 Boyden Chamber Assay 84
3.3.5 Acumen Cell Cycle Analysis 86
3.3.6 Chapter Conclusion 87

Chapter Four Design and Construction of a GRIN2D-Based Vaccine 88

4.1 Targeting GRIN2D 89
4.1.1 The Structure of GRIN2D 89
4.1.2 Identification of an Appropriate Target Sequence 90

4.2 Expression of GRIN2D Fusion Proteins 94
4.2.1 The GRIN2D Target Sequence 94
4.2.2 Expression of hGRIN2D-Fc and mGRIN2D-Fc Fusion Protein 96
4.2.3 Expression of GST-hGRIN2D and GST-mGRIN2D Fusion Protein 103

Chapter Five **Investigating GRIN2D as a Tumour Endothelial Marker in a Murine Model of Colorectal Cancer** **108**

5.1 GRIN2D as a TEM in Murine Colorectal Tumours 109
5.1.1 The CT26 Cell Line 110
5.1.2 Isolation of Murine Endothelial Cells 110
5.1.3 The Expression Profile of GRIN2D in Murine Tissues and Colorectal Cancer 111

5.2 The Effect of a GRIN2D-Fc Protein Vaccine in Murine Models of Angiogenesis and Colorectal Cancer 113
5.2.1 Establishment of a Murine GRIN2D Vaccine Model 113
5.2.2 The Effect of GRIN2D Vaccination on Physiological Angiogenesis 117
5.2.3 Establishment of a Murine Subcutaneous Colorectal Cancer Model 120
5.2.4 The Effect of GRIN2D Vaccination on Subcutaneous CT26 Tumour Growth 123
5.2.5 Chapter Conclusion 126

Chapter Six **Discussion** **127**

Appendix **141**

References **142**

List of Figures

Chapter One

Figure 1.1 The Adenoma-Carcinoma Sequence 3
Figure 1.2 The Contrast Between Sprouting and Intussusceptive Angiogenesis 10
Figure 1.3 Tumour-Induced Angiogenesis 12
Figure 1.4 The Structure of Ionotropic NMDA Receptors 17
Figure 1.5 Correlation of Antibody Titers to the Various Phases of the Vaccine Response 23

Chapter Three

Figure 3.1 The Mechanism of RTqPCR 73
Figure 3.2 Quantitative analysis of the relative expression of candidate genes between patient-matched Colorectal Cancer (CRC) and Normal Colon (NC). 74
Figure 3.3 Candidate Expression in Further Biological Replicates 75
Figure 3.4 Endothelial Candidate Expression. 76
Figure 3.5 Immunohistochemical Validation of GRIN2D as a Tumour Endothelial Marker in Colorectal Cancer 78
Figure 3.6 siRNA Knockdown of GRIN2D in HUVEC 80
Figure 3.7 Scratch Wound Assay 81
Figure 3.8 Matrigel Assay 83
Figure 3.9 The Modified Boyden Chamber Assay 85
Figure 3.10 Acumen cell cycle analysis 86

Chapter Four

Figure 4.1 Bioinformatic Prediction of Transmembrane regions of GRIN2D 90
Figure 4.2 Human and Murine Sequence Alignment of the GRIN2 Subgroup 92
Figure 4.3 Bioinformatic Prediction of the Secondary Structure of the N-terminal Domain of GRIN2D 93

Figure 4.4 Vector Map of the Human GRIN2D-IDT Construct 95
Figure 4.5 Representative Vector Map of the pIgG-GRIN2D Vector 97
Figure 4.6 Restriction digest of pIgG-GRIN2D 98
Figure 4.7 Trial GRIN2D-Fc Production and Purification 99
Figure 4.8 Large-scale purification of hGRIN2D 100
Figure 4.9 Contaminant Fc-fusion Protein 101
Figure 4.10 UV Absorbance analysis of Size Exclusion Chromatography for mGRIN2D-Fc 102
Figure 4.11 Fractions Collected from SEC for mGRIN2D-Fc 103
Figure 4.12 Vector Map of the pGEX2T-hGRIN2D Vector 105
Figure 4.13 Isolation of GST-GRIN2D from Bacterial Lysate 106

Chapter Five

Figure 5.1 Expression of GRIN2D in Murine Tumours and Tissues 112
Figure 5.2 GRIN2D Vaccination Protocol 115
Figure 5.3 Antibody Response to GRIN2D-Fc Vaccination in Balb/c Mice 116
Figure 5.4 Combined Protocol of Vaccination and Subcutaneous Sponge assays 117
Figure 5.5 Sponge Vascular Density 118
Figure 5.6 Macroscopic Evaluation of Sponge Assay 119
Figure 5.7 The CT26-Luc Tumour Model 122
Figure 5.8 Protocol for GRIN2D Vaccination Followed by Subcutaneous CT26 Tumour Growth Monitoring. 123
Figure 5.9 Vaccination with mGRIN2D-Fc Significantly Decreases Subcutaneous CT26 Tumour Growth. 124
Figure 5.10 Tumour Vascular Density is Decreased by mGRIN2D-Fc Vaccination 125

List of Tables

Table 1 Pathology, Prevalence, Standard Treatment and Survival by Dukes' Stage 4
Table 2 Transmembrane Gene Candidates from Microarray Analysis of CRC versus Patient-Matched Normal Colon 66
Table 3 Summary of the Literature Review of Candidate TEMs in CRC 67-70
Table 4 Gene Candidates Taken Forward for Further Study 71

List of Abbreviations

ADC	Antibody-Drug Conjugate
ANOVA	Analysis of Variance
BBB	Blood Brain Barrier
BSA	Bovine Serum Albumin
bFGF	Basic Fibroblast Growth Factor
cDNA	Complementary DNA
CEA	Carcino-Embryonic Antigen
CRC	Colorectal Cancer
cRNA	Complementary RNA
CT26	Colon Tumour 26 Murine Cell Line
DMSO	Dimethyl sulfoxide
EC	Endothelial Cell
EDTA	Ethylenediaminetetraacetic acid
ELISA	Enzyme-Linked Immunosorbent Assay
Fc	Fragment crystallizable Region of Human Immunoglobulin
FCA	Freund’s Complete Adjuvant
FIA	Freund’s Incomplete Adjuvant
GRIN2D	Glutamate Receptor, Ionotropic, NMDA Receptor Subunit 2D
GST	Glutathione S-Transferase
H&E	Haematoxylin and Eosin
HUVEC	Human Umbilical Vein Endothelial Cells
IHC	Immunohistochemistry
IL-8	Interleukin 8
IVIS	*In Vivo* Imaging System
KD	Knockdown
LB	Lysogeny Broth
MAb	Monoclonal Antibody
NF	Nuclease Free
NMDA	N-methyl D-aspartate
OD	Optical Density

PAGE	Polyacrylamide Gel Electrophoresis
PCR	Polymerase Chain Reaction
PECAM	Platelet Endothelial Cell Adhesion Molecule
PMSF	Phenylmethylsulfonyl fluoride
RIN	RNA Integrity Number
RNA	Ribonucleic Acid
RT	Room Temperature
RTqPCR	Real-time Quantitative Polymerase Chain Reaction
SAGE	Serial Analysis of Gene Expression
SDS	Sodium dodecylsulfate
SEC	Size Exclusion Chromatography
siRNA	Small Interfering RNA
TEM	Tumour Endothelial Marker
UV	Ultraviolet
VEGF	Vascular Endothelial Growth Factor
VEGFR	Vascular Endothelial Growth Factor Receptor

CHAPTER ONE

INTRODUCTION

1.1 COLORECTAL CANCER

Colorectal Cancer (CRC) represents the third most commonly diagnosed malignancy in humans worldwide, with 33,218 cases diagnosed in 2010 in England alone(1). The mainstay of curative treatment relies upon a histologically clear resection margin at surgery(2), and the long-term absence of metastatic spread. Around 80% of surgical resections for CRC result in complete local microscopic clearance of disease, but of these, 50% will relapse to metastatic disease, due to micrometastases which were present at the time of original resection(3). This premise is the basis for routine adjuvant treatment of poor prognostic groups (Dukes stage C/D) with systemic therapies. Chemotherapeutic agents have been in established use as an adjuvant treatment in CRC for over 50 years(4), but despite introduction of new agents, and the use of monoclonal antibodies, presentation with macroscopic or microscopic metastatic disease still carries a poor prognosis(5). Targeting of the vasculature of CRCs has been shown to be of interest(6), with anti-angiogenic agents licensed for advanced disease. However, vascular targeting in the form of a targeted specific immunotherapy in CRC has not been described. This thesis describes the process of identification of an endothelial specific target in CRC, the development of a tumour-vessel specific vaccine, and the investigation of its effects in *in vivo* murine models of angiogenesis and tumour growth.

1.1.1 Histology of Colorectal Cancer

More than 90% of CRCs are adenocarcinomas, originating from the glandular epithelium of the colon. Identification of malignancy within glandular epithelium is confirmed by the presence of invasion beyond the mucosa into the submucosa, and that of a desmoplastic, or fibrous, reaction in the surrounding stroma secondary to tumour infiltration(7).

1.1.2 The Adenoma – Carcinoma Sequence

The development of sporadic CRC is associated with a multi-step series of genetic changes that promote proliferation of the epithelium(8). The progression from normal epithelium, through dysplasia, and eventual progression to invasive malignancy is governed by a series of genetic mutations via a consistent pathway.

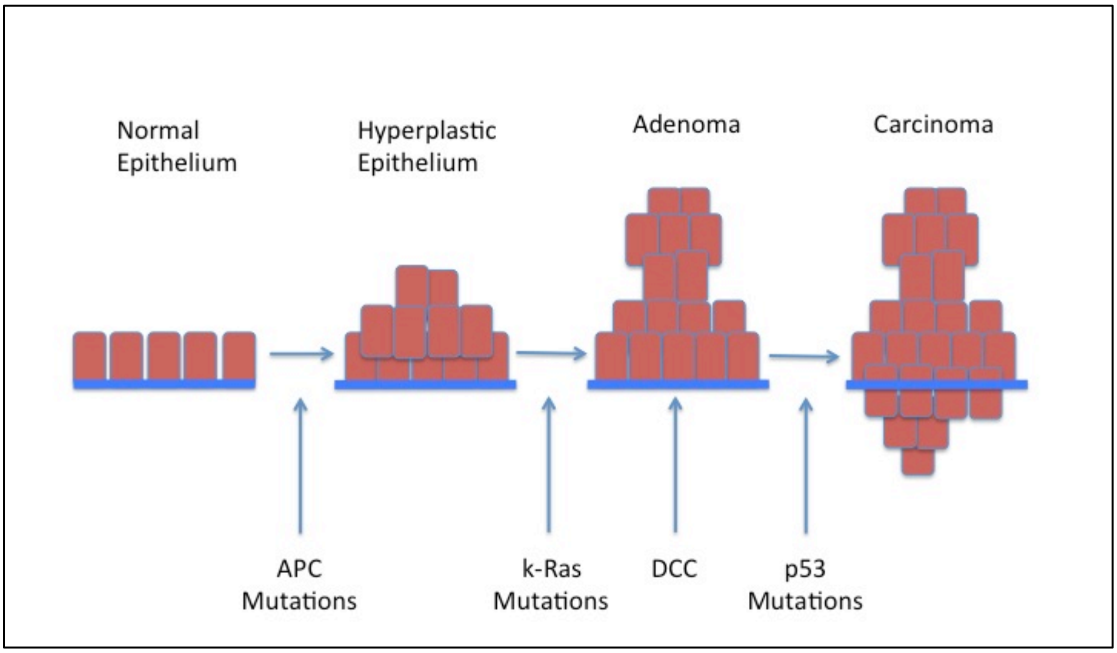
Normal Epithelium
Hyperplastic Epithelium
Adenoma
Carcinoma
APC Mutations
k-Ras Mutations
DCC
p53 Mutations

Figure 1.1 – The Adenoma-Carcinoma Sequence. APC – adenomatous polyposis coli; k-RAS – Kirsten Rat Sarcoma oncogene; DCC – Deleted in Colorectal Cancer.

These mutations are thought to occur via two pathways – chromosomal instability and microsatellite instability(8). Chromosomal instability describes alterations in chromosome complement (aneuploidy) or deletion or amplification of specific, detectable loci, where microsatellite instability describes the acquisition of errors in DNA mismatch repair.

1.1.3 Staging and Prognosis of Colorectal Cancer

The prognosis of patients with colorectal cancer depends upon the extent of locoregional and distant spread. The staging system for colorectal cancer, originally described by Cuthbert Dukes in 1958(9), has subsequently been modified to include the presence of distant metastasis. It now forms the basis for treatment planning in the United Kingdom.

Dukes Stage	Tumour Extent	Prevalence	1st Line Treatment	5-year Survival
A	Tumour extends into but not beyond muscularis mucosa	13.2%	Surgery	93.2%
B	Tumour penetrates into subserosa and beyond, including invasion into other organs	37.3%	Surgery	77.0%
C	Involvement of local lymph nodes.	35.9%	Surgery + Adjunctive Treatment	47.7%
D	Any Distant Metastasis	14.0%	Adjunctive Treatment +/- Surgery	6.6%

Table 1 – Pathology, Prevalence, Standard Treatment and Survival by Dukes' Stage. Data is adapted from Cancer Research UK (CRUK)(10):

While surgical management can be curative in early stage tumours, once there is evidence of loco-regional spread, relative survival falls rapidly. Current management initiatives such as the bowel cancer screening programme in the UK are aimed at identifying tumours at an early or pre-malignant stage. An alternative route for improvement of patient prognosis is the development of novel adjuvant treatments with the aim of down-staging disease, and decreasing the effects of micrometastases already present in the circulation or distant organs, or eliminating them entirely.

1.1.4 Treatment of Colorectal Cancer

1.1.4.1 Surgical Treatment of Primary Colorectal Cancer

Successful surgical resection of colorectal cancer depends upon an *en bloc* excision of the tumour and its draining lymph nodes, while maintaining optimal blood supply to the remaining bowel. Classically this has been performed via a large incision in the abdominal wall, or laparotomy, but more recently, advances in technique have enabled successful bowel resection by keyhole, or laparoscopic(11), methods, including the use of robotic resection(12).

1.1.4.2 Chemotherapy for Colorectal Cancer

Chemotherapeutic agents broadly work by interrupting the cell cycle, thereby limiting mitosis and hence tumour growth. The majority achieve this by directly inducing DNA damage, or by interfering with intracellular mechanisms that limit the process(13). Chemotherapy has been the primary adjuvant treatment in patients with CRC for over 30 years. It is efficacious in terms of increasing longevity and quality of life in patients with Dukes stage C and D disease. In Dukes C disease it has been shown to increase five-year disease-free survival by 8-13%(14). There is also evidence for its neoadjuvant use in decreasing tumour burden prior to surgical resection in locally advanced cases(15). However, there is only limited evidence of benefit in so-called early stage disease, in the absence of lymph node involvement at the time of diagnosis. The National Institute of Health and Care Excellence (NICE) in the UK, only recommends its use in ‘high-risk’ Dukes B disease – those tumours with histological evidence of lymphovascular invasion, peritoneal tumour involvement or evidence of pre- or peri-operative perforation(16,17).

The first agent successfully used in CRC was 5-Fluorouracil (5FU), an antimetabolite agent which inhibits the action of thymidylate synthase, thereby blocking DNA synthesis(18). It remains the agent of choice in first line treatment, in its oral form, capecitabine, either alone or in combination with oxaliplatin and folinic acid(17). The intravenous regimen (utilising 5FU) is known as FOLFOX, with its oral counterpart (utilising capecitabine) known as CAPOX. These are the treatment regimens of choice in advanced or metastatic disease, with irinotecan (FOLFIRI) reserved for refractory disease(19).

1.1.4.3 Radiotherapy for Colorectal Cancer

Radiotherapy works by the direct damage of cellular DNA, leading to apoptosis, and a large inflammatory response. Because of these actions, and the lack of tissue specificity involved in this treatment modality, radiotherapy has to be carefully planned and targeted to minimise exposure of surrounding non-malignant tissues to damaging ionising radiation. In colorectal cancer, pre-operative radiotherapy is reserved for low rectal tumours where the circumferential resection margin (CRM) for surgery is compromised by the tumour. This situation risks leaving malignant cells behind following resection, so the cytotoxic effect of radiotherapy is used to downsize the tumour, in combination with chemotherapy. Post-operatively, radiotherapy can be utilised in both colonic and rectal malignancy under the following circumstances(20):

i. Where there is involvement of the surgical resection margin
ii. Where there is invasion of the peritoneal or abdominal wall identified either pre- or peri-operatively.
iii. Where there are post-operative findings of High Risk Dukes B, or Dukes C disease in disease that was ‘under staged’ pre-operatively, and therefore did not undergo pre-operative chemoradiotherapy.

1.1.4.4 Immunotherapy for Colorectal Cancer

The development of antigen-specific immunotherapies relies upon identification of a specific, over-expressed antigen in the malignancy of interest (21), and can be divided into passive and active immunotherapies.

Passive immunotherapy in the form of monoclonal antibodies (MAb) has gained widespread interest in the last 20 years, with effective treatment available in Renal Cell Carcinoma (Anti-VEGF-A MAb, Avastin®, bevacizumab), Breast cancer (Anti-Her2 MAb, Herceptin®, trastuzumab) and haematological malignancies (Anti-CD20 MAb, MabThera®, Rituximab). However, primary colorectal cancer remains a difficult target for immune therapies(22), with no currently licenced immunotherapies for the Dukes A-C disease. Cetuximab, bevacizumab, and a third monoclonal antibody, panitumumab, are also currently licenced for use in the treatment of advanced colorectal cancer, although evidence of benefit is limited, with response rates below 5% when used as a monotherapy (23). Improved outcomes are found when these compounds are used in combination with established chemotherapy regimens. This lack of response has also been coupled with observations in animal models that an initial stabilization in tumour size is then followed by a rapid growth of a more aggressive tumour, as a result of the tumour acquiring functional ways to avoid VEGF in angiogenesis, as demonstrated in a mouse model of pancreatic neuroendocrine tumour(24). There are also surgical considerations becoming apparent with bevacizumab, with a recent meta-analysis identifying prior treatment being an independent risk factor for anastomotic leak following resection(25).

Active specific immunotherapy in CRC is discussed in section 1.4

1.2 ANGIOGENESIS

The role of the vascular network is to both deliver nutrients and substrates to the tissues, and to conduct metabolic by-products to end organs for deactivation and excretion. Angiogenesis describes the generation of new blood vessels from the pre-existing vascular network(26). It is preceded by vasculogenesis, which lays down the original vascular network during embryonic development through differentiation of angioblasts. Physiologically, angiogenesis occurs during wound healing, menstruation and pregnancy, with the process also being involved in numerous pathological conditions, the most notable of which is malignancy(27).

1.2.1 Physiological Angiogenesis

Angiogenesis can be divided into sprouting and non-sprouting angiogenesis, the latter of which is also known as intussusception(26).

Sprouting angiogenesis is the longest lived, and hence considered the conventional pathway of angiogenesis. It occurs both in the yolk sac, and in the embryo, and is characterised by the disruption of the basement membrane of existing vasculature by a group of enzymes produced by activated endothelial cells - the matrix metalloproteinases (MMPs) and their inhibitors. Following the activation of cell surface receptors on endothelial cells by substances such as VEGF(28), the cell membrane is destabilised and this leads to formation of filopodia. These cells in turn secrete MMPs, and dissolve the basement membrane supporting the existing vasculature, causing proliferation of endothelial cells towards the source of the angiogenic stimulus. This results in an increase in both the number of blood vessels, and an increase in the total endothelial cell number.

Intussusceptive angiogenesis was first described in 1986(29), and is an intravascular phenomenon resulting from the formation of pillars into the vessel lumen, which subsequently leads to establishment of an endothelial junction between two newly divided vessels(30). This method can increase the surface area of a capillary network without increasing the underlying number of endothelial cells, making it especially important during embryological development where there are a limited number of endothelial cells available(31).

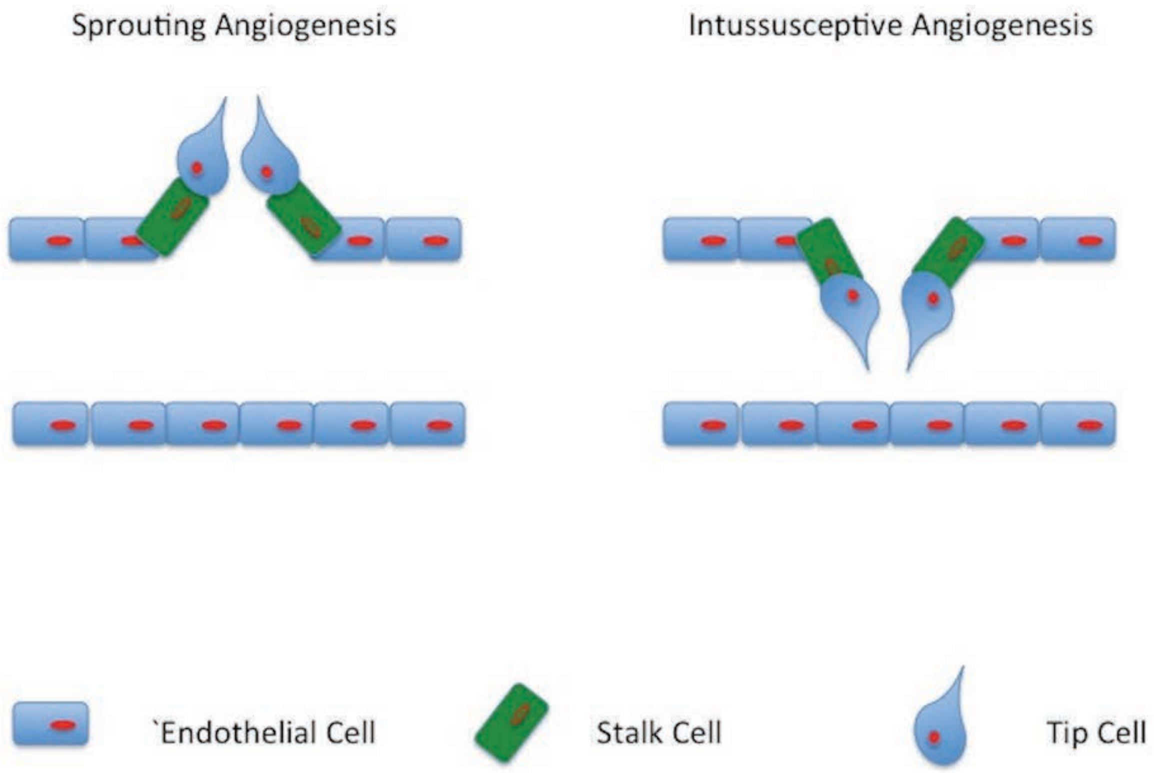
Sprouting Angiogenesis
Intussusceptive Angiogenesis
`Endothelial Cell
Stalk Cell
Tip Cell

Figure 1.2 – The Contrast Between Sprouting and Intussusceptive Angiogenesis.

1.2.2 Tumour Angiogenesis

While there is significant variation in the doubling time for capillary endothelium in physiological tissues, ranging from 47 to 20 000 days, this is considerably shorter, at 2-13 days, in tumour vasculature(32). This indicates that angiogenesis is a tightly controlled process in normal physiology, which has been overcome in the growth of malignant tumours.

Below the volume of around 2 mm^3, tumours can absorb the necessary nutrients from the surround tissues by diffusion(33). However, just as in normal physiological situations, as tumours grow their metabolic demand increases, creating relative hypoxia. This results in a period of dormant growth, as the immature tumour lacks the ability to stimulate angiogenesis. Future mutations result in the production of substances such as VEGF, IL-8 and bFGF which promote the formation of new blood vessels, thereby perpetuating tumour growth, and allowing the potential for metastasis(33-35). This genetic change forms part of the ‘angiogenic switch’, which describes a tumours’ change to an angiogenic phenotype. This switch has been attributed to(36):

i. The capability of tumour to recruit their own blood supply
ii. Recruitment of endothelial stem cells towards the vascular bed of tumours
iii. Amplification of the angiogenic signal by stromal cells such as macrophages, pericytes and vascular smooth muscle cells.
iv. Vessel co-option, whereby tumour cells cause endothelial cell apoptosis and induce neovascular sprouts from neighbouring vessels within normal tissues.

It has subsequently been shown that targeting of the process of tumour angiogenesis can starve the tumour of substrates, and cause regression. This has the theoretical advantage over the targeting of tumour cells that endothelial cells are relatively genetically stable and homogenous, rather than being prone to frequent mutations(37), as is the case with tumour cells.

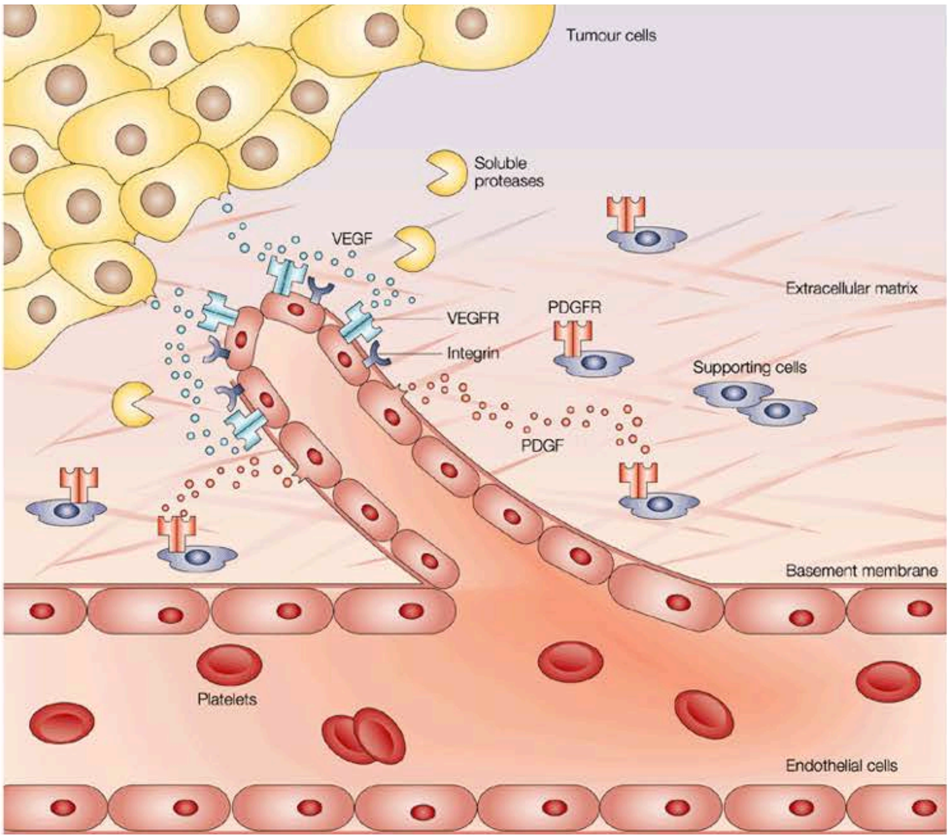
Tumour cells
Soluble proteases
VEGF
Extracellular matrix
VEGFR
PDGFR
Integrin
Supporting cells
PDGF
Basement membrane
Platelets
Endothelial cells

Figure 1.3 – Tumour-Induced Angiogenesis. Taken from (38), with permission from Nature Publishing Group.

1.2.3 Anti-angiogenic Therapies

Anti-angiogenic agents act by preventing the generation of new blood vessels, and consequently have a cytostatic effect, resulting in a stabilisation of tumour size(39). These agents aim to return a tumour to a status of dormancy, and are therefore a useful adjunct to chemotherapy regimens, radiotherapy or surgery. Many chemotherapeutic agents have both a direct cytotoxic and an anti-angiogenic effect. Broadly, a compound is considered to be primarily anti-angiogenic if its anti-angiogenic action occurs at a lower concentration than its cytotoxic threshold(36). Three categories of anti-angiogenic agents have been proposed(40):

i. Direct anti-angiogenics, which act by the targeting of either the endothelial cells or their functions, which are involved in angiogenesis (proliferation, migration or the formulation of new blood vessels (e.g. angiostatin, thalidomide).
ii. Indirect antiangiogenic drugs which impair the production of angiogenic factors by the tumour cells, and those cells within the tumour microenvironment, or to interfere with resultant extracellular processes (e.g. cetuximab, gefitinib)
iii. Mixed anti-angiogenic drugs that may be able to interfere with both endothelial and tumour cells (e.g. bevacizumab).

1.2.4 Vascular Targeting Therapies

These methods aim to disrupt or destroy existing vasculature, thereby starving the tumour of oxygen and metabolic substrates. Tumours are much more dependent on their microvasculature than physiologically normal tissues, with potentially hundreds of cell layers being dependent on a single endothelial cell. As a consequence, direct vascular disruption can result in significant, rapid tumour apoptosis and acute regression(41). These methods can be mechanical, such as the embolization of isolated liver metastases(42), or can be pharmacological. This latter group can be divided into three classes(39):

i. Ligand-directed vascular targeting agents

   These agents rely upon the identification of a target that is sufficiently upregulated on tumour-associated endothelium compared to that of the normal vasculature for there to be specific action within the tumour, without causing significant systemic toxicity. Studies have focused upon antibodies to such targets which are then conjugated to directly toxic or pro-thrombotic compounds(43), termed antibody-drug conjugates.

ii. Small-molecule vascular targeting agents

   This group of agents is analogous to tubulin-binding agents (e.g. combretastatin(44)). The small molecules bind to the tubulin cytoskeleton of endothelial cells and cause a conformational change. This exposes the basement membrane, resulting in activation of the coagulation cascade.

iii. Cationic liposome-based vascular targeting therapy.

   Cationic liposomes selectively target activated tumour endothelium, as opposed to neutral and anionic liposomes which extravasate into the tumour interstitium(45). These liposomes can then be used to encapsulate cytotoxic compounds (e.g. paclitaxel), and thereby mediate concentrated vascular-targeted effects.

1.3 VASCULAR ENDOTHELIUM

Vascular endothelium forms the lining of all vascular and lymphoid vessels within the body. Endothelium has specialised roles including a role in angiogenesis, but also as an endocrine organ, having functions in regulating blood pressure, inflammation and coagulation(46). This thin monolayer controls the transport of proteins solutes and gases across the blood vessel wall(47). It is supported by a basement membrane, and in the case of capillaries, is partially covered by pericytes. In larger veins and arteries, vascular smooth muscle cells and collagenous connective tissue surround this layer. They are generally considered to be quiescent in normal physiology, but their abnormal activation, or errors in their inactivation have been shown to be responsible for a variety of vascular disorders(48).

It has recently been appreciated that there is significant interdependence between endothelial cells, and their surrounding microenvironment, with the endothelial transcriptome influenced by that of nearby tumour cells(49).

1.3.1 Isolation of Endothelial Cells

In order to perform endothelial specific assays, it is important to be able to effectively isolate endothelial cells from surrounding tissues. The initial reports of endothelial cell isolation and culture date back to the 1970’s(50,51), but conventional tissue culture techniques have been found to significantly affect the transcriptome of cultured endothelial cells, due to lack of flow, and acidic stress(52). As a result, it is important that *in vivo* samples of tissue for endothelial cell isolation and assays to determine genetic expression profile are obtained expediently.

1.3.2 Tumour Endothelial Markers (TEMs)

There is significant evidence that capillaries within tumours differ in terms of their structure, integrity and flow characteristics compared to that of surrounding normal tissue(53). As a consequence, the genetic profile, and hence protein expression on the endothelial cell surface of tumour-associated endothelium differs significantly to that within normal tissues. This difference in expression can be exploited to identify potential therapeutic targets.

The work of St. Croix published in 2000 contained the first reference to tumour endothelial markers (TEMs)(53). Within this work, endothelial cells were extracted from CRC tumour samples, and neighbouring normal colon, followed by RNA extraction and SAGE (Serial Analysis of Gene Expression) to identify and quantify consistently upregulated genes. The resultant identified markers were termed TEM1-10, and have formed the basis of many pre-clinical papers. However, despite considerable interest in these targets(54), clinical data has been lacking.

1.3.3 GRIN2D

GRIN2D (Glutamate Receptor, Ionotropic, N-Methyl D-aspartate (NMDA) receptor subunit 2D), also known as the NMDA receptor subunit 2D (NMDAR2D/NR2D), and NMDA receptor subunit 2ε, is a subunit of a glutamate dependent calcium channel, conventionally found in neuronal tissues. Chromosomally, GRIN2D is localized within the region 19q13.1–qter(55). Each NMDA Receptor is comprised of two NR1 subunits, and two NR2 or NR3 subunits. These heterotetramers are transmembrane proteins, with an intracellular C-terminus and an extracellular N-Terminus (Figure 1.4). NR2 subunits both provide the glutamate-binding sites in the NMDA receptor complex(56), and also modify the channel properties, particularly in terms of ion flux(57,58).

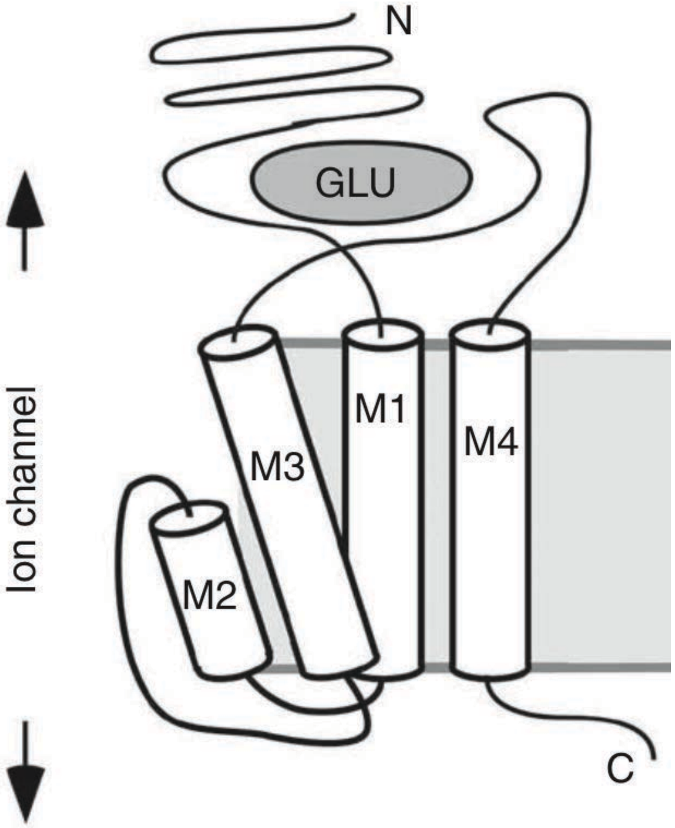

Figure 1.4 – The Structure of Ionotropic NMDA Receptors. GLU – Glutamate binding Site. Taken from (59), with permission from Nature Publishing Group.

The NMDA receptors are involved in long-term potentiation within the central nervous system – a process that is intimately involved in the processes of learning and memory(60), as well as synaptic plasticity(61). GRIN2D is most highly expressed in the embryonic and early neonatal rodent brain, with expression declining, and becoming more focally expressed in the brain stem and cerebellum(60) with progressing age. These initial findings of central nervous system expression in rats have since been corroborated in human studies(62). Subsequently, NMDA Receptors have been identified within the enteric nervous system, and are implicated in the modulation of visceral sensitivity and pain, where activation of peripheral NMDA receptors in colonic tissue sections in rats has shown to cause calcium-dependent release of pro-inflammatory neuropeptides(63). These early animal studies have laid the foundation for studies which have shown the association between the up-regulation of NMDA receptors and the presence of visceral pain in patients with Ulcerative Colitis(64). This influx of calcium, regulated by NMDA receptors, has been shown to protect against apoptosis(65), and this, alongside its association with colonic inflammation offers logical reasons for its presence as a tumour endothelial protein in CRC. Indeed, GRIN2D has previously been shown to be ubiquitously present within human tumour cell lines in vitro, including the HT29 colorectal adenocarcinoma line(66).

1.4 VACCINATION

Vaccination was developed as a method of inducing protection against communicable diseases in the late 18th Century. The work of Edward Jenner modified the practice of variolation, which involved the direct inoculation of the ground scabs of smallpox sores into wounds to offer protection(67). His work, published in 1798, described the inoculation of fluid from cow-pox lesions into 23 patients, with consequent protection offered against smallpox in the medium term(68). This resultant protection afforded by the exposure of a patient to a less pathogenic form of a contagion has formed the basis of all future vaccine development, whether these vaccines be directed against a communicable disease or a malignancy, as is now the case with the human papilloma virus in cervical cancer(69).

1.4.1 Vaccine Design

The development of a vaccine essentially relies upon the identification of a target that is specific to the intended target pathology (the antigen), and a compound to induce an immune response (the adjuvant)(70).

Optimisation of the antigen by selection of only specific areas of its structure is necessary to prevent autoimmune responses, to target immune responses against particular strains or forms of the pathogen, and to prevent predominant immune responses to areas of the pathogen prone to genetic (or antigenic) drift. However, the selected peptide must cover enough of the target protein to prevent vaccine inactivity due to clonal variability(70).

The use of an adjuvant to induce immune response is often necessary, as many epitopes lack the molecular cues necessary to be innately immunogenic. This is the case when self-antigens are the targets of interest. Within humans, the only approved adjuvant is Alum, as many of the bacterial-derived compounds are toxic(71). However, these bacterial compounds are widely used in animal studies.

Some of the more recent vaccines for human use have been engineered within specific delivery systems. These have been developed, as some antigens are broken down within the circulation prior to presentation to immune reactive cell types. Examples of these would be enclosure of the vaccine within recombinant viral vectors or conjugation to antibodies which are specific to immune reactive cells, such as Clec-9A(72).

1.4.2 The Immune Response to Vaccination

The first requirement of a vaccine is for it to trigger an immune reaction mediated by the cells of the innate immune system(73). Following administration of a vaccine, circulating dendritic cells are recruited to the site of inoculation, and undergo maturation. This maturation stimulates the modulation of specific cell surface molecules such as inflammatory cytokines and chemokines(74). Locally, this promotes an inflammatory microenvironment with extravasation and attraction of monocytes, granulocytes and natural killer cells. Systemically, this maturation causes migration of dendritic cells towards secondary lymph nodes. It is at this site where the induction of T- and B- lymphocyte response occurs(75).

B-Cell Responses

Within the lymph nodes, B-cells are activated by the presence of vaccine antigens, and move towards the marginal zone, where they are exposed to activated dendritic cells, and activated T-helper cells. This leads to the differentiation of B-cells into plasma cells within germinal centres, which produce large amounts of antibody to the vaccine antigen. In rodents, Th1 T-cells promote a switch towards IgG2a, whereas Th2 T-cells support the generation of IgG1 and IgE (via IL-4) and IgG2b and IgG3 (via TGF-β)(76). This differentiation is less predominant in humans, where the IgG1 subtype predominates regardless of the helper T-cell subtype. This portion of the immune response lasts only for around 28 days. However, a fraction of plasma cells that differentiated into germinal centres acquire the capacity to migrate towards long-term survival niches mostly located within the bone marrow, from where they may produce vaccine-derived antibodies for extended periods. These are then termed memory B-Cells. An additional exposure to the antigen, or a ‘booster’ vaccination will reactivate these memory cells, and lead to a longer, more pronounced immune response(77) (Figure 1.5).

T-Cell Responses

Activated dendritic cells display major histocompatibility complex (MHC) proteins on their surface, and are transported to the peripheral zone of lymph nodes. CD4+ T-Cells, which are activated by MHC Class II proteins, proceed down one of two pathways with differentiation into either Th1-type or Th2-type cells. Th1-cells produce IFN-γ and TNF-α, leading to the elimination of intracellular pathogens both via cytokine responses and through their support of macrophage activation and $CD8^+$

T-cell differentiation (78). Th2-type $CD4^+$ T cells produce IL-4, IL-5 and IL-13 which are directly implicated in the defense against extracellular pathogens such as helminths(79).

The ongoing immune response beyond around 28 days relies upon T-cell memory. The degree to which a T-cell memory response is maintained depends predominantly upon the amount of antigen present during initial vaccination(80). The degree of future immune response also depends upon whether there is predominantly an effect via effector memory B-cells, which are mobile throughout the non-lymphoid organs, or central memory B-cells, which traffic through the spleen and lymph nodes. Effector memory cells have a high cytotoxic capacity, so can act swiftly, but lack the proliferative potential of central memory cells(81).

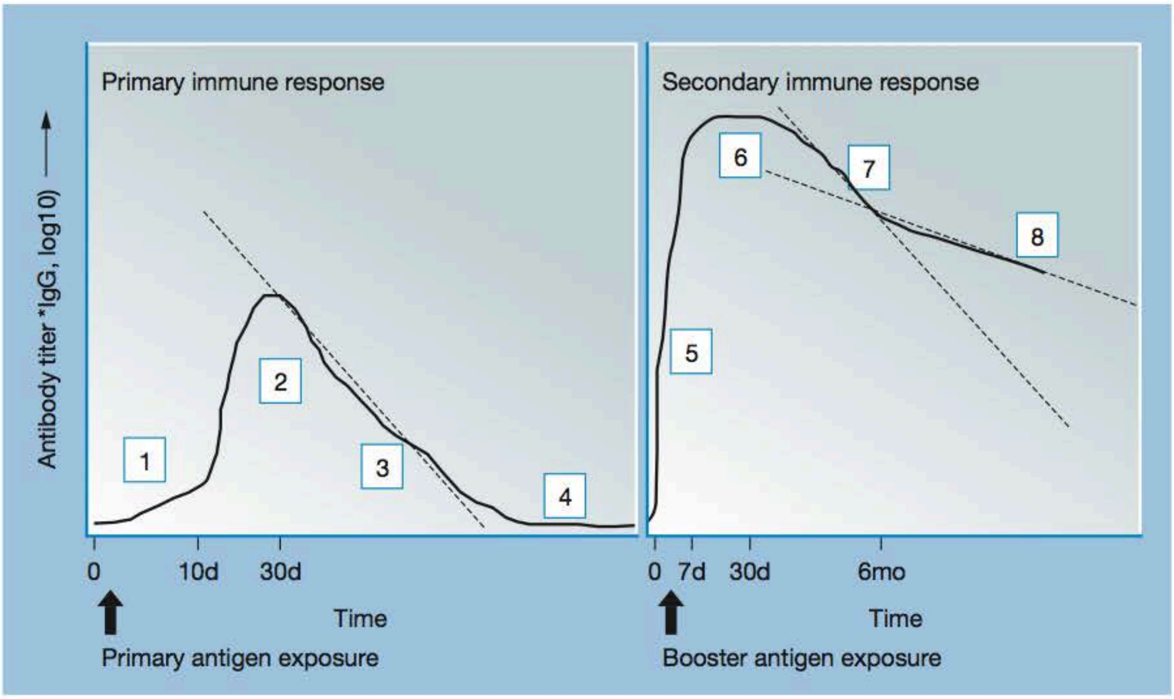

Figure 1.5 - Correlation of Antibody Titers to the Various Phases of the Vaccine Response. An initial antigen exposure stimulates an extra-follicular response [1]. This results in the rapid production of low concentrations of IgG antibody. As B-cells proliferate in germinal centers, with differentiation into plasma cells, IgG antibody levels increase to a peak value [2]. This is usually reached 4 weeks after immunisation. The short life plasma cells results in a rapid fall in antibody titers [3], which eventually return to baseline levels [4]. In secondary immune responses, a secondary exposure to an antigen reactivates memory cells, resulting in a rapid increase of IgG antibody titer [5]. 'Short-lived' plasma cells maintain peak antibody levels [6] for the first few weeks, after which titers decline with the same rapid kinetics as that which follows primary immunisation [7]. 'Long-lived' plasma cells, which have reached survival niches, continue to produce antigen-specific antibodies, which then decline over a slower course [8]. Taken from (75), with permission from Elsevier.

1.4.3 Therapeutic Vaccination in Colorectal Cancer.

Active specific immunotherapy in the form of a vaccination has developed as a new route of targeting both primary tumours and potentially unidentified distant micrometastases in CRC(22).

Clinically, it has been stated that endothelial cell vaccines may be beneficial in subgroups of patients following colorectal resection(22), and early studies in a mouse model of metastatic CRC have yielded encouraging results(82), with a detectable immune response to injected hepatic sinusoidal cells – a highly angiogenic endothelial cell line. Indeed, Vermorken et al. describe successful vaccination using an autologous tumour cell-BCG conjugate vaccine with excellent results in Dukes B Cancers (83). This had led to the development of the OncoVax™ tumour vaccine. While this has shown good results in a Phase III randomised controlled trial (84), it is patient specific, and therefore requires individual tumour profiling and generation of an individualised vaccine. Economically, this is not ideal, and the search for a more generaliseable vaccine is ongoing. Early experience with vaccination of human umbilical vein endothelial cells (HUVEC) in patients with metastatic CRC demonstrated little response(85). Since these initial targets were studied, a large number of tumour-specific antigens have been identified in GI malignancies, the most frequently targeted of which are CEA and Ep-CAM (Epithelial cell-adhesion molecule)(21). Early clinical results of a CEA-based vaccine within a phase II clinical trial in patients with metastatic CRC, have indicated an objective clinical response in 40% of enrolled patients when combined with a chemotherapeutic regime(86).

A further therapeutic vaccine known as TroVax® has also undergone phase-I and early phase-II trials in metastatic colorectal cancer(87). This vaccine is targeted against a pan-cancer tumour target, 5T4, and has demonstrated a stimulation of immune response in these early clinical trials, with some evidence of disease response in those patients demonstrating a 5T4-specific immune response.

1.5 HYPOTHESIS, AIMS AND OBJECTIVES

1.5.1 Hypothesis

That a putative TEM can be identified in CRC by sequential genetic analysis of endothelial isolates from multiple biological replicates, and that this marker can be targeted through a vaccination-based approach to produce anti-angiogenic effects in a murine model of CRC, leading to a decrease in tumour growth.

1.5.2 Validation of Potential Tumour Endothelial Markers in Colorectal Cancer

A list of potential TEMs will undergo literature review, and those that prove to be novel within colorectal cancer will be taken forward to validation by real-time quantitative polymerase chain reaction (RTqPCR) and immunohistochemistry (IHC) on locally acquired clinical tissue samples.

1.5.3 Functional Characterisation of TEMs in Endothelial Cell Behaviour

Candidate genes of interest will be knocked down in human umbilical vein endothelial cells (HUVEC) using siRNA (small interfering RNA) duplexes. Manipulated cells will undergo assessment of cellular migration by a modified Boyden Chamber assay, vascular tube formation by Matrigel assay, chemotaxis and cellular communication by scratch wound assay and assessments of cell viability and proliferation will be made using the Acumen™ cell imager.

1.5.4 Investigation of Novel TEMs as Therapeutic Vaccines in Colorectal Cancer

Newly identified TEMs, which are successfully validated, will be taken forward to a murine vaccine model. Self-antigens will be vaccinated against, using an adjuvant to facilitate breaking of immune tolerance. Vaccine effects on physiological angiogenesis will be investigated using the murine subcutaneous sponge assay, with tumour effects assessed using a subcutaneous tumour model.

CHAPTER 2

MATERIALS AND METHODS

2.1 MATERIALS

2.1.1 Equipment

Centrifuges	**Source**
Biofuge Primo	Heraeus, Newport Pagnell, UK
Accuspin Micro	Fisher Scientific, Loughborough, UK
Mikro22R	Hettich Zentrifugen, Tuttlingen, Germany
Avanti J-20 XP	Beckman Coulter, Brea, USA
Harrier 18/80R	MSE (UK) Ltd, London, UK

Microscopes	**Source**
Leica DM6000	Leica, London, UK
Leica DM1L Inverted Microscope	Leica, London, UK
USB 2.0 2M Xli Camera	Xli, Carrollton, USA

Spectrophotometer	**Source**
ND-1000 Spectrophotometer	Nanodrop Technologies, Wilmington, USA

Microtome	**Source**
5040 Microtome	Bright Instruments, Cambridge, UK

Biochemistry	**Source**
XCell SureLock™ Mini-Cell Electrophoresis Apparatus	Invitrogen, Paisley, UK
XCell II™ Blot Module Wet Transfer Apparatus	Invitrogen, Paisley, UK
Electrophoresis Power Supply EPS 301	Amersham Biosciences, Sweden
Polyvinylidene Difluoride Membranes	Immobilon-P, Billerica, USA
Block Heater SBH 200D	Stuart, Stone, UK
Accublock™ Digital Dry Bath	Labnet International Inc., Woodbridge, USA
Gyro-rocker SSL3	Stuart, Stone, UK
Rotator SB3	Stuart, Stone, UK
Heating Magnetic Stirrer FB15001	Fisher Scientific, Loughborough, UK
EK-300i Measuring Scale	A&D, Seoul, South Korea
Roto-shake Genie	Scientific Industries, New York, USA
Compact x4 X-Ray Film Developer	Xograph Imaging System, Tetbury, UK
3510 pH Meter	Jenway, Stone, UK
HiTrap Protein A Column	GE Healthcare Life Sciences, Little Chalfont, UK

Molecular Biology	**Source**
Orbital Incubator	Gallenkamp, The Netherlands
Stuart SI500 Shaking Incubator	Stuart, Stone, UK
GeneGenius Gel Imaging System	Syngene, Cambridge, UK
DNA Gel Tank	Jencons (Scientific) Ltd, East Grinstead, UK
Thermal Water Bath	Fisher Scientific, Loughborough, UK
DYAD DNA Engine Multi-Bay Thermal Cycler	Life sciences, Little Chalfont, UK
Rotor-Gene RG-3000	Corbett Life Sciences, Qiagen, Crawley, UK
Vibracell Ultrasonic Processor	Sonics & Materials, Newtown, CT, USA

Cell Biology	
Sterile Cell Culture Hood, Advanced BioSafety Cabinet Class 2	Microflow, Andover, UK
Incubator, 37°C, 5% CO_2, 95% Filtered Air	Heraeus, Newport Pagnell, UK
Water Bath	Fisher Scientific, Loughborough, UK
Haemocytometer	Marienfeld, Lauda-Königshofen, Germany

Facilities	
Biomedical Services Unit	Birmingham, UK
DNA Sequencing Service	Technology Hub, Birmingham, UK
Mass Spectroscopy Unit	Technology Hub, Birmingham, UK

2.1.2 Consumables, Chemicals and Reagents

Biochemistry	**Source**
Protein A Sepharose Beads	Sigma, Gillingham, UK
Glutathione Sepharose Beads	GE Healthcare, Little Chalfont, UK
Histoclear	National Diagnostics
Ultrapure ProtoGel	Geneflow, Lichfield, UK
Tween 20	Sigma, Gillingham, UK
Ponceau S	Sigma, Gillingham, UK
TEMED	Sigma, Gillingham, UK

Molecular Biology	**Source**
ProbeLibrary Realtime PCR Assay System	Exiqon, Woburn, USA
Agarose	Sigma, Gillingham, UK
SYBR-safe DNA Gel Stain	Invitrogen, Paisley, UK
LB Broth	Sigma, Gillingham, UK
LB Agar	Sigma, Gillingham, UK
SOC Media	Bioline, London, UK
10mM dNTP	Fermentas, Cambridge, UK
EXPRESS qPCR Supermix	Invitrogen, Paisley, UK
6x DNA Loading Dye	New England Biolabs, Herts, UK
Fusion DNA Polymerase	New England Biolabs, Herts, UK
Taq DNA Polymerase	Bioline, London, UK
EcoR1	New England Biolabs, Herts, UK
BamH1	New England Biolabs, Herts, UK
EcoR1 Buffer	New England Biolabs, Herts, UK
Antarctic Phosphatase	New England Biolabs, Herts, UK
T4 Ligase	Thermo Scientific, California, USA
α-Select Competent *E.coli* Gold Efficiency	Bioline, London, UK
α-Select Competent *E.coli* Bronze Efficiency	Bioline, London, UK
BL 21 *E.coli*	Bioline, London, UK

Cell Biology	**Source**
RNAiMAX Lipofectamine	Life Technologies, California, USA
Actinomycin	Life Technologies, California, USA
Collagenase Type 1A	Sigma, Gillingham, UK
Collagenase Type 5	Sigma, Gillingham, UK
Polyethylenimine (PEI)	Sigma, Gillingham, UK

2.1.3 Oligonucleotides

Primers for RTqPCR / DNA Sequencing		
Oligonucleotide	**Organism**	**Sequence**
KCNJ8	Human	F: 5’-CGCTACCCGGAGTCTGAG-3’ R: 5’-CAGCTTAGCCACCTCCCTCT-3’ Probe 34
P2RY6	Human	F: 5’-TGCTCCACGAGTGGGAAT-3’ R: 5’-GGTGGGTTTCCTATGTTCAGG-3’ Probe 67
GRIN2D	Human	F: 5’-GGCTCAGTGACCGCAAGT-3’ R: 5’-GCACGGTCCCAAACTTCA-3’ Probe 57
GRIN2D	Mouse	F: 5’-CCATTCTCGACTTCCTGTCG-3’ R: 5’-GCTGTTGCTCTGTGGAGGA-3’ Probe 4
GRIN2D Reverse Cloning	Human	5’-CTGATCGAATTCGCGCCCGGGCTG CGCACCGCCGCCGCCGCCACGGC-3’
LOC541471	Human	F: 5’-CAGATCTTCACAGCACAGTTCC-3’ R: 5’-TGCTGATCCACTTTGCTTGT-3’ Probe 39
LILRB4	Human	F: 5’-ACCTTCACGGCTCTGCTCT-3’ R: 5’-CCCCCAGCTGATCACAGA-3’ Probe 57
VASN	Human	F: 5’-CGCCAGGAAAGACTGAGG-3’ R: 5’-ACCCTGGAGCACATCTTCTG-3’ Probe 70
OR51E1	Human	F: 5’-CAGCCTGCCAGACCTCTT-3’ R: 5’-CAGCACCAGGCAGGTAGAG-3’ Probe 69
GJA4	Human	F: 5’-CCTCAAACCCTCTCCTCACA-3’ R: 5’-GCTCTGTCTGTGCGATCAAG-3’ Probe 3
RGS16	Human	F: 5’-GATCCGATCAGCTACCAAGC-3’ R: 5’-GTGGGTCTCATGGTCAATGTT-3’ Probe 37
ADAP2	Human	F: 5’-ACACCAGGAACCTGTTTGTGT-3’ R: 5’-GGAGGGCATTGAACCAGTC-3’ Probe 12
PECAM	Human	F: 5’-GCAACACAGTCCAGATAGTCGT-3’ R: 5’-GACCTCAAACTGGGCATCAT-3’ Probe 14
PECAM	Mouse	F: 5’-CGGTGTTCAGCGAGATCC-3’ R: 5’-ACTCGACAGGATGGAAATCAC-3’ Probe 45
β -Actin	Human	F: 5’-CCAACCGCGAGAAGATGA-3’ R: 5’-CCAGAGGCGTACAGGGATAG-3’ Probe 64

β -Actin	Mouse	F: 5’- GGAGGGGGTTGAGGTGA-3’ R: 5’-GTGTGCACTTTTATTGGTCTCAA-3’ Probe 71
Flotillin	Human	F: 5’-GATCCTCAGCTTCACCATCAA-3’ R: 5’-TCAGCATCTCTCTGCACCAC-3’ Probe 61
NOX4	Mouse	F: 5’-AGTATCAGACAAATGTAGACACTCACC-3’ R: 5’-CTGGGATGATGTCTGGTTAAGA-3’ Probe 71
STRA6	Mouse	F: 5’-CTCAGCAAGGCCTCTCTCTTTC-3’ R: 5’-TGGGATGGGAGATATTCAGG-3’ Probe 9
CMV Promoter	Vector	F: 5’-CGCAAATGGGCGGTAGGCGTG-3’
pGEX Sequencing Primers	Vector	F: 5'-GGG-CTGGCAAGCCACGTTTGGTG-3' R: 5'-CCG-GGAGCTGCATGTGTCAGAGG-3

2.1.4 Antibodies

Specificity	Characteristics	Application/ Dilution	Source	Catalogue Number
Anti-GST	Goat, anti-GST	Western Blot 1 in 2000; ELISA 1 in 500	GE Healthcare, Little Chalfont, UK	27-4577-62
Anti-Sheep Ig-HRP	Rabbit, anti-sheep, HRP conjugated	Western Blot 1 in 5000	R&D Systems, Abingdon, UK	HAF016
Anti-Goat Ig-HRP	Rabbit, anti-goat, HRP conjugated	ELISA 1 in 5000	Dako, Ely, UK	P0160
Anti-Mouse Ig-HRP	Rabbit, anti-mouse IgG, HRP conjugated	ELISA 1 in 5000	Dako, Ely, UK	Z 0420
Anti-Rabbit Ig-HRP	Donkey, anti-rabbit Ig, HRP conjugated	Western Blot 1 in 5000 ELISA 1 in 5000	R&D Systems, Abingdon, UK	HAF008
Anti-Mouse IgG1	Goat, anti-mouse	ELISA 1 in 500	Sigma, Gillingham, UK	M5532
Anti-Mouse IgG2a	Goat, anti-mouse	ELISA 1 in 500	Sigma, Gillingham, UK	M5657

Anti-Mouse IgG2b	Goat, anti-mouse	ELISA 1 in 500	Sigma, Gillingham, UK	M5782
Anti-Mouse IgG3	Goat, anti-mouse	ELISA 1 in 500	Sigma, Gillingham, UK	M5907
Anti-Mouse IgA	Goat, anti-mouse	ELISA 1 in 500	Sigma, Gillingham, UK	M6032
Anti-Mouse IgM	Goat, anti-mouse	ELISA 1 in 500	Sigma, Gillingham, UK	M6157
Anti-Human Clec-14a	Sheep Anti-human	Western Blot 1 in 1000	R&D Systems, Abingdon, UK	AF4968
Anti-Fc-HRP	Goat Anti-human, HRP conjugated	Western Blot 1 in 1000	Abcam, Cambridge, UK	ab97265
Anti-GRIN2D-N-Terminus	Rabbit Anti-Human, custom polyclonal serum	Western Blot 1 in 500 IHC undiluted	Eurogentec, Seraing, Belgium	ZGB14072 - 0685
Anti-GRIN2D-N-Terminus	Rabbit Anti-Human, polyclonal serum	Western Blot 1 in 500 IHC undiluted	Eurogentec, Seraing, Belgium	ZGB14072 - 0686
ImmPRESS HRP Universal Secondary Antibody	Donkey Anti-mouse Ig & Donkey Anti-rabbit Ig, HRP Conjugated	IHC As supplied	Vector Laboratories, Peterborough, UK	MP-7500

2.1.5 siRNA Duplexes

Specificity	**Source**	**Catalogue Number**
Scrambled Control	Origene, Rockville, MD, USA	SR30004
Human GRIN2D	Origene, Rockville, MD, USA	SR301958A
Human GRIN2D	Origene, Rockville, MD, USA	SR301958C

2.1.6 DNA Vectors and Plasmids

Vector	Characteristics	Source
pcDNA3.1	Mammalian Expression Vector. Human Fc Tag at C-Terminus	Invitrogen, Paisley, UK
pGEX-2T	Bacterial Expression Vector. GST Tag at N-Terminus	GE Healthcare, Life Sciences, Little Chalfont, UK
MSCV-Luc	Retroviral Mammalian expression Vector. Luciferase insertion sequence.	Clontech, California, USA

2.1.7 Cell Lines

Cell Line	Source
Human Umbilical Vein Endothelial Cells (HUVEC)	Bicknell Lab, Birmingham University, UK
SHSY5Y	Nagy Lab, Birmingham University, UK
HEK293-T	Bicknell Lab, Birmingham University, UK
CT26	Life Technologies, California, USA
Phoenix-ampho	Gary Nolan, Stanford, USA

2.1.8 Cell Culture Media

Media	Source
Foetal Calf Serum	CRUK Central Services, London, UK
Penicillin 10 000 units/ml + Streptomycin 10 000 μg/ml	Gibco, Life Sciences, Gillingham, UK
L-Glutamine	Gibco, Life Sciences, Gillingham, UK
OptiMEM Serum Low Media	Invitrogen, Paisley, UK
Medium 199	Sigma, Gillingham, UK
Bovine Brain Extract	Bicknell Laboratory, UK
Heparin	Sigma, Gillingham, UK
Trypsin 0.5%	Gibco, Life Sciences, Gillingham, UK
DMEM	Sigma, Gillingham, UK

2.1.9 Biological Materials and Solutions

Material	**Company**
Balb/c Mice	Charles River, Margate, UK
Umbilical Cords	NHS, Birmingham, UK
Colorectal Cancer	NHS, Birmingham, UK
Normal Colon	NHS, Birmingham, UK
Matrigel	BD Biosciences, Oxford, UK
D-Luciferin	PerkinElmer, Seer Green, UK
Freund's Complete Adjuvant	Sigma, Gillingham, UK
Freund's Incomplete Adjuvant	Sigma, Gillingham, UK

2.1.10 Buffers and Solutions

Buffer	**Recipe**
4x SDS Loading Buffer	2ml 1M Tris HCl(pH6.8), 0.8g SDS, 0.04g Bromophenol Blue, 4ml 100% Glycerol, 4ml 1M DTT
RIPA Buffer	300µl 5M NaCl, 1ml 10% NP40, 500µl 10% DOC, 100µl 10% SDS, 500µl 1M Tris HCl (pH 7.5), 7.6ml dH_2O
4x Resolving Buffer (250ml)	1g SDS, 42.25g Tris HCl pH8.8
4x Stacking Buffer (250ml)	1g SDS, 15.125g Tris HCl pH6.8
10x Western Blot Running Buffer (1L)	50ml 20% SDS, 30.2g Tris, 144g Glycine
10x Western Blot Transfer Buffer (1L)	2.5ml 20%SDS, 2g Tris, 75g Glycine.
Phosphate Buffered Saline – Tween 20 (PBS-T)	1L PBS, 500µl Tween-20
Blocking Buffer	10% Skimmed Milk in PBS-T
TAE Buffer	40mM Tris Base, 18mM Glacial Acetic Acid, 1mM EDTA
E.coli Lysis Buffer	50mM Tris pH7.5, 100mM NaCl, 2mM EGTA, 2mM EDTA, 1mM DTT, 0.5mM PMSF
GST Wash Buffer	50mM Tris pH8.5, 100mM NaCl, 1mM DTT, 0.5mM PMSF
GST Elution Buffer	30mM Reduced Glutathione, 50mM Tris pH8.5, 100mM NaCl, 1mM DTT, 0.5mM PMSF, Protease inhibitors.
GST-GRIN2D Storage Buffer	50mM MES pH 5.5, 150mM NaCl

2.2 METHODS

2.2.1 Molecular Biology

2.2.1.1 DNA/RNA Handling and Quantification

All work with DNA or RNA was carried out using sterile pipette tips and nuclease-free (NF) water. DNA Samples were stored at -20^{o}C and RNA samples at -80^{o}C. DNA and RNA quantification was performed using the NanoDrop spectrophotometer (Thermoscientific, Wilmington, DE, USA), with the OD 260/280 ratio used as a measure of sample purity.

2.2.1.2 RNA Extraction

Total RNA was isolated from primary cells or cell lines using the RNeasy Mini-Kit (Qiagen, Crawley, UK) as per the kit protocol. To summarise: The cells were suspended in 700 µl Qiazol Lysis buffer, and then 140 µl chloroform was added. This mix was then centrifuged at 14,000*g* at 4^{o}C for 15 mins, and the upper aqueous phase separated off. This phase was combined with 100% ethanol, and added to a centrifuge column. The column is then washed with Buffer RWT (Qiagen, Crawley, UK), and treated with RNase-free DNase. The column is further washed, and finally the RNA sample was eluted in RNase-free Water.

2.2.1.3 Generation of Complementary DNA (cDNA)

Following RNA isolation, cDNA was generated using the High-Capacity cDNA Reverse Transcription Kit (Life Technologies, California, USA), without RNase Inhibitor.

Reaction components:

Component	Volume per reaction (μl)
10x RT Buffer	2.0
25x dNTP Mix (100 mM)	0.8
10x RT Random Primers	2.0
Multiscribe™ Reverse Transcriptase	1.0
Nuclease-Free H_2O	4.2
Total Volume Per Reaction	10.0

The reaction master mix was then combined with an equal quantity (20 ng-2 μg) of RNA made up to 10 μl with H_2O. Total reaction volume = 20 μl

Thermal Cycler Conditions:

	Step 1	Step 2	Step 3	Step 4
Temperature	25°C	37°C	85°C	4°C
Time	10 min	120 min	5 min	∞

2.2.1.4 Real-Time Quantitative Polymerase Chain Reaction (RTqPCR)

All RTqPCR Reactions were performed using the Rotor-Gene RG3000 Thermal Cycler, and the ProbeLibrary PCR Assay System. Beta-Actin was used as the housekeeping gene to which the expression of each potential endothelial target was normalised unless otherwise stated. Primer and Probe sets were designed using ProbeFinder Software (Roche Applied Science, Indianapolis, USA). Reaction mix was prepared in triplicate, and 10 μl of cDNA used for each reaction. Serial dilutions of 1:10, 1:100 and 1:1000 of cDNA were used to ensure internal experimental validity.

Primer mix:

Component	Volume (μl)
Forward Primer	10
Reverse Primer	10
Nuclease Free H_2O	180

Reaction Mix per reaction:

Component	Volume (µl)
Primer Mix	2
Probe	0.25
Nuclease Free H_2O	0.25
Express qPCR Supermix (Life Technologies, Paisley, UK)	12.5

2.2.1.5 Agarose Gel Electrophoresis

1% or 2% agarose gel was prepared in TAE Buffer with the addition of 1:10 000 SYBR safe DNA gel stain (Invitrogen, Paisley, UK). 6x loading dye was added to the DNA, and the samples loaded. The samples were run at 100V for 30-45 mins. An ultraviolet (UV) image was acquired of the gel using the BIO Imaging System machine. Annotations were performed using Genesnap Software (Gene Genius, Cambridge, UK).

2.2.1.6 Agarose Gel Extraction

All procedures were performed using the GeneJET Gel Extraction Kit (Thermoscientific, Wilmington, DE, USA). Desired bands were visualised using UV light, and excised using a scalpel. A 1:1 ratio of binding buffer was added to the excised gel slice, and incubated with agitation at 60°C for 10 mins. For DNA fragments ≤500bp, a 1:2 ratio of isopropanol was added to aid DNA isolation. The solution was then added to a centrifugation column, washed using wash buffer, and eluted in 50 µl elution buffer. Samples were then stored at -20°C. Concentration of extracted DNA was confirmed on agarose gel.

2.2.1.7 Restriction Enzyme Digestion

Appropriate restriction enzymes were utilised in appropriate buffers with BSA at 0.1 mg/ml. Digestion was performed in accordance with the manufacturer's instructions. To summarise, 2 μg of DNA vector was combined with 1 μl of each enzyme (usually equivalent to 10 units) for 60 mins at 37^{o}C.

2.2.1.8 Vector Dephosphorylation

When necessary, the digested vector ends were dephosphorylated using antarctic phosphatase. 1 μl (5 units) of antarctic phosphatase was added to the restriction digest product, alongside a 1/10 volume of 10x of antarctic phosphatase reaction buffer. This was incubated at 37^{o}C for 15-30 mins, and then heat inactivated at 65^{o}C for 5 mins.

2.2.1.9 Ligation

All DNA constructs were generated using T4 ligase. Appropriate ratios of vector and insert DNA were calculated using online software, and combined with 1 μl T4 ligase and an appropriate volume of 10x ligase buffer. The reaction mix was then incubated at 22^{o}C overnight.

2.2.1.10 Bacterial Transformation

'Gold efficiency α-select' competent *E.coli* (Bioline Reagents, London, UK) were used for transforming ligation products, while 'Bronze efficiency α-select' competent cells were used for plasmid amplification. BL21 cells (Bioline Reagents, London, UK) were used for protein expression. 50 μl of cells were thawed on ice for 30 mins. 5-50 ng of plasmid DNA was added to the cells, mixed by flicking, and incubated on ice for 30 mins. The mixture was then heat shocked in a water bath at 42°C for 30-45 seconds. The mix was then placed on ice for a further 2 mins, after which 200 µl of SOC media was added, and the resultant mix incubated at 37°C on an agitator for 60 mins. 100 µl was then plated onto LB Agar plates containing an appropriate antibiotic.

2.2.1.11 Plasmid DNA extraction from bacteria

All extractions were performed using the GeneJET Plasmid Miniprep Kit (Fermentas, Thermoscientific, Wilmington, DE, USA). Briefly, cultured cells were centrifuged and pelleted. The pellet was then resuspended in 250 µl resuspension buffer, containing RNase, 250 µl lysis solution and 350 µl of neutralisation solution, mixing between each addition by inversion. The resultant mix was then centrifuged and the supernatant transferred to a spin column. Here, the DNA is bound, washed, and then eluted using either elution buffer or NF Water.

2.2.1.12 DNA Sequencing

This was performed by the Functional Genomics and Proteomics Facility, School of Biosciences, University of Birmingham, UK. Briefly, 250 ng of DNA was combined with 1 µl of forward or reverse primer (final primer concentration 3.2pM), and the mix made up to 10µl using NF water. This was then combined with 10 µl BigDye® Reaction Mixture (Life Technologies, California, USA) for further processing. Data outputs were analysed using Sequencher software (Gene Codes Corporation, Ann Arbor, USA

2.2.1.13 Haematoxylin and Eosin Staining

Slides were incubated twice in xylene for 5 mins, then twice for 2 mins in 100% ethanol, 2 mins in 70% ethanol, and then washed in distilled water. The slides were then incubated with Mayer's haematoxylin for 10 mins, followed by washing in warm tap water for 3 mins, and then in eosin for a further 10 mins. The slides were then washed sequentially in tap water, 70% ethanol, 100% ethanol, then twice in xylene for 2 mins. The sections were then mounted in DPX.

2.2.1.14 Immunohistochemical Staining

Paraffin embedded sections were initially placed in xylene for 5 mins, then into 100% ethanol for 5 mins, then rehydrated by washing in water. Endogenous peroxidase block was performed using 0.3% hydrogen peroxide for 15 mins. The slides were then washed with water, and antigen retrieval was performed by incubating overnight in 1 mM EDTA pH 8.0 with 0.1% Tween in a beaker at 65^{o}C, with stirring overnight. The following day, the beaker was cooled with running water until at room temperature. The slides were then washed with PBS for 5 mins, and then were treated with 100 µl of 2x casein block. The slides were then incubated with primary antibody at the desired concentration for 1 hour. Following this, the slides were washed with PBS-T for 5 mins, and then incubated for 30 mins with Vector ImmPRESS universal secondary antibody. Then the slides were washed with PBS-T for 5 mins, and then washed in PBS prior to visualisation by incubation with Vector ImmPACT DAB chromogen for 5 mins. The slides were then washed with water for 5 mins prior to a 1 min counterstain using Meyer's Haematoxylin. The slides were then dehydrated using sequential 5 min washes with water, 100% ethanol, and xylene, and then mounted in DPX.

2.2.2 Cell Biology

All cell biology work was performed in a Class 2 isolation hood, utilising aseptic precautions.

2.2.2.1 HUVEC Isolation and Culture

HUVEC were isolated from fresh umbilical cords acquired from the Birmingham Bio Bank following patient consent in accordance with UK ethics Approval. Cords were washed with sterile PBS to remove any residual blood or debris. 1 mg/ml Collagenase A diluted in Medium-199 was then injected into the umbilical vein at an appropriate volume to the cord size, and incubated at 37°C for 20 mins to detach the endothelial cells. The cord was then flushed with Medium-199 supplemented with 10% FCS, 10% large vessel endothelial cell growth supplement, 4 mM L-glutamine (cM199) to isolate the HUVEC. They were then seeded onto plates coated with 0.1% Type 1 porcine gelatine, and cultured in cM199. The cells were then passaged one in three when they reached confluence.

2.2.2.2 Adherent Cell Culture

All cell culture was performed at 37°C in a 5% CO_2 atmosphere. HEK 293T, CT26 and SHSY5Y cells were cultured in Dulbecco's Modified Eagle's Medium (DMEM) supplemented with 10% FCS, 4 mM L-Glutamine, 50 000 Units Penicillin and 50 000 µg Streptomycin (cDMEM), with HUVEC cultured in cM199.

2.2.2.3 Trypsinisation of Adherent Cells

Media was removed from the plate, and the cells washed with sterile PBS. For a 10 cm Plate, 1 ml of 2x Trypsin/EDTA was applied, and incubated at 37°C for 10 mins. Cells were totally detached by pipetting of the trypsin over the plate surface. 10 ml of cDMEM was used to neutralise the trypsin and place the cells into suspension. The cells were then centrifuged for 5 mins at 1100 rpm, and the cell pellet subsequently resuspended in media at a suitable volume for cell counting, or for replating.

2.2.2.4 Cell Counting

10 µl of suspended cells were added to a haemocytometer (Marienfeld-Superior, Lauda-Königshofen, Germany). The cell number per ml was calculated using the following formula: (Count from 4x4 grid)x10^4 = cell number/ml

2.2.2.5 Freezing and Thawing of Cells

Cryopreservation of cells was achieved following release of adherent cells and centrifugation at 1100 rpm for 5 mins. Cells were resuspended in filtered FCS containing 10% DMSO at 4°C. 1 ml of suspended cells were aliquoted into cryovials, which were placed into a freezing container (Thermo Scientific, Langenselbold, Germany) at room temperature, then immediately transferred to the -80°C Freezer, ensuring a cooling of 1°C per minute. The following day, the cryovials were transferred to Liquid Nitrogen storage.

Thawing of cells was conducted by transferring cryovials from liquid nitrogen storage to at circulating water bath at 37°C. The suspended cells were then transferred to a 15 ml falcon tube, and diluted with 9ml of complete media. These suspended cells were then centrifuged at 1100 rpm for 5 mins, and this process completed twice to remove the DMSO. Finally cells were resuspended in complete media and replated.

2.2.2.6 Isolation of Endothelial Cells from Human Colon

Method adapted from ‘Validation and identification of tumour endothelial markers and their uses in cancer vaccine.’ Zhuang, Xiaodong (2013) Ph.D. thesis, University of Birmingham:

Fresh specimens of both colorectal cancer and patient matched normal colonic tissue were obtained from the Queen Elizabeth Hospital Birmingham with patient consent and ethical approval (South Birmingham Local Research Ethics Council: 2003/242). Normal colonic tissue was taken from the proximal margin of the resection specimen to ensure the greatest distance from the tumour, without affecting histopathological staging. Endothelial isolation was commenced within 1 hour of the specimen being removed from the patient.

Tissues were mechanically disrupted with a scalpel, and then digested to a cell suspension in DMEM containing 2 mg/ml Collagenase Type V (Sigma, Gillingham, UK), 7.4 mg/ml of actinomycin (Sigma, Gillingham, UK), and 30 kU/ml of RNase-free DNase (Qiagen, Crawley, UK) for 90-120 mins at 37^{o}C on an agitator. 50 μl of Streptavidin-coated Dynabeads® (Invitrogen, Paisley, UK) per sample were incubated with 25 μl of 20 mg/ml of biotinylated lectin from *Ulex Europaeus* for 30 mins at 4^{o}C.

The cell suspension was then passed through a 70μm filter, the flow-through centrifuged at 1100 rpm for 5 mins, and the pellet resuspended in sterile PBS. This process was repeated a further two times. Dynabead-bound endothelial cells were then isolated by passage alongside a magnet, and suspended in 700 µl Qiazol lysis buffer (Qiagen, Crawley, UK) for subsequent RNA extraction.

2.2.2.7 Isolation of Endothelial Cells from Murine Tissue

On the day before endothelial isolation, 50 µl of Dynabeads ((Invitrogen, Paisley, UK) per sample were washed and suspended in 2 ml of 0.1% BSA. 5 µl Anti-mouse PECAM-1 antibody was then added to the Dynabeads, and the tube mixed on a rotator overnight at 4^{o}C. Following euthanasia by a Schedule 1 method, mice were submerged in 70% ethanol, and the organs dissected out, and stored in cDMEM. Each specimen was mechanically disrupted using a scalpel, and then suspended in 25 ml Type 1 Collagenase (Sigma, Gillingham, UK) 2 mg/ml 1% BSA supplemented with 1 µl 1M $CaCl_2$ and 1 µl $MgCl_2$. The sample suspension was then agitated at 37^{o}C for 60 mins, and subsequently passed through a 70 µm cell strainer into a fresh 50 ml tube. The filtrate was subsequently centrifuged at 1300 rpm for 5 mins at 4^{o}C, and the supernatant discarded. The pellet was then resuspended in 25 ml 0.1% BSA, and the centrifugation and aspiration repeated. The resulting pellet was resuspended in 1 ml 0.1% BSA, and the Dynabead-bound endothelial cells were then isolated by passage alongside a magnet, and suspended in Qiazol lysis buffer (Qiagen, Crawley, UK) for subsequent RNA extraction.

2.2.2.8 Generation of Luciferase-Transduced CT26 (CT26-Luc) Cell Line

Initially, a lentiviral supernatant was generated by lipofectamine transfection: Phoenix-ampho cells (courtesy of Gary Nolan, Stanford, USA) were cultured in high glucose DMEM. 2x10^6 cells were then seeded to each 6 cm plate in high glucose DMEM. The following day, 10 µg of MSCV-Luc (88) plasmid DNA (Clontech, California, USA) in 500 µl Optimem medium was combined with 20 µl Lipofectamine 2000 (Life Technologies, California, USA) in 500 µl Optimem to make a total of 1ml. This was incubated at room temperature for 20 mins. The medium was removed from the plated cells, and they were washed with 3 ml Optimem. This was discarded, and a further 4 ml Optimem, and the 1 ml of transfection mix were added to the plate. This was then incubated overnight at 37°C, 5% CO2. The following day, the medium was changed to 4 ml cDMEM, and the plate was then incubated at 32°C, 5% CO_2. Viral supernatant was then collected over the next five days, centrifuged at 1100 rpm for 10 mins to remove cellular debris and stored at -80°C.This was followed by transduction of CT26 Cells:

1x10^5 CT26 Cells were plated per well of a 6-well plate in cDMEM. The following day, the medium was replaced with 2 ml DMEM with 4 µg/ml polybrene, and incubated for 5 mins at room temperature. 2 ml viral supernatant supplemented with 4 µg/ml polybrene was then added to the plate and the plate centrifuged for 1 hr at room temperature at 300*g.* The medium was then replaced with 4 ml DMEM, and incubated again for two days. Following this, the cells were assayed for gene expression following puromycin selection using the *In Vivo* Imaging System (PerkinElmer, Waltham, MA, USA) (IVIS) to detect bioluminescence. Technique optimised by Joseph Wragg (Bicknell Laboratory).

2.2.2.9 Generation of Vector containing GRIN2D-Fc Fusion DNA

The insert DNA for the extracellular domain of GRIN2D was generated by IDT Technologies, and delivered in the pIDTSmart-Amp Vector. The insert was digested from the pIDTSmart vector using the *Eco*R1 and *Bam*H1 restriction sites using a double digestion technique, and ligated in a single reaction into the pIgG (pcDNA3-Fc) vector using the same sites and T4 ligase. Following ligation, heat-shock transformation of 'gold efficiency α-select' cells was performed, followed by overnight culture on ampicillin plates. Colonies were picked and grown up overnight, and then DNA extracted using the GeneJET Miniprep kit. These samples were sequence verified using GRIN2D Gene Expression Reverse primer and Forward primer to the CMV Promoter region of the PIgG plasmid. The derived construct was scaled up by maxi-prep and stored at -20^{o}C. It is referred to as the pIgG-GRIN2DVector.

2.2.2.10 Generation of Vector containing GRIN2D-GST Fusion DNA

The insert DNA for the extracellular domain of GRIN2D was digested out of the GRIN2D-PIgG vector using the *Eco*R1 and *Bam*H1 restriction sites using a double digestion, and ligated in a single reaction into the pGEX-2T vector (GE Healthcare, Life Sciences, Little Chalfont, UK) using the same sites and T4 ligase. Following ligation, heat-shock transformation of 'gold efficiency α-select' cells was performed, followed by overnight culture on ampicillin plates. Colonies were picked and grown up overnight, and then DNA extracted using the GeneJET Miniprep kit. These samples were sequence verified using the forward and reverse pGEX sequencing primers (GE Healthcare, Life Sciences, Little Chalfont, UK). The derived construct was scaled up by maxi-prep and stored at -20°C. This vector was named the pGEX2T-GRIN2D Vector.

2.2.2.11 Polyethylenimine (PEI) Transfection of HEK293T Cells

For a 15 cm plate, on the day before transfection $6x10^6$ HEK293T cells were plated out in 20 ml cDMEM. The following day, 18 µg of DNA was combined with 2 ml of Optimem serum-free media, and mixed by flicking of the tube. 72 µg of PEI was then added and briefly vortexed at low speed to mix, followed by a 10 min incubation at room temperature. The mixture was then gently added to the HEK293T cells and mixed by north/south east/west movements.

2.2.2.12 – siRNA Knockdown of Novel TEMs in HUVEC

$1.75x10^5$ HUVEC at passage 3 were plated into each well of a 6-well plate coated in 0.1% gelatine. These cells were incubated overnight at 37°C. A mix of 2.5 µl of 20 µM siRNA duplex and 167.5 µl Optimem (final duplex concentration of 50 nM), and a mix of 3 µl RNAiMAX lipofectamine and 27 µl Optimem were incubated at room temperature for 10 mins. 30 µl of lipofectamine mix was added to the duplex mix, flicked to combine, and incubated at RT for 10 mins. The seeded cells were then washed twice with PBS, and 800 µl of Optimem was added. Then 200 µl of lipofectamine/duplex mix was added to the cells, and incubated at 37°C for 4 hrs. At this stage, the media was aspirated off, and replaced with cM199 without antibiotics. The following day, the cells were harvested and assays performed.

2.2.2.13 – Scratch Wound Assay

$3x10^5$ HUVEC were plated into each well of a 6-well plate and cultured in cDMEM at 37^oC. Once the cells were confluent, a P200 pipette tip was used to make three parallel scratches both vertically and horizontally, resulting in 9 intersections. The plate was then washed twice with PBS to remove any floating cells. Images were taken at 0 hrs, 6-8 hrs and 16-24 hrs to measure wound closure.

2.2.2.14 – Matrigel Tube Forming Assay

A 1 ml aliquot of Matrigel was retrieved from the -80^oC freezer, and allowed to defrost overnight in the cold room at 4^oC and on ice. The following day, the wells of a 12-well plate were moistened with PBS, which was then removed to leave a thin film within the well. 70 µl of Matrigel was added to each well, and then allowed to solidify at 37^oC for 30 mins. $1.4x10^5$ cells were added to each well in 1 ml cM199. The assay was incubated for 16-24 hrs, and then images acquired to measure tube number, length and branching.

2.2.2.15 – Transwell Filter Assay (Modified Boyden Chamber Assay)

700 µl of 0.1% gelatine was added to each well of a 24-well plate, and then a cell permeable membrane was placed into the well, followed by a further 200 µl of gelatine. This was incubated at 37^oC for 10 mins, then aspirated off. 700 µl of cM199 was added to the bottom of the well, with $3x10^4$ HUVEC in low-serum M199 (1% FCS & no brain extract) placed on top of the filter. The assay was then incubated for 16-24 hrs.

Following incubation, the media was removed, and the wells washed with 700/200 µl of PBS. The PBS was then removed and replaced with equivalent volumes of fixing solution containing 2% Formaldehyde in PBS + 2 µg/ml bisbenzamide for 15 mins. The fixing solution was then removed and the wells and filters washed with PBS.

To mount the filter, initially a drop of PBS was placed onto a slide, and then the filter was placed on top of this. A scalpel was used to excise the filter from its mounting, and the excess PBS wiped away. A drop of Shandon Immu-Mount(TM was added to the filter, and a coverslip applied. The slides were then stored in the dark at 4^{o}C until ready to be imaged. To quantify this assay, the slide was visualised at 20x magnification, and counts made of those cells atop and below the filter by adjustment of the focus. These scores from 5-10 sites on the slide were averaged, and the figures used to quantify percentage transmigration.

2.2.2.16 – Acumen

On Day 2 following siRNA knockdown, media was removed and cells fixed using 100 µl 100% ethanol at -20^{o}C. The cells were then washed with PBS and incubated with RNase in PBS (0.2 mg/mL, DNase free) for 4 hrs at room temperature. Subsequently, nuclei were stained with propidium iodide (3 µM) for 15 mins at room temperature. The plate was scanned on an Acumen Explorer fluorescence microplate cytometer (TTP LabTech, Royston, Herts, UK), (Nagy Laboratory, Birmingham UK).

2.2.2.17 – Cytospin

A suspension of $5x10^5$ cells/ml was made. 200 µl of this cell suspension was then loaded into the cytospin cuvette, above blotting paper and a cytospin slide. The cells were then centrifuged at 800 rpm for 3 mins with a Cytospin 3 machine (Shandon, Loughborough, UK). The blotting paper and cuvette were carefully removed, and the slide air-dried. Cells were then fixed by immersion in 50% Ethanol / 50% Acetone for 10 mins. Following this, they were stored at room temperature until further assays were performed.

2.2.3 Protein Analysis

2.2.3.1 Protein Quantification

Protein was quantified either by using the Protein A280 protocol on the NanoDrop machine, or by utilisation of the Pierce™ BCA™ Protein Assay Kit (Thermoscientific, Wilmington, DE, USA). This latter method was used when low protein concentrations were expected, or particularly accurate readings were necessary. The nanodrop spectrophotometer was used for more approximate readings.

2.2.3.2 Western Blotting

Cell lysates were prepared using RIPA buffer. Protein samples were mixed with 4x SDS Loading buffer in an appropriate volume, and denatured by boiling for 3 mins. Samples were loaded onto an SDS-Polyacrylamide Gel for electrophoresis (SDS-PAGE). Electrophoresis was performed in running buffer at 200V with time dependent on gel concentration and expected band size. The gel was then blotted onto a polyvinylidene fluoride (PVDF) membrane in transfer buffer at 30V for 120 mins at 4^{o}C. The membrane was blocked for 60 mins at RT with 10% milk in wash buffer (PBS with 0.05% Tween-20). Following blocking, the membrane was washed (4x 5 min) in wash buffer, then incubated with primary antibody in wash buffer with 3% BSA for 60 mins at RT. Following further washes, horseradish peroxidase (HRP)-conjugated secondary antibody with a 1 in 10 000 dilution in blocking buffer was applied for 60 mins at RT.

Following antibody staining, the membrane was washed further and 500 µl of enhanced chemiluminescent western blotting detection agent was added for 3 mins. A piece of photographic film was then exposed to the membrane for different lengths of time dependent on the luminescence of the HRP.

2.2.3.3 Coomassie Brilliant Blue Staining

Following SDS-PAGE, when non-specific protein identification was required, overnight staining in Coomassie brilliant blue at RT was utilised. The gel was then washed in dH_20 to remove non-specific binding and visualised using a yellow filter and the BIO Imaging System Machine.

2.2.3.4 Enzyme-Linked Immunosorbent Assays (ELISA)

A Nunc Maxi-Sorp™ ELISA plate (eBioscience, Hatfield, UK) was coated with 100 µl of 2 µg/ml of GRIN2D-GST or Fc protein, and incubated overnight at 4^oC. The plate was blocked using 200 µl 3% BSA in PBS-T for at least 2 hrs. The plate was then washed 5 times with 100 µl PBS-T, and then 5 µl of serum in 45 µl PBS was incubated overnight in each well at 4^oC. The following day, the serum was removed, and the plate washed 5 times. For antibody isotyping, 100 µl of primary antibodies at 1 in 500 were incubated for 90 mins. The plate was then washed 5 times. Peroxidase-conjugated anti-mouse IgG antibody (1 in 5000) was then applied as a secondary for 90 mins. The plate was incubated for 15 mins in detection solution (10 mg o-phenylenediamine dihydrochloride (OPD) in sodium perborate/phosphate citrate buffer), and then quenched with 50 µl 3M HCl. Imaging was performed using a plate reader at 490 nm.

2.2.4 Protein Production

2.2.4.1 Production and Purification of GRIN2D-Fc fusion protein

Following PEI transfection of twenty 15 cm tissue culture plates, cells were grown in cDMEM until near confluence. Then the media was replaced with Optimem serum-free media, and the media collected and refreshed every two to three days for up to 21 days, giving a total conditioned media volume of 3-5 litres. 1 mM EDTA and a few phenylmethylsulfonyl fluoride (PMSF) crystals were added to the collected media to inhibit any contaminant proteases present.

A HiTrap Protein-A column (GE Healthcare, Life Sciences, Little Chalfont, UK) was flushed with filtered 20% ethanol, and pH equilibrated using monosodium phosphate (NaH_2PO_4) at pH 7.0. Conditioned media was run through the column at 1 ml/min at 4^oC followed by a further 30 ml wash with NaH_2PO_4 to remove non-specific protein. The protein was eluted using sodium citrate 100 mM pH 3.0 in 500 µl fractions and immediately pH neutralised using 110 µl 1M Tris-HCl pH 9.5. Fractions were analysed for the presence of protein, and those with a significant eluate pooled. Final protein concentration was measured by BCA Protein assay, after which the protein was sterile filtered and stored at 4^oC.

2.2.4.3 Production and Purification of GRIN2d-GST fusion protein

50 µl BL21 *E.coli* were transformed as previously described using the pGEX-2T-GRIN2D Vector. Overnight cultures of transformant colonies underwent DNA extraction using the mini-prep protocol, and were then sequence verified. Stock

cultures were made by dilution of 10 ml overnight culture in 10 ml of LB Broth with 10% glycerol, aliquoted to 1 ml, and stored at -80^{o}C.

For large-scale protein expression, 1 ml of stock culture was diluted in LB Broth with 100 µg/ml ampicillin, and incubated overnight while shaking at 37^{o}C. The following day, 25 ml of this overnight culture was inoculated into 500 ml LB broth with ampicillin, and again incubated at 37^{o}C while agitating for 120 mins to achieve an OD_{600} of 0.6, indicating the bacteria were in the log growth phase. At this stage, Isopropyl β-D-1-thiogalactopyranoside (IPTG) at 1 mM concentration was added to induce protein expression. The cells were then incubated for 4 hrs at 37^{o}C. Following incubation, the cells were centrifuged at 5 500 rpm at 4^{o}C for 15 mins. Bacterial pellets were then washed in *E.coli* lysis buffer and stored at -80^{o}C.

Pellets were thawed on ice, and resuspended in 2 ml E.coli Lysis Buffer per 100 ml of original bacterial culture. The sample was then sonicated at 10W for 4 mins on ice (20s on, then 10s off to prevent warming of sample. 100x Triton was the added to the sample to a final concentration of 1%, and the sample vortexed, then incubated on ice for 30 mins. The sample was then divided into 1ml aliquots and centrifuged at 14 000 rpm at 4^{o}C for 15 mins. The supernatant was then pooled.

Glutathione sepharose beads (Sigma, Gillingham, UK) were washed three times in *E.coli* lysis buffer, and then combined with the pooled bacterial lysate. 1 ml of beads was used for 2 litres of bacterial culture. This was incubated on a wheel at 20 rpm at RT for 2 hrs. Following incubation, the beads were washed twice with 20 ml wash buffer. The GST-fusion protein was then either eluted off the beads or on-bead thrombin digestion was performed. For elution, the beads were incubated with 1 ml of elution buffer, containing 30 mM reduced glutathione, for 30 mins at room temperature. A second elution was performed to ensure complete protein retrieval.

2.2.4.4 Buffer exchange

Following elution of GRIN2D-GST, buffer exchange was performed using at PD10 Desalting Column (GE Healthcare, Life Sciences, Little Chalfont, UK). Briefly, the column was equilibrated by washing with 25 ml of the collection buffer of choice, and the flow-through discarded. 2.5 ml of sample was added, and the flow-through discarded. Then a further 3.5 ml of collection buffer was added, and the eluate collected.

2.2.4.6 Size Exclusion Chromatography (SEC)

Protein samples that required purification underwent SEC using a HiLoad 16/600 Superdex 200 PG column (GE Healthcare, Little Chalfont, UK), with an AKTA Fast Protein Liquid Chromatography (FPLC) machine (Bio-Rad Healthcare, GE, Little Chalfont UK). Briefly, the column was washed with 2 column volumes of an appropriate FPLC Buffer. The sample was then loaded at room temperature, and passed through the column at 3 ml/min. 5 ml fractions were collected, and the fractions analysed by SDS-PAGE prior to pooling and concentrating with a VivaSpin Column (eBioscience, Hatfield, UK) to a useable concentration.

2.2.5 Animal Models

2.2.5.1 Home Office Licence Training

In order to undertake scientific procedures on animals, Home Office training for a personal license under the Animal (Scientific Procedures) Act 1986 was undertaken and successfully completed. The personal license number 70/25131 was gained, and subsequently transferred to the electronic license system, with the designation I350D34BB.

All work was carried out under the Project License 40/3339 held by Roy Bicknell.

2.2.5.2 Murine Subcutaneous Colorectal Cancer Model

Balb/c mice were anaesthetised using inhaled Isofluorane, and following confirmation of depth of anaesthesia with a toe pinch, the left flank was shaved. Anaesthesia was maintained using a facemask. $1x10^5$ Luciferase-transduced CT26 (CT26-Luc) colorectal cancer cells were injected into the left flank of each mouse. A one-week tumour establishment period was allowed, following which regular tumour calliper measurement was performed. This was combined with intraperitoneal injection of 200 μl of 15 mg/ml D-Luciferin in PBS, and tumour growth measurement using the intravital imaging system (IVIS).

2.2.5.3 Murine Subcutaneous Sponge Model

Buprenorphine was administered 1 hour prior to surgery. NSAIDs were avoided due to potential confounding effects on angiogenesis. Balb/c mice were anaesthetised using inhaled Isofluorane, and following confirmation of depth of anaesthesia with a toe pinch, both flanks were shaved. The skin was cleansed with ethanol. A small incision was made in the flank and a subcutaneous pocket created by blunt dissection. A 0.5 x 1.0 cm cylindrical sponge was inserted into the sub-cutaneous pocket and the skin closed using 6/0 absorbable subcuticular sutures. This was then repeated for the other flank. Over the next 14 days, 100 µl of 20 ng/ml bFGF was injected into the sponge a total of 7 times, with a minimum of 12 hrs between injections. Animals were culled by a schedule 1 method, and the sponges fixed in 4% formalin prior to histological analysis.

2.2.5.4 Murine Vaccination Model

Balb/c mice were anaesthetised using inhaled Isofluorane, and following confirmation of depth of anaesthesia with a toe pinch, 100µl Freund's Complete Adjuvant was injected subcutaneously with 50µg of either treatment or control protein. After 14 days, 100µl Freund's Incomplete Adjuvant was injected subcutaneously with 50µg of either treatment or control protein to boost the host antibody response. Tail vein bleeds were performed at days 0, 14 and 28, with antibody response quantified by ELISA.

2.2.5.6 Colonic Tissue Acquisition and Ethical Considerations

The acquisition of colorectal cancer and normal colon tissue was approved by the South Birmingham Local Research Ethics Committee, with the approval number 2003/242.

Informed consent for acquisition of tissue was taken from patients by one of three researchers (Henry Ferguson, Steven Ward, Elizabeth Hepburn), using both the University Hospitals Birmingham NHS Trust's formal consent form, and the approved University of Birmingham consent form.

Following surgical resection, the named researchers entered theatre with permission, and retrieved the resection specimen. This was then transported to the Department of Histopathology, where it was sectioned for histological diagnosis by a Consultant histopathologist. Only remnants of the resection specimen not necessary for patient care or diagnosis were then taken for further processing.

The patient information that was collected for the purpose of this research was limited to name, gender, date of birth and hospital number, alongside a diagnosis of a colorectal malignancy. These details were stored on the patient consent form only, in a secured, locked filing cabinet in a non-public secured office within the Institute for Biomedical Research at the University of Birmingham. All samples were subsequently anonymised, and no patient identifiable data was released or used within any analysis, nor will it be included in any publications or presentations of this work in an academic or public forum.

2.2.6 Bioinformatic Websites

Universal ProbeLibrary Assay Design Centre:

https://www.roche-applied-science.com

NCBI:

http://ncbi.nlm.nih.gov/

TMHMM Server v2.0 (Transmembrane Region Prediction):

http://www.cbs.dtu.dk/services/TMHMM

Clustal Omega Genome Sequence Alignment Tool:

http://www.ebi.ac.uk/Tools/msa/clustalw2/

Protease cutting site prediction:

web.expasy.org/peptide_cutter

Protein Secondary Structure Prediction:

http://bioinf.cs.ucl.ac.uk/psipred and http://swissmodel.expasy.org/

Vector Insert Ratio Calculator

http://www.insilico.uni-duesseldorf.de/Lig_Input.html

Statistical Testing:

http://vassarstats.net/

2.2.7 Statistical Methods

A minimum 95% confidence interval was used in all statistical tests. All error bars depict standard error of the mean (SEM). Non-parametric data distributions were assumed in all analyses. Mann-Whitney U Tests were used to compare two groups, with ANOVA tests used to compare multiple groups.

p-value	Depiction
<0.001	***
To 0.01	**
0.01 to 0.05	*
>0.05	Non-Significant (ns)

CHAPTER THREE

IDENTIFICATION AND VALIDATION OF NOVEL TUMOUR ENDOTHELIAL MARKERS IN COLORECTAL CANCER

3.1 IDENTIFICATION OF NOVEL TEMs IN COLORECTAL CANCER

This chapter describes the process of the identification of GRIN2D as a putative endothelial target in CRC from an initial list of candidates provided by microarray analysis of gene expression, through RTqPCR analysis of multiple biological replicates, and finally confirmation of endothelial expression through immunohistochemistry. Later, the *in vitro* effects of knockdown of the genetic expression of GRIN2D in HUVEC are described, focussing on its effects on angiogenesis.

3.1.1 – Isolation of Endothelial Cells from Fresh Colorectal Resection Specimens

In order to maintain the RNA expression profile of the specimens, fresh colorectal resection specimens were obtained in person from the operating theatres at the Queen Elizabeth Hospital in Birmingham, and transferred to the histopathology department of the same hospital. Here, an available consultant histopathologist cut small sections of the specimen from both the malignant lesion, and from non-diseased proximal colon, away from areas needed for clinical diagnosis or prognostication. The sections were then processed within 2 hrs of resection, as described in Section 2.2.2.6. RNA was extracted, and assessed for integrity using the Agilent Bioanalyzer 2100 (by Steve Kissane, Birmingham University, UK). Those paired samples with an RNA integrity number (RIN) of greater than 7.0 were taken forward. The RIN is a validated method for estimation of RNA integrity, which has been shown to reliably predict, quantify the quality of extracted RNA(89). Essentially, it measures the number of RNA fragments present, and their size by means for laser induced fluorescence, and is an integral function of the Agilent Bioanalyzer 2100.

Endothelial enrichment was confirmed by RTqPCR quantification of the expression of platelet endothelial cell adhesion molecule (PECAM-1 or CD31) when normalised to the consistently expressed, ‘housekeeper’ molecule beta-actin. PECAM is a highly endothelial-specific protein(90), and can hence be used to quantify enrichment of endothelial cells within a sample. Relative expression was calculated using the $2^{-\Delta\Delta CT}$ method, a validated mode of analysis for this purpose(91). PCR analyses were performed in triplicate for each sample to eliminate internal experimental error, and repeated using multiple biological replicates.

3.1.2 – Microarray Identification of Gene Candidates (Performed by Joseph Wragg)

Differential gene expression profiles between four colorectal cancer specimens, and patient-matched normal colon was performed using an Agilent™ Microarray. Briefly, the extracted RNA from fresh colorectal samples was confirmed as having an RIN>7, and then utilised to generate complimentary DNA. This cDNA was used to generate complementary RNA, which was then fluorescently labelled with the cyanine dye Cy3. This cRNA was hybridised onto the microarray chip (Steve Kissane, Birmingham University, UK), and then imaged.

The resultant data gave absolute gene expression values across the human genome in triplicate (3x20 000 genes per sample). Those genes that were predicted to code for transmembrane proteins, and were greater than five times upregulated consistently across the multiple biological replicates used for the microarray were taken forward as potentially targetable endothelial proteins. This gave 28 potential candidates:

EGFL6	THBS2	HSD11B1	TRIB3
IL6	NOTCH3	PLXDC1	GJA4
GRIN2D	PDGFRB	FZD10	VASN
WNT2	LOC541471	LILRB4	IL13RA2
FCGR3A	P2RY6	LINGO1	PGF
LZTS1	KCNJ8	SLAMF8	RGS16
MARCO	OR51E1	GJA4	ADAP2

Table 2 – Transmembrane Gene Candidates from Microarray Analysis of CRC versus Patient-Matched Normal Colon.

3.1.3 – Narrowing the Shortlist

From this long-list, extensive literature and bioinformatic review was undertaken to reduce the shortlist. Those genes that were previously published as tumour endothelial markers, or were under study or patent with another institution were excluded from further work. Preference was given to those genes encoding known endothelial proteins, or those with published links to the vasculature or carcinogenesis. All gene-coding details were taken from GeneCards (www.genecards.org), as was all data on protein function and associated pathology unless otherwise referenced.

Candidate Gene	**Existing Evidence**	**Take Forward?**
EGFL6	• Codes for a member of the epidermal growth factor superfamily • Previously identified in ovarian cancer endothelial cells(92) • Widespread expression outside the colon(93) • Likely to be a secreted protein rather than transmembrane(94,95)	No
THSB2	• Codes for Thrombospondin-2 • Well known to be a potent inhibitor of tumour growth(96) and angiogenesis(97)	No
HSD11B1	• Codes for the microsomal enzyme Hydroxysteroid (11-Beta) Dehydrogenase 1 • Not transmembrane.	No
TRIB3	• Codes for Tribbles Pseudokinase 3, a negative regulator of NF-kappB, which sensitizes cells to TNF- and TRAIL-induced cellular apoptosis. • Has been previously implicated and studied as a biomarker for CRC prognosis(98), and in breast cancer(99).	No
IL6	• Codes for interleukin 6. • Widespread mediator of fever and acute phase response. • Well known to have systemic high levels in malignancies, including CRC(100).	No
NOTCH3	• Codes for a protein which has a role in intercellular communication, particularly in neuronal development • Previously implicated in CRC as a nuclear protein(101).	No

PLXDC1	• Codes for plexin domain containing 1 protein • Known to be found as endothelial marker in glioblastomas(102). • One of the original TEMs, TEM7(53).	No
GRIN2D	• Codes for the NMDA Receptor Subunit 2D • Has been raised as a non-endothelial candidate in Breast Cancer(103). • Upregulated in tumour cell lines in vitro(66)	Yes
PDGFRB	• Codes for Platelet Derived Growth Factor Receptor Beta • PDGF Very well known to be tumour endothelium associated, so disregarded.	No
FZD10	• Codes for Frizzled Receptor 10 • Previously implicated in CRC(104)	No
GJA4	• Codes for Connexin-37, a gap junction protein • Implicated in tumour cell proliferation(105).	Yes
WNT2	• Codes for the wingless-type MMTV integration site family member 2 • WNT pathway well known in carcinogenesis(106).	No
LOC541471	• Predicted non-coding locus on chromosome 2 • No literature •	Yes
LILRB4	• Codes for a member of the leukocyte immunoglobulin-like receptor family • Role identified in gastric cancer(107). • Appears to suppress host immune response to a tumour(108).	Yes
VASN	• Codes for Vasorin • Known endothelial protein linked to the arterial response to injury(109). • No literature on malignancy	Yes

FCGR3A	• Codes for the Fc fragment of IgG receptor, low affinity IIIa, (CD16a) • Trials of the monoclonal antibody ofatumumab in patients with metastatic CRC, has shown response to be predicted by FCGR3A genotype expression(110).	No
P2RY6	• Codes for a G-protein coupled nucleotide receptor • Considered important in bone development, and implicated in the pathogenesis of osteosarcomas(111).	Yes
LINGO1	• Codes for the Leucine-Rich Repeat And Immunoglobulin Domain-Containing Protein 1 • Role in axonal regeneration • Implicated in Parkinson's disease	No
IL13RA2	• Codes for the IL13 Receptor A2 • Function in internalisation of IL13 • Linked with pathogenesis of adrenocortical tumours	Yes
LZTS1	• Codes for the leucine zipper, also known as putative tumour suppressor 1. • Implicated in multiple tumour types(112) • Ubiquitously expressed in normal tissues(112)	No
KCNJ8	• Codes for a G-protein controlled Potassium Channel subunit. • Linked to cardiac arrhythmias and hypotension(113).	Yes
SLAMF8	• Codes for a member of the CD2 family of cell surface proteins • Involved in lymphocyte activation	No

PGF	• Codes for placental growth factor • Also known as VEGF-related protein. • Well known to promote tumour growth, including in colorectal cancer(114).	No
MARCO	• Codes for a receptor for bacteria on macrophages. • Not endothelially associated	No
OR51E1	• Codes for an olfactory receptor. • Potential marker of small bowel neuroendocrine tumours(115). • Also implicated in prostate cancer(116).	Yes
RGS16	• Codes for Regulator of G-Protein Signalling 16 • Previously implicated in pancreatic cancer(117).	Yes
ADAP2	• Codes for ArfGAP with dual PH domains 2 • Associated with an increased risk of malignancy in neurofibromatosis(118).	Yes

Table 3 – Summary of the Literature Review of Candidate TEMs in CRC.

3.2 VALIDATION OF NOVEL TEMs IN COLORECTAL CANCER

Having refined the long-list of 28 candidate genes to a manageable list of 10 candidates, the FASTA nucleotide sequences were submitted to the Roche primer design service, and forward and reverse primer sequences obtained, with a corresponding Universal ProbeLibrary Probe for ongoing real-time quantitative PCR (RTqPCR) validation in further biological replicates. One target, IL13RA2, was excluded at this stage, as no primers could be designed, leaving a final short-list of nine:

LOC541471	KCNJ8	VASN
P2RY6	OR51E1	ADAP2
GRIN2D	GJA4	RGS16

Table 4 – Gene Candidates Taken Forward for Further Study

Following RTqPCR, those targets with sufficiently consistent expression on the RNA level were submitted to immunohistochemical analysis on paraffin embedded sections of colorectal cancer and normal colon.

3.2.1 – Real-time Quantitative PCR Validation of Gene Shortlist

The method of real-time quantitative PCR was originally described in 1996 by Heid et al(119). It developed as a modification of the earlier methods of quantitative gene analysis(120), and reverse-transcriptase PCR(121). Early incarnations of the method used quantitation resulting from Sybr Green DNA dye concentrations on agarose gel, but the modified method utilising a TaqMan probe-based system has been shown to be preferable both in terms of sensitivity and accuracy(122). The method relies upon an engineered probe which recognises a specific region within the DNA sequence, as described by the method of Higuchi et al.(123). The probe has both a fluorophore (or reporter) at the 5’ end and a quencher compound at the 3’ end, which prevents the emission of light by the fluorophore. However, when the gene sequence is present, the probe anneals downstream from one of the primer sites and is cleaved by the 5´-nuclease activity of Taq DNA polymerase. The cleavage of the probe liberates the fluorophore into solution. This occurs in a directly proportional concentration to that of the original DNA in the sample, where it can then be measured and quantified (Figure 3.1).

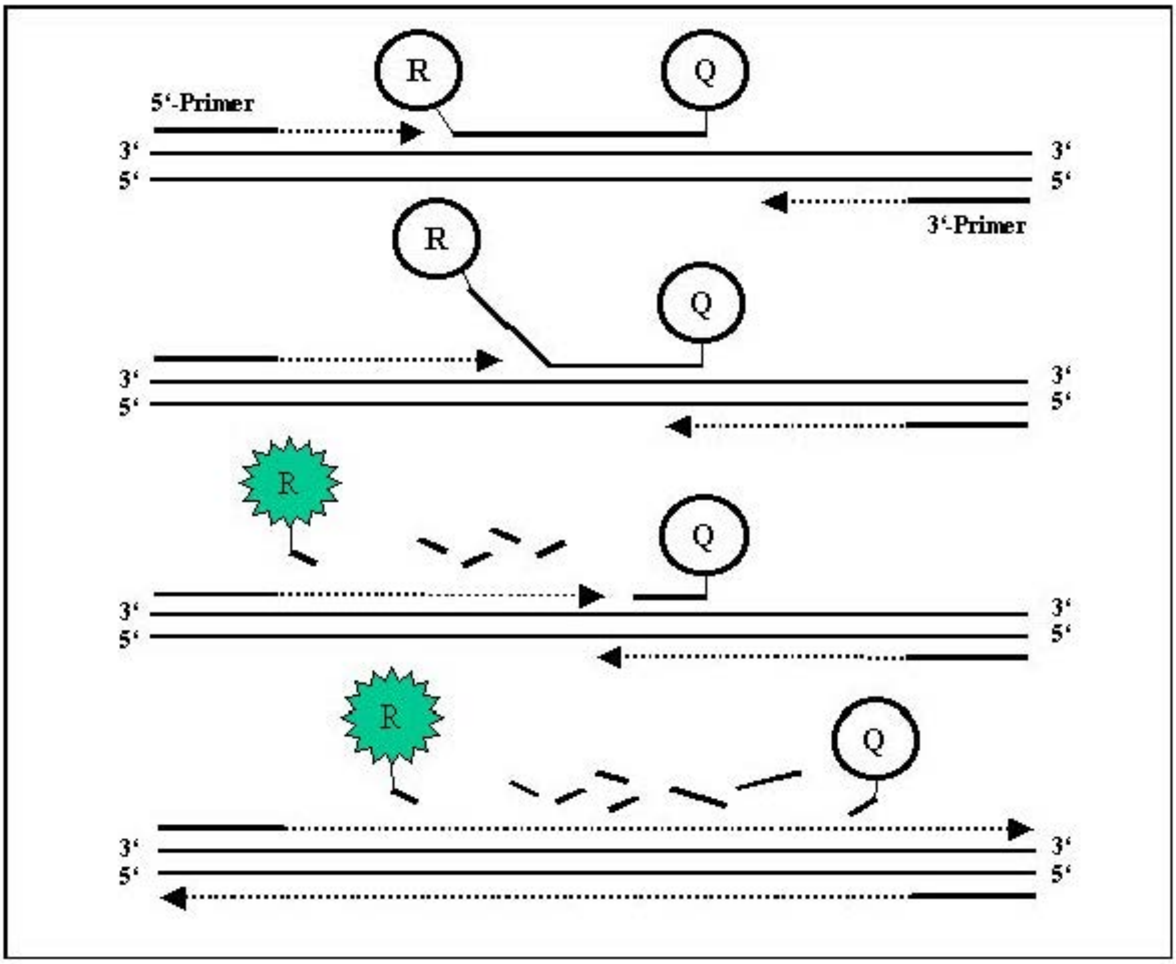
R
Q
5'-Primer
3'
5'
3'
5'
3'-Primer
R
Q
3'
5'
3'
5'
R
Q
3'
5'
3'
5'
R
Q
3'
5'
3'
5'

Figure 3.1 – The Mechanism of RTqPCR. The liberation of the reporter ('R') into solution is detected and quantified in proportion to the gene expression in the sample. Taken with permission from http://edoc.hu-berlin.de/dissertationen/kuner-ruprecht-2002-07-02/HTML/Kuner-ch2.html

In order to further narrow the short list, RTqPCR was performed in a further biological replicate as described in section 2.2.1.4. On the basis of these results, only those candidates with confirmed expression greater than two-fold were taken forward.

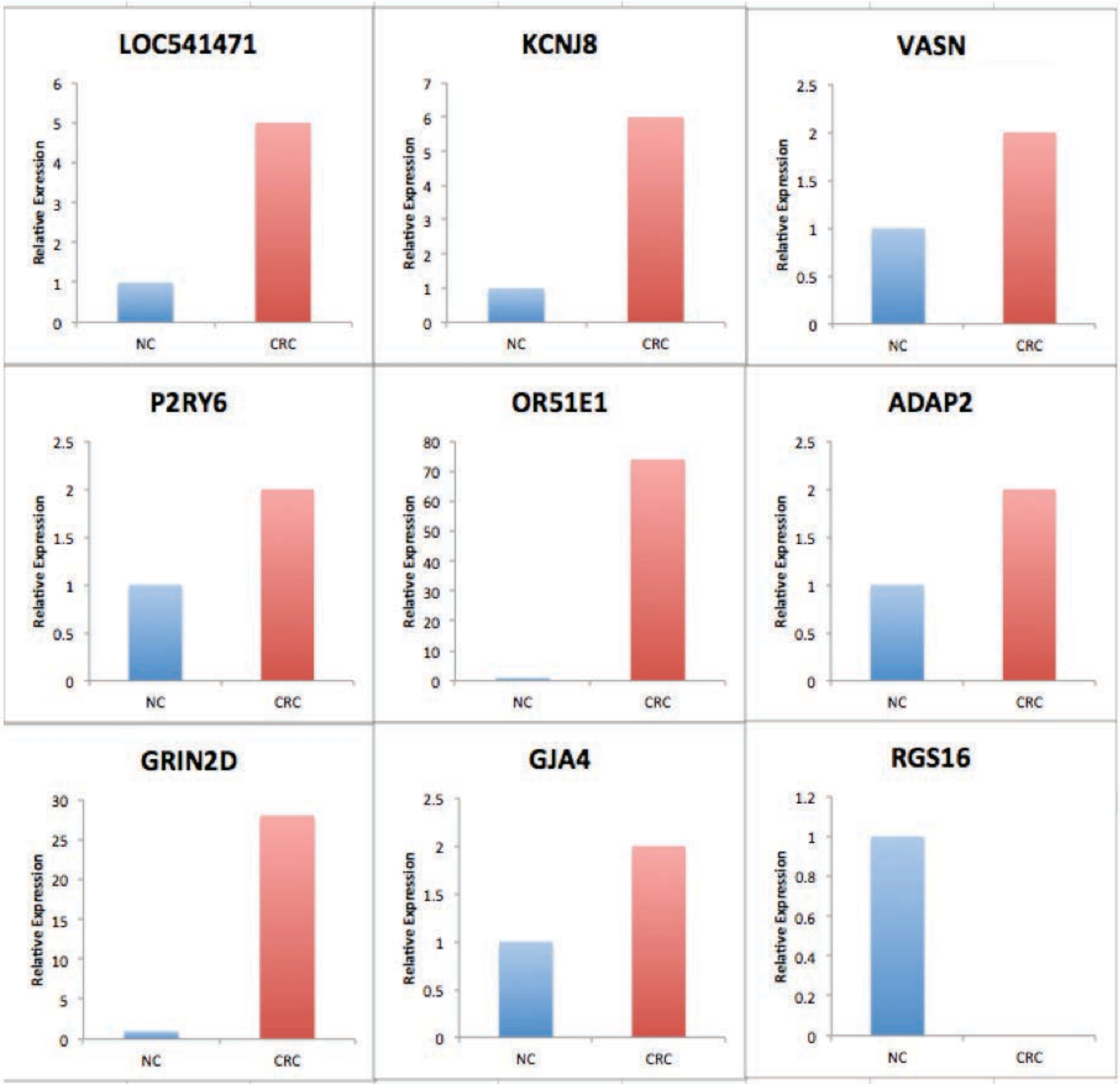

Figure 3.2 – Quantitative analysis of the relative expression of candidate genes between patient-matched Colorectal Cancer (CRC) and Normal Colon (NC). Normalised to Beta Actin.

This led to the shortlist being narrowed to include LOC541471, GRIN2D, OR51E1 and KCNJ8. Further RTqPCR analysis was undertaken in five further paired biological replicates:

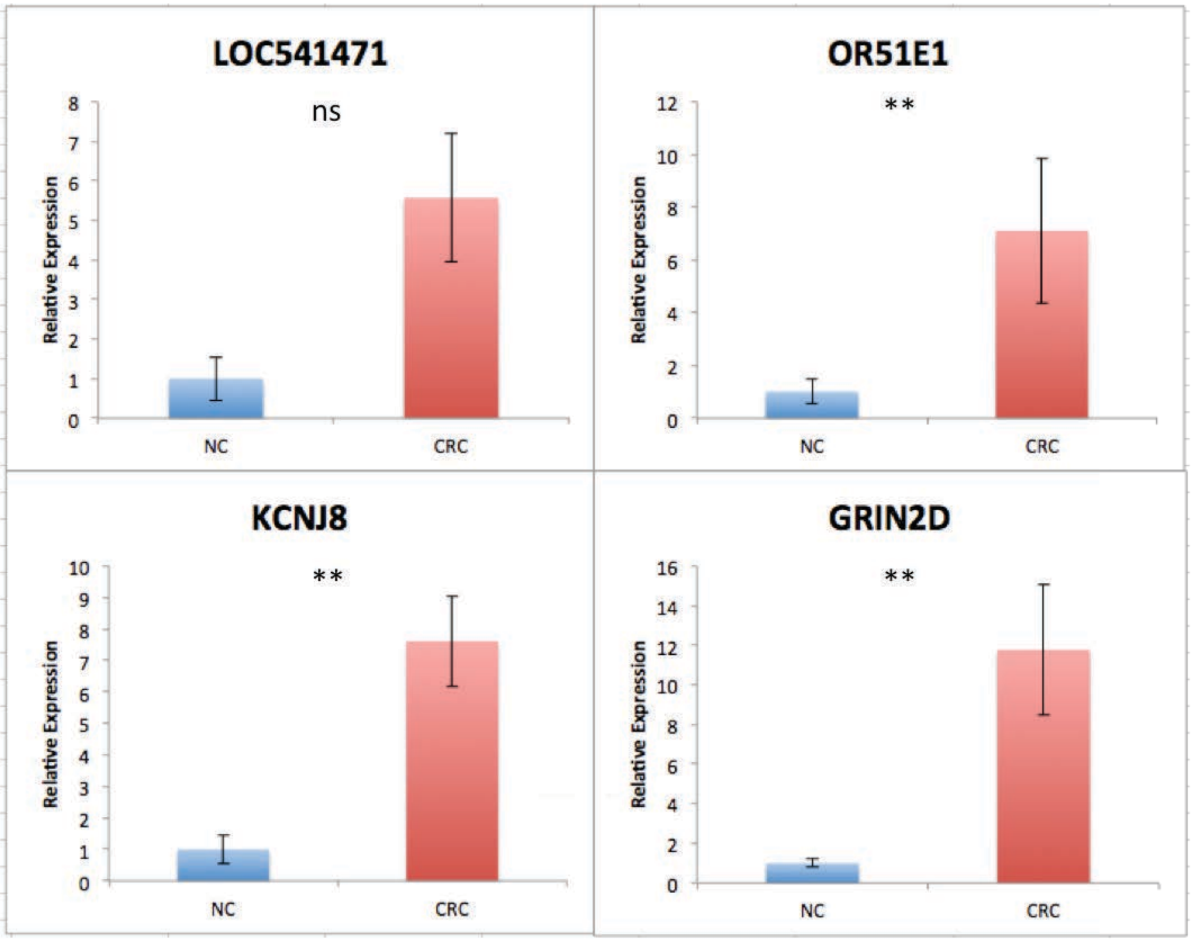

Figure 3.3 – Candidate Expression in Further Biological Replicates. Normalised to Beta Actin. (n=5).

While OR51E1, KCNJ8 and GRIN2D looked promising at this stage, there had been no adjustment for the degree of endothelial enrichment between the samples. Therefore further RTqPCR was performed with normalisation against beta actin for cell number, but also against PECAM to adjust for endothelial cell enrichment:

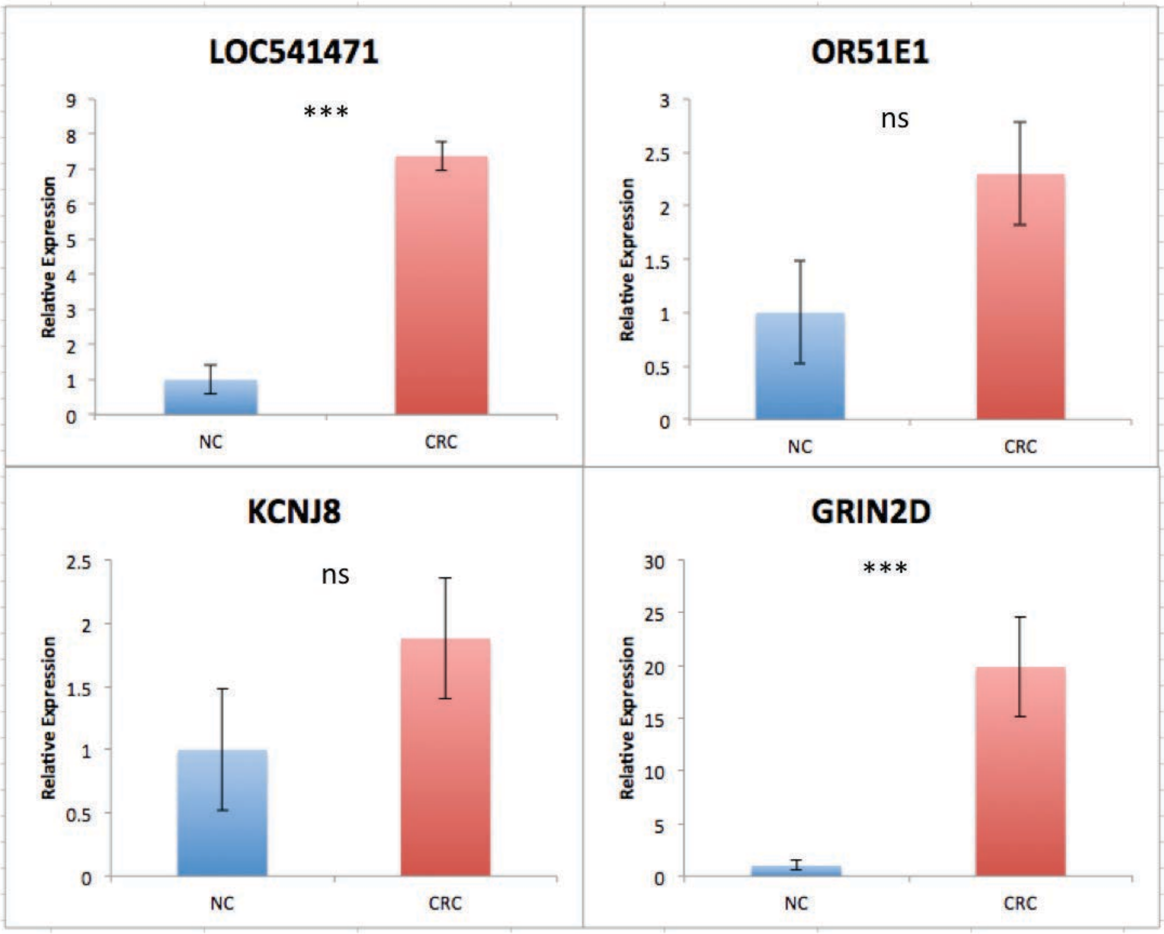

Figure 3.4 – Endothelial Candidate Expression. Normalised to PECAM. All statistical significance measured by Mann Whitney.

As can be seen from Figure 3.3, the promising raw expression levels of both OR51E1 and KCNJ8 were negated by adjustment for endothelial enrichment. However, expression levels of LOC541471 (p=0.006) and GRIN2D (p<0.0001) were confirmed as statistically upregulated in CRC compared to patient-matched normal colon.

3.2.2 – Immunohistochemical Validation

While RTqPCR offers validation on an RNA level for the differential expression, this does not always translate into expression on a protein level(124). The process of immunohistochemistry (IHC) depends upon the specific interaction of an antibody and an antigen within a histological tissue section. Successful IHC depends upon two factors – the presence of the protein of interest within the tissue section, and an antibody that is highly specific to the target of interest. Two commercially available monoclonal antibodies were used for validation by IHC and Western blot. They were termed the 43 and 48 antibodies based upon catalogue number. However, both blots and IHC were unsatisfactory, with non-specific binding present using both methods. While neither antibody was specific enough to conclusively validate the presence of GRIN2D on endothelial cells, staining with the GRIN2D 48 antibody did suggest an endothelial pattern, alongside the non-specific staining. It was therefore concluded that endothelial expression was possible. Once a human GRIN2D-GST construct had been generated (as explained in Chapter 4), Protein was sent to Eurogentec for custom polyclonal serum generation in rabbits. This polyclonal serum was then utilised as a primary antibody in immunohistochemistry. It positively stained in HEK293T cells transfected to express GRIN2D-Fc (as described in Chapter 4), and also exhibited an endothelial expression pattern within paraffin embedded sections of colorectal cancer, but not in its matched controls (Figure 3.5). Unfortunately, within the time constraints of this project, the IHC process could not be optimised to gain better images than those presented, but this work has been subsequently completed within the group.

On the basis of these preliminary results obtained in histological sections of colorectal cancer (NHS, Birmingham, UK), GRIN2D was taken forward as a potential endothelial target in colorectal cancer.

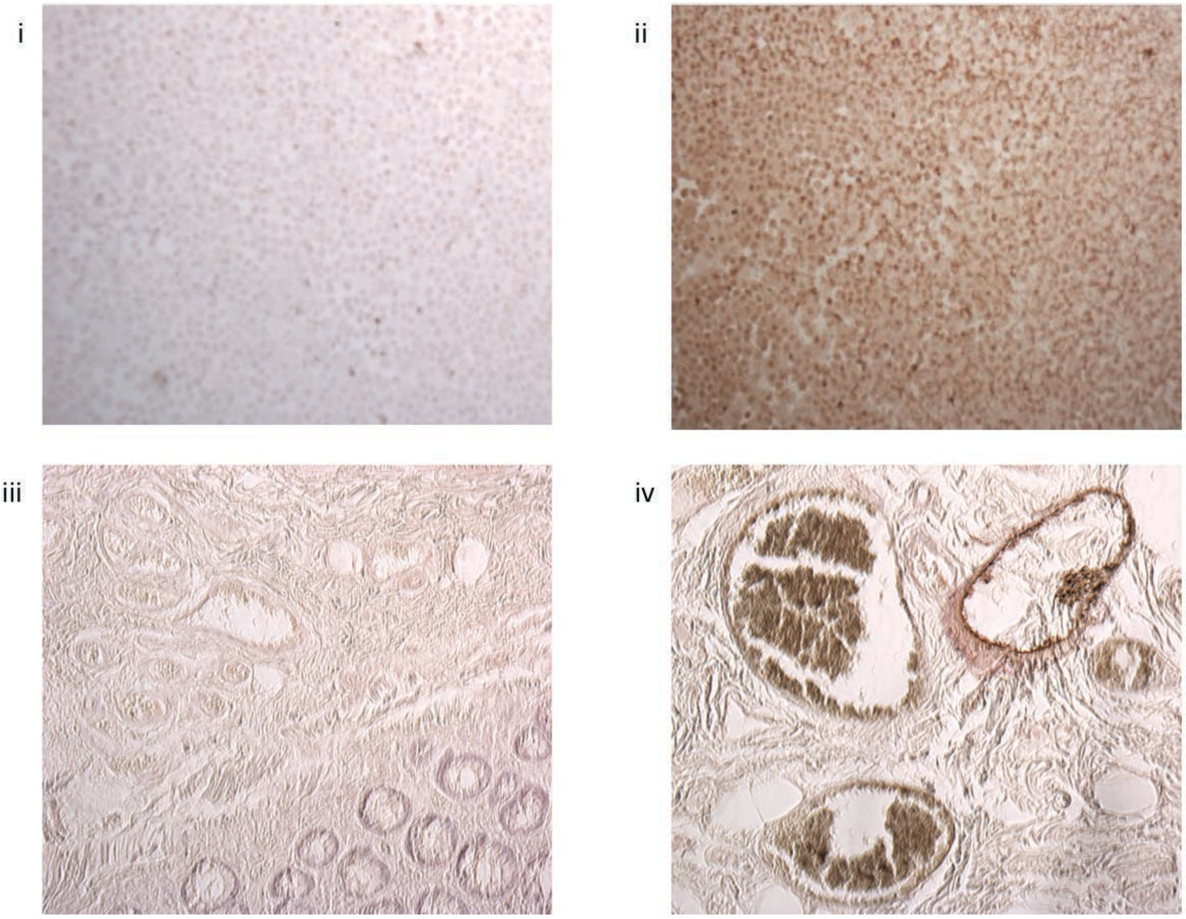

Figure 3.5 – Immunohistochemical Validation of GRIN2D as a Tumour Endothelial Marker in Colorectal Cancer. Differential staining is seen between control (i) and GRIN2D-expressing (ii) HEK293T cells in cytospin slides. Equally, an endothelial staining pattern is seen when staining in colorectal cancer (iv), but not in patient-matched normal colon (iii). Serum is utilised undiluted as primary antibody.

3.3 FUNCTIONAL CHARACTERISATION OF GRIN2D

Available evidence suggests that endothelial specific genes are often involved in endothelial cell biology and angiogenesis(125,126). Having identified GRIN2D as an endothelial specific protein in colorectal cancer, this section describes work performed in conjunction with Joseph Wragg (Bicknell Group, University of Birmingham, UK), to outline the effects of gene knockdown on HUVEC biology *in vitro*. To ensure generalisability of the results, assays were performed on HUVEC isolated from three separate umbilical cords, and with two different siRNA duplexes. The results presented are summarised from all cord/duplex combinations for clarity of presentation.

The assays were selected to quantify each stage of angiogenesis, namely cellular migration, proliferation and tube formation.

3.3.1 – siRNA Knockdown of GRIN2D in HUVEC

Knockdown of GRIN2D gene function in HUVEC was performed using lipofectamine transfection, and relative GRIN2D expression following knockdown quantified using RTqPCR. Duplex A achieved a knockdown of 80% of gene expression, with Duplex C achieving a knockdown of 65% expression on RTqPCR when compared to a scrambled knockdown (Figure 3.6).

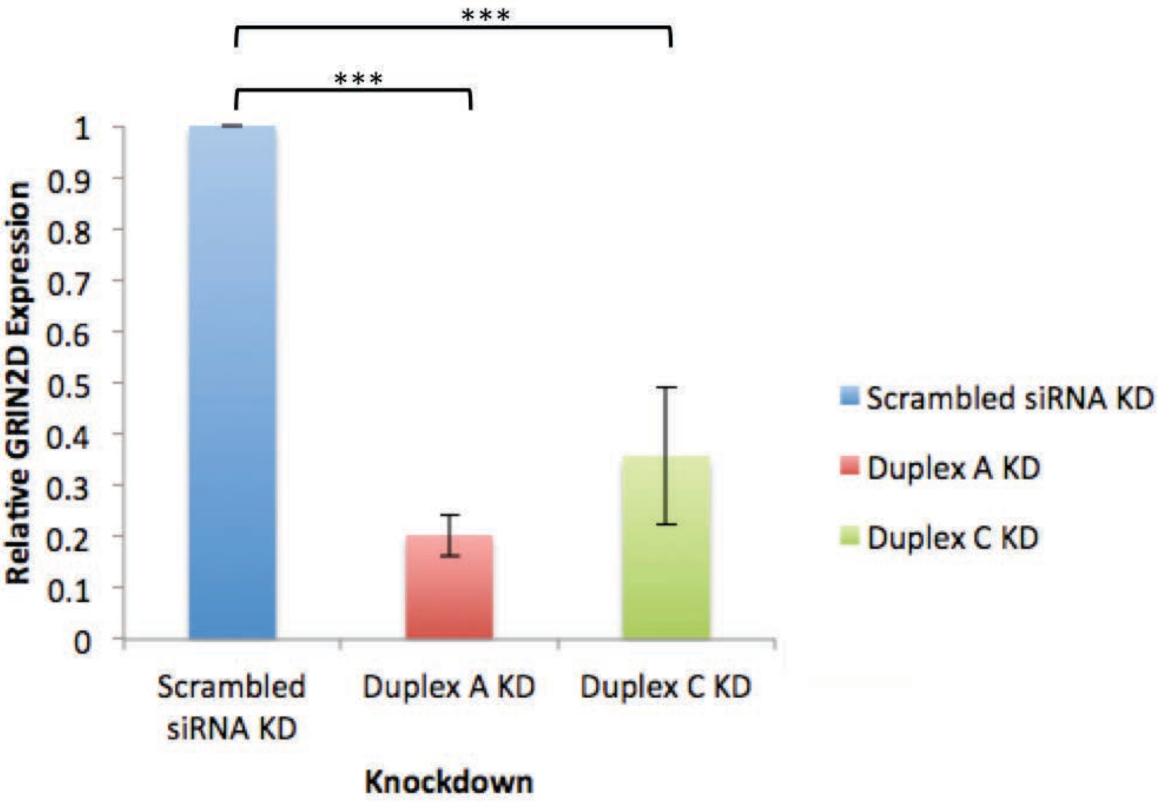

Figure 3.6 – siRNA Knockdown of GRIN2D in HUVEC. Quantified by RTqPCR, normalised to Beta Actin.

3.3.2 – Scratch Wound Assay

The scratch wound assay is a well-established approach to investigate cell migration *in vitro,* especially in combination with siRNA knockdowns(127). The assay involves disrupting a confluent monolayer of cells in a consistent formation, then subsequently monitoring the closure of the wound over a number of time points.

Measurements of the open area of a scratch wound were quantified using ImageJ software, and results generalised across HUVEC from three different umbilical cords. Due to the differences in HUVEC behaviour across cords, exact matching time points were inappropriate for analysis, so the start, midway closure point and end of the control wound closure was used in each case, with the results summarised. siRNA knockdown of GRIN2D is associated with a significant impairment in cellular migration as measured by scratch wound closure (p<0.0001, Mann-Whitney Test).

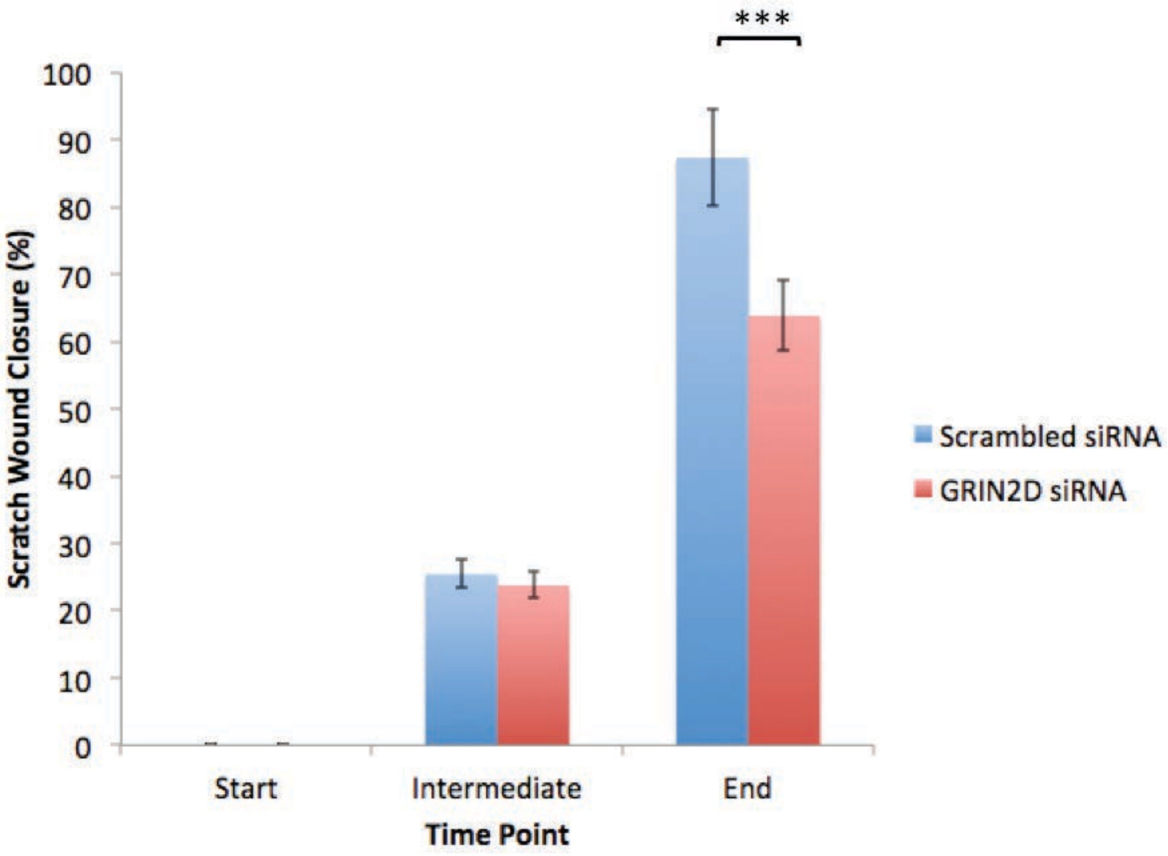

Figure 3.7 – Scratch Wound Assay. Quantification of wound closure by ImageJ software, indicating a significant decrease in closure following siRNA knockdown of GRIN2D compared to scrambled control (p<0.0001, Mann-Whitney Test).

3.3.3 – Matrigel Cellular Interaction Assay

Matrigel contains a number of extracellular matrix proteins that have been extracted from Englebreth-Holm-Swarm murine sarcomas. It primarily consists of laminin, collagen IV, and entactin, and is considered to be a reconstituted basement membrane preparation(128). It also contains cellular growth factors such as basic fibroblast growth factor, epidermal growth factor, platelet-derived growth factor, insulin-like growth factor 1, transforming growth factor beta, and nerve growth factor(129). At 37^{o}C, it forms a gel on which cells can be grown, and cell-cell interactions observed. The effect of siRNA knockdown on vascular tube formation in HUVEC was investigated by quantifying the number of nodes in a microscopic field, and the number of sprouts from each node after 16 hrs. siRNA knockdown of GRIN2D resulted in both a significant decrease in node formation (Mann-Whitney, p=0.0008), and the number of sprouts per node (Figure 3.8). These results indicated that knockdown of GRIN2D interferes with HUVEC cell-cell interaction, and impairs tube formation in vitro.

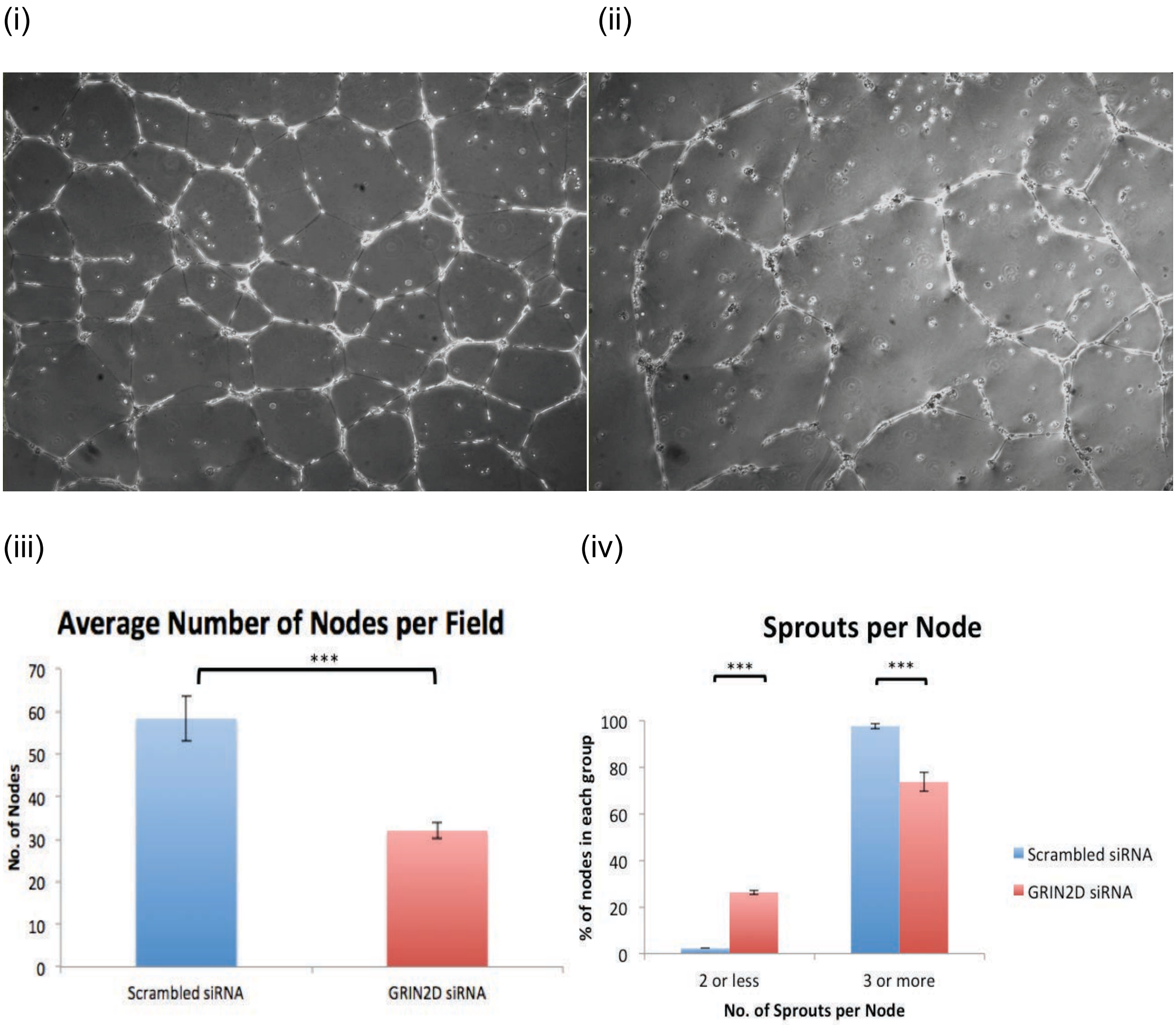

Figure 3.8 – Matrigel Assay. A decrease in visible cell-cell interaction was observed between control knockdown (i) and GRIN2D knockdown (ii) after 16 hrs. This was demonstrated both in terms of the average number of nodes observed (iii) (Mann-Whitney, $p=0.0008$), and the total number of sprouts per node (iv) (Mann-Whitney, $p<0.0001$ between both low number of sprouts (2 or less) and high numbers of sprouts (3 or more) per node.)

3.3.4 – Boyden Chamber Assay

The modified Boyden Chamber Assay, also known as the Transwell migration assay is used to quantify cellular chemotaxis and migration in response to pro-angiogenic stimuli(130). Briefly, HUVEC are loaded above a porated membrane in serum deplete media, with enriched media beneath (Figure 3.9,i). The percentage of cells migrating from above to below the membrane is microscopically quantified as a measure of cell migration following 4',6-diamidino-2-phenylindole (DAPI) staining of the formalin-fixed membrane. siRNA knockdown of GRIN2D significantly impairs cellular migration and chemotaxis, when measured in five random fields per replicate, with three replicates per condition (Figure 3.9,ii).

(i)

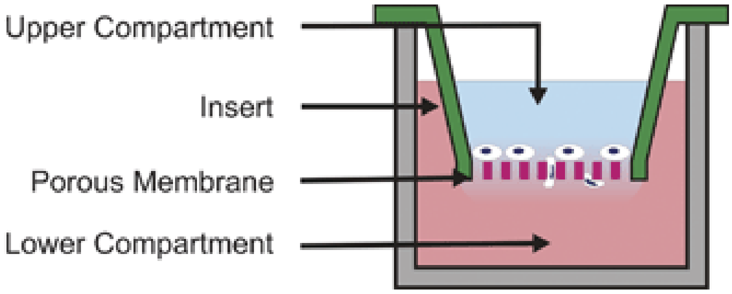
Upper Compartment
Insert
Porous Membrane
Lower Compartment

ii)

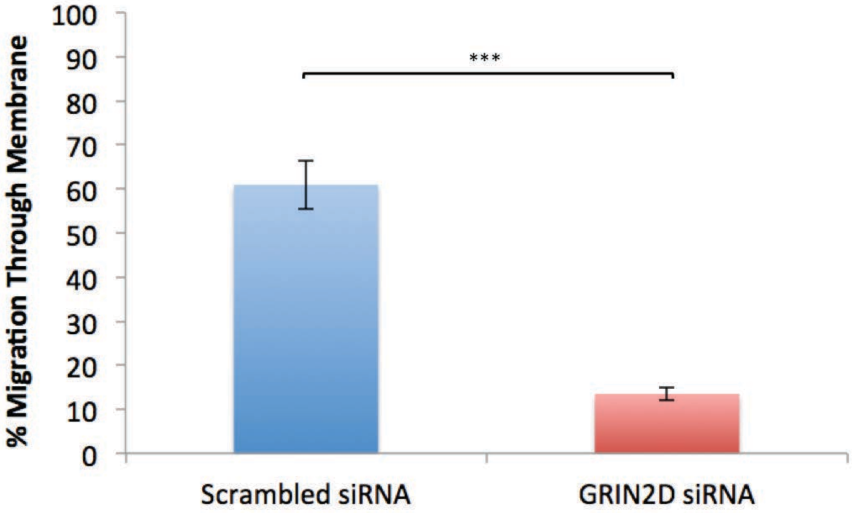

Figure 3.9 – (i) The Modified Boyden Chamber Assay. (ii) siRNA knockdown of GRIN2D impairs cellular migration in HUVEC, demonstrating a significant decrease in cellular migration and chemotaxis with GRIN2D knockdown ($p<0.001$, Mann-Whitney).

3.3.5 – Acumen Cell Cycle Analysis

The Acumen™ Cell Analyser (TTP Labtech, Melbourn, Herts, UK) was utilised to make an assessment of the effect of siRNA knockdown of GRIN2D on HUVEC cell cycle and viability(131). DNA was labelled using Hoechst stain, and measured using 405 nm laser excitation.

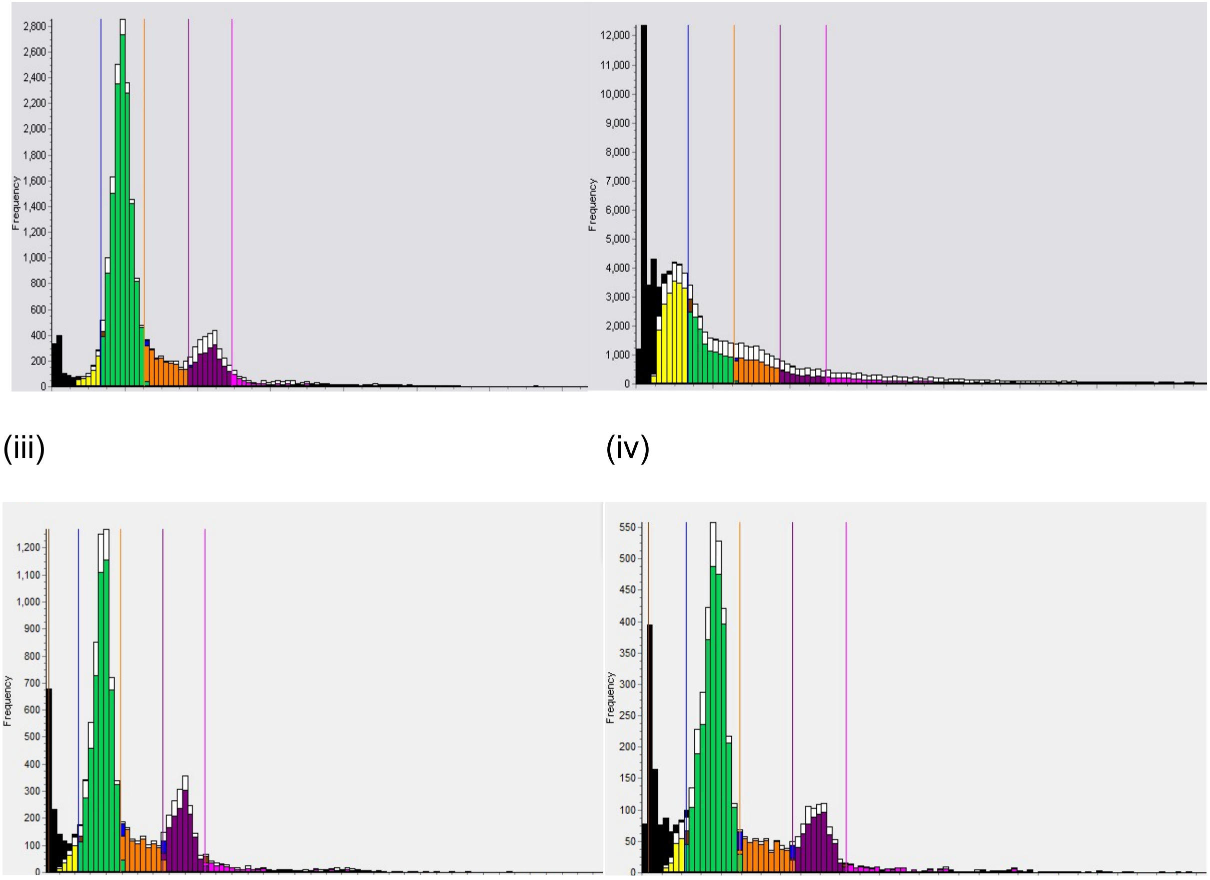
(i)

(ii)

(iii)

(iv)

Figure 3.10 – Acumen™ cell cycle analysis. Images (i) and (ii) are stock images showing healthy and apoptosing cells respectively. Image (iii) shows the effect of a scrambled siRNA knockdown, and image (iv) that of GRIN2D siRNA knockdown. Black = Dead cells, Yellow = apoptosing cells, Green = G0/1 Phase, Orange = S Phase, Purple = G2/M Phase.

While the process of siRNA knockdown clearly affects overall cell viability, with a visible increase in the proportion of dead (black) cells, there was not a significant difference between the scrambled control siRNA knockdown and the GRIN2D knockdowns. It can also be seen that there was a normal proportion of mitotic (G2/M Phase) cells within the GRIN2D knockdown cells. In combination, this indicated that siRNA does not affect cell viability.

3.3.6 Chapter Conclusion

GRIN2D has been identified and validated as a putative tumour endothelial marker in colorectal cancer through a sequential process of endothelial cell isolation, RNA extraction and microarray analysis, followed by quantitative PCR and immunohistochemical analyses.

By utilising siRNA knockdown, it has been demonstrated that a decrease in GRIN2D gene expression significantly decreases cellular migration, communication and chemotaxis, without adversely affecting cell viability or proliferation *in vitro.*

CHAPTER FOUR

DESIGN AND CONSTRUCTION OF A GRIN2D-BASED TUMOUR VACCINE

4.1 TARGETING GRIN2D

In order for a protein to be utilised as a vascular endothelial target for a vaccine based approach, it is important for there to be target-specific epitopes to stimulate an antibody response, which is readily accessible to the bloodstream. This chapter describes the process of identification of a suitable target region within the GRIN2D protein, and the processes pursued in order to produce an appropriate protein for use as a protein-based vaccine *in vivo*.

4.1.1 – The Structure of GRIN2D

GRIN2D is an ionotropic NMDA receptor subunit, and as such has been predicted to have an intracellular C-terminus, and an extracellular N-terminus(59). Between these termini, there are predicted to be four transmembrane regions, the second of which forms the ion channel in conjunction with three other subunits. This has been described as a putative structure for the NR2 subunits, with analogous structures in the AMPA glutamate receptor confirmed by fluorescence-detection size-exclusion chromatography(132). However, this structure has not been confirmed for GRIN2D. Bioinformatic prediction suggested that both the N- and C- termini were extracellular, and hence targetable (Figure 4.1), in contrast to the published proposed structure. Evidence suggests that the structure of the amino-terminal domain of each NR2 subunit defines the behavior of the NMDA receptor(59), and therefore it was considered that this region should be focused upon when identifying a targetable sequence. This decision also negated any concerns regarding the intra- or extra-cellular position of the carboxyl-terminal domain.

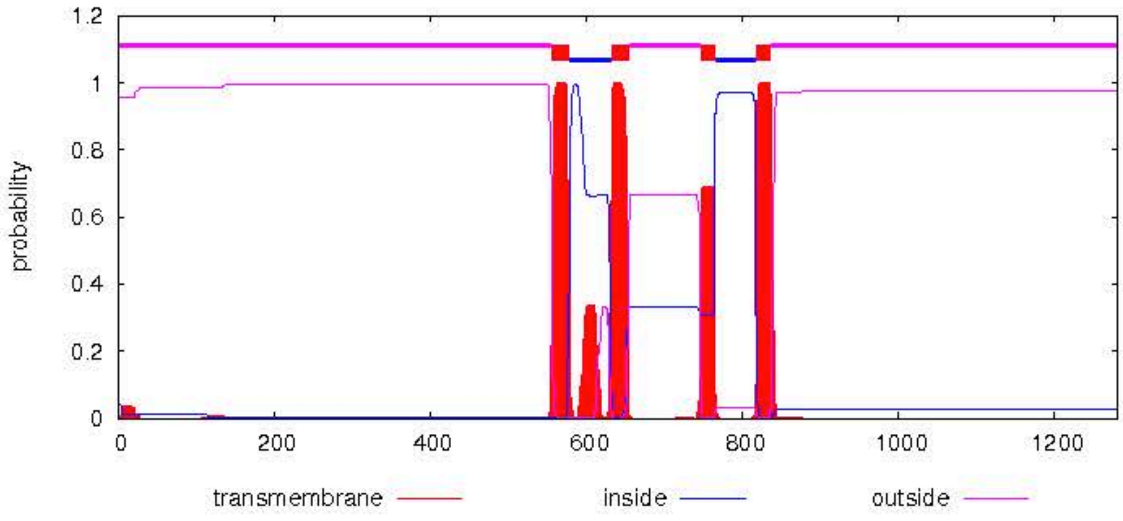

Figure 4.1 – Bioinformatic Prediction of Transmembrane regions of GRIN2D. Suggestive of both an extracellular N- and C-Terminus (Centre for Biological Sequence Analysis, The Technical University of Denmark, CTU.)

4.1.2 – Identification of an Appropriate Target Sequence

Clinical response to antibody-directed therapy, with minimal side-effects, depends on the identification of an antigen which is highly specific to the target tissue of interest(133). However, this specificity must also extend to the region of the target molecule of interest, if off target effects are to be avoided.

The GRIN2 subgroup has molecular regions that are highly conserved and unique compared to other subgroups. Specifically, the transmembrane region and ligand-binding regions are highly conserved, both across species and between GRIN2 subtypes. The greatest variability occurs in both the N- and C- terminal regions(134). As previously stated, the published consensus errs towards the C-terminal region being intracellular, with it therefore being inaccessible to circulating immune cells. Focus was therefore concentrated on the N-terminal region of the GRIN2 family. Multiple sequence alignment was performed, and an 81 amino acid sequence was identified which was unique to human GRIN2D, and an equivalent 78 amino acid sequence in mouse GRIN2D, corresponding to the same region. These target sequences underwent comparative sequence analysis using the Protein Basic Local Alignment Search Tool (BLASTp) tool from NCBI to ensure there was no significant sequence homology with any other human or murine protein, thereby decreasing the likelihood of any off-target effects of any future targeted therapy. Sequence alignment with the other members of the GRIN2 subgroup were also performed in human and mouse to ensure there was no sequence homology within the target region of interest (Figure 4.2).

While the primary amino acid sequence is important in predicting specific immunological reactions, the secondary structure also contributes significantly. Peptide sequences inevitably form different secondary structures to the full-length protein, and efforts were made to predict the secondary structure of the N-terminal sequence of human GRIN2D to ensure that some of its secondary structure remained. These indicated that the helical structure of the predicted peptide was consistent with the same segment of the predicted full-length protein (Figure 4.3).

```
Human

Base        1
GRIN2D      MRGAGGPRGPRGPAKMLLLLALACASPFPEEAPGPGGAGGPGGGLGGARPLNVALVFS--
GRIN2A      ----------MGRVGYWTLLVLPALLVWRGPAPSAAAEKG-------PPALNIAVMLGHS
GRIN2B      ----MKPRAECCSPKFWLVLAVLAV-----SGSRARSQKS-------PPSIGIAVILVGT
GRIN2C      ---MGG---ALGPALLLTSLF----GAWA--------GLGPGQG---EQGMTVAVVFSSS
                               *                   .          : :*:::

Base        60                      81
GRIN2D      G--PAYAAEAARLGPAVAAAVRSPGLDVRPVALVLNGSDPRSLVLQLCDLLSGLRVHGVV
GRIN2A      H-DVTERELRTLWGP---EQAAGLPLDVNVVALLMNRTDPKSLITHVCDLMSGARIHGLV
GRIN2B      SDEVAIK---DAHEK---DDFHHLSVVPRVELVAMNETDPKSIITRICDLMSDRKIQGVV
GRIN2C      G--PPQAQFRARLTPQ---SFLDLPLEIQPLTVGVNTTNPSSLLTQICGLLGAAHVHGIV
                                     :  .   : :* ::* *:: ::* *:.  :::*:*

Base        120
GRIN2D      FEDDSRAPAVAPILDFLSAQTSLPIVAVHGGAALVLTPKEKGSTFLQLGSSTEQQLQVIF
GRIN2A      FGDDTDQEAVAQMLDFISSHTFVPILGIHGGASMIMADKDPTSTFFQFGASIQQQATVML
GRIN2B      FADDTDQEAIAQILDFISAQTLTPILGIHGGSSMIMADKDESSMFFQFGPSIEQQASVML
GRIN2C      FEDNVDTEAVAQILDFISSQTHVPILSISGGSAVVLTPKEPGSAFLQLGVSLEQQLQVLF
            * *:    *:* :***:*::*  **:.: **:::::: *:  * *:*:* * :**  *::


Mouse
Base        1
GRIN2D      MRGAGGPRGPRGPAKMLLLLALACASPFPEEVPGPGAAGGGTGGARPLNVALVFS--GPA
GRIN2A      ----------MGRLGYWTLLVLPALL----VWHGPAQNAAAEKGTPALNIAVLLG-HSHD
GRIN2B      ----MKPSAECCSPKFWLVLAVLAV---------SGSKARSQKSAPSIGIAVILVGTSDE
GRIN2C      ---MGGA---LGPALLLTSL------------LGAWAGLGAGQGEQAVTVAVVFGSSGPL
                               *                    .  .   : :*:::   .

Base        60                 78
GRIN2D      YAAEAARLGPAVAAAVRSPGLDVRPVALVLNGSDPRSLVLQLCDLLSGLRVHGVVFEDDS
GRIN2A      VTERE-LRNLWGPEQATGLPLDVNVVALLMNRTDPKSLITHVCDLMSGARIHGLVFGDDT
GRIN2B      VAI----KDAHEKDDFHHLSVVPRVELVAMNETDPKSIITRICDLMSDRKIQGVVLADDT
GRIN2C      QAQARTRLTPQ---NFLDLPLEIQPLTIGVNNTNPSSILTQICGLLGAARVHGIVFEDNV
             :                  :  .   : :* ::* *:: ::* *:.  :::*:*: *:

GRIN2D       RAPAVAPILDFLSAQTSLPIVAVHGGAALVLTPKEKGSTFLQLGSSTEQQLQVIFEVLEE
GRIN2A       DQEAVAQMLDFISSQTFIPILGIHGGASMIMADKDPTSTFFQFGASIQQQATVMLKIMQD
GRIN2B       DQEAIAQILDFISAQTLTPILGIHGGSSMIMADKDESSMFFQFGPSIEQQASVMLNIMEE
GRIN2C       DTEAVAQLLDFVSSQTHVPILSISGGSAVVLTPKEPGSAFLQLGVSLEQQLQVLFKVLEE
             :;:*:* :***:*:**  **:.: **:::::: *:  * *:*:* * :**  *:::::::

* - full alignment, : - Alignment in 3 of 4 sequences, ; - alignment in 2
of 4 sequences.
```

Figure 4.2 – Human and Murine Sequence Alignment of GRIN2 Subgroup.

Unique, extracellular sequences within the human and mouse amino acid sequences for GRIN2D are indicated in yellow..

(i) (ii)

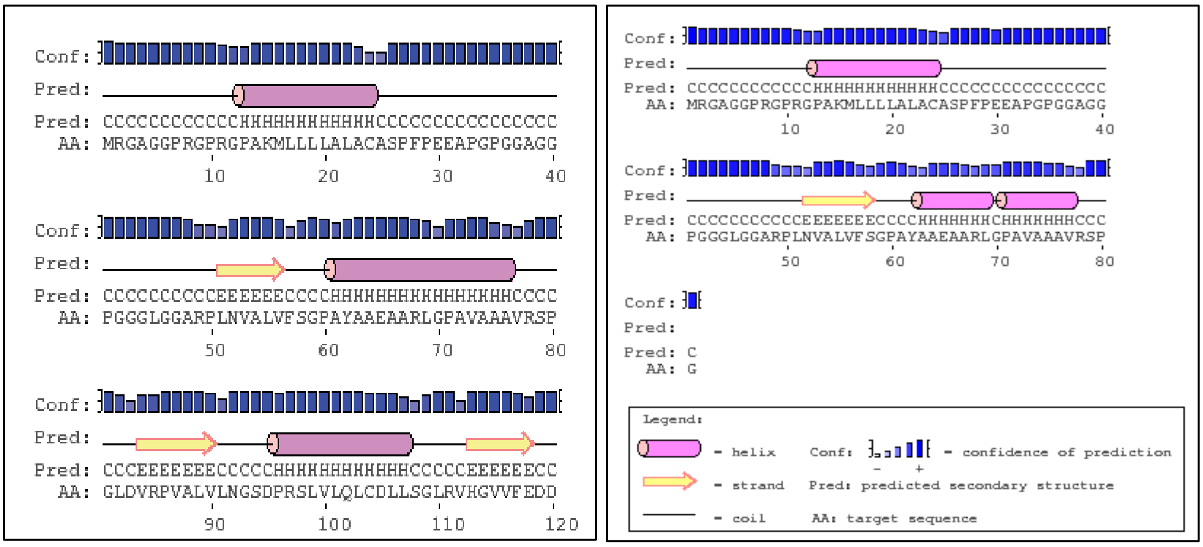

(i)

```
Conf:
Pred:
Pred: CCCCCCCCCCCCHHHHHHHHHHHHCCCCCCCCCCCCCCCC
  AA: MRGAGGPRGPRGPAKMLLLLALACASPFPEEAPGPGGAGG
              10        20        30        40

Conf:
Pred:
Pred: CCCCCCCCCCEEEEEECCCCHHHHHHHHHHHHHHHHCCCC
  AA: PGGGLGGARPLNVALVFSGPAYAAEAARLGPAVAAAVRSP
              50        60        70        80

Conf:
Pred:
Pred: CCCEEEEEEECCCCCHHHHHHHHHHHHCCCCCEEEEEECC
  AA: GLDVRPVALVLNGSDPRSLVLQLCDLLSGLRVHGVVFEDD
              90       100       110       120
```

(ii)

```
Conf:
Pred:
Pred: CCCCCCCCCCCCHHHHHHHHHHHHCCCCCCCCCCCCCCCC
  AA: MRGAGGPRGPRGPAKMLLLLALACASPFPEEAPGPGGAGG
              10        20        30        40

Conf:
Pred:
Pred: CCCCCCCCCCCEEEEEEECCCCHHHHHHHCHHHHHHHCCC
  AA: PGGGLGGARPLNVALVFSGPAYAAEAARLGPAVAAAVRSP
              50        60        70        80

Conf:
Pred:
Pred: C
  AA: G
```

Legend:
- helix
- strand
- coil
Conf: - confidence of prediction
- +
Pred: predicted secondary structure
AA: target sequence

iii)

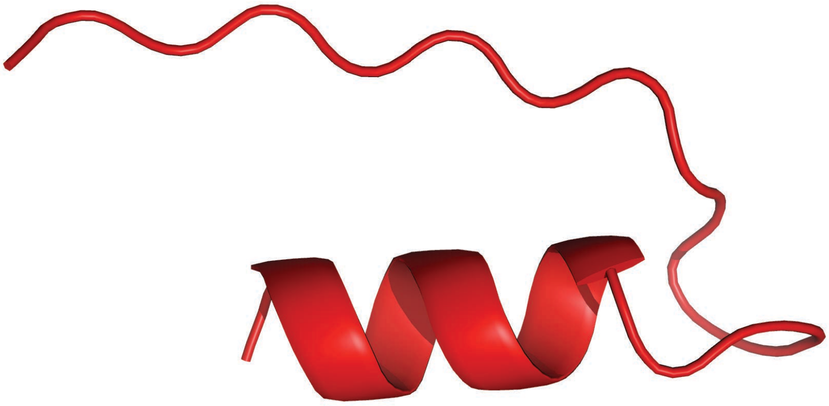

Figure 4.3 – Bioinformatic Prediction of the Secondary Structure of the N-Terminal Domain of GRIN2D. Calculated from (i) the full-length human GRIN2D sequence, and (ii) from the 81 amino acid N-terminus peptide to be taken forward (ii) by PSIPRED software (UCL Dept. of Computer Software). An alternate prediction giving a three-dimensional representation of the GRIN2D N-Terminus peptide is also shown (iii) (http://swissmodel.expasy.org). Indications are of significant homology between the two entities in terms of secondary structure.

4.2 EXPRESSION OF GRIN2D FUSION PROTEINS

In order to take GRIN2D forward as a TEM in colorectal cancer, it was necessary to generate protein based upon the identified human and mouse target sequences. The generation of conjugate proteins was favoured in this process, as protein ‘tags’ can be used for downstream purification, and can also be useful in identifying proteins in analytical processes where no reliable antibody exists, as is the case with GRIN2D.

4.2.1 The GRIN2D Target Sequence

In order to produce the target regions of human and mouse GRIN2D, it was necessary to generate sufficient corresponding DNA to enable transfection into bacterial or mammalian expression hosts. For human GRIN2D, initial attempts were made to achieve this through PCR amplification from complementary DNA derived from a neuronal cell line, SHSY5Y (Nagy Lab, University of Birmingham, UK), which had demonstrated high levels of expression of GRIN2D when quantified by RTqPCR. However, despite numerous attempts, with varying concentrations of DMSO and Magnesium, amplification failed, presumably as the sequence is highly ‘GC’ rich. Therefore, the sequence was designed to provide the in-frame message for subsequent expression in both the pcDNA3 and pGEX2T vectors, and was commercially synthesised (Integrated DNA Technologies, Coralville, Iowa, USA) with the *Bam*HI and *Eco*RI restriction sites in place:

hGRIN2D

*Bam*HI
GGATCCATGCGCGGCGCCGGTGGCCCCCGCGGCCCTCGGGGCCCCGCTAAGATGCTGCTGCT
GCTGGCGCTGGCCTGCGCCAGCCCGTTCCCGGAGGAGGCGCCGGGGCCGGGCGGGGCCGGTG
GGCCCGGCGGCGGCCTCGGCGGGGCGCGGCCGCTCAACGTGGCGCTCGTGTTCTCGGGGCCC
GCGTACGCGGCCGAGGCGGCACGCCTGGGCCCGGCCGTGGCGGCGGCGGTGCGCAGCCCGGG
CAAGAATTC
*Eco*RI

The DNA was received within a transport Vector, the IDTSmart-Amp Vector:

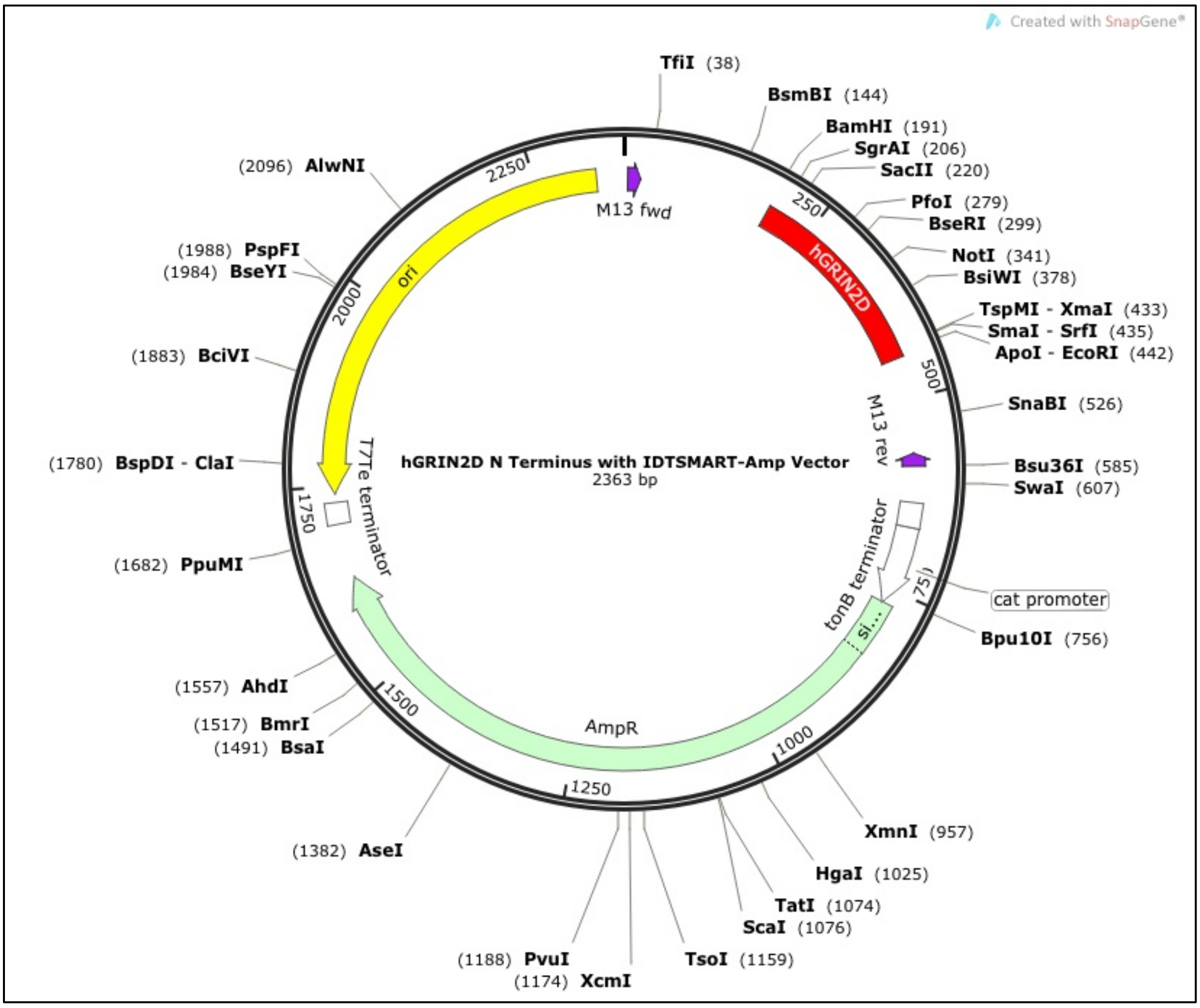
Created with SnapGene®
TfiI (38)
BsmBI (144)
BamHI (191)
SgrAI (206)
SacII (220)
PfoI (279)
BseRI (299)
NotI (341)
BsiWI (378)
TspMI - XmaI (433)
SmaI - SrfI (435)
ApoI - EcoRI (442)
SnaBI (526)
Bsu36I (585)
SwaI (607)
cat promoter
Bpu10I (756)
XmnI (957)
HgaI (1025)
TatI (1074)
ScaI (1076)
TsoI (1159)
(1174) XcmI
(1188) PvuI
(1382) AseI
(1491) BsaI
(1517) BmrI
(1557) AhdI
(1682) PpuMI
(1780) BspDI - ClaI
(1883) BciVI
(1984) BseYI
(1988) PspFI
(2096) AlwNI
M13 fwd
hGRIN2D
M13 rev
tonB terminator
si...
AmpR
T7Te terminator
ori
250
500
750
1000
1250
1500
1750
2000
2250
hGRIN2D N Terminus with IDTSMART-Amp Vector
2363 bp

Figure 4.4 – Vector Map of the Human GRIN2D-IDT Construct.

An equivalent sequence was synthesised for mouse GRIN2D, and received within the same transport vector:

mGRIN2D

*Bam*HI
GGATCCATGCGCGGCGCCGGTGGCCCCGCGGCCCTCGGGGCCCCGCTAAGATGCTGTTGCT
GCTGGCGCTGGCGTGCGCCAGCCCGTTCCCGGAGGAGGTGCCGGGGCCGGGCGCGGCCGGCG
GGGGCACGGGCGGGGCGCGGCCGCTCAACGTGGCGCTGGTCTTCTCTGGCCCGGCGTACGCG
GCCGAGGCGGCGCGCTTGGGCCCGGCCGTGGCGGCGGCAGTGCGCAGCCCGGGCAAGAATTC
*Eco*RI

4.2.2 – Expression of hGRIN2D-Fc and mGRIN2D-Fc Fusion Protein

Informed by the work of Zhuang et al.(135), an Fc-fusion protein was chosen as the primary conjugate protein for production. The Fc tag is formed of a 230 amino acid sequence encoding for the Fc chain of human IgG1. The Fc tag enables efficient purification by the use of Protein A affinity chromatography(136), and has also been shown to increase the solubility and stability of the fusion partner protein both *in vitro* and *in vivo*(137). For our particular purpose of the utilisation of Fc-fusion proteins as therapeutic tumour vaccines, the tag also enables interaction with the Fc receptors of circulating immune cells, thereby increasing the immune response against the fusion partner(138).

The pIgG vector (pcDNA3.Fc) is a vector previously constructed within the Bicknell Laboratory whereby the constant region of the Fc Heavy chain has been cloned into the pcDNA3 vector using the *Not*I and *Xba*I restriction sites, enabling flexible positioning of the fusion partner protein. It has previously been shown to be a high copy vector in this application(135). It also codes for the CMV and SV40 promoters, enabling protein expression in mammalian cell lines. The full construct post-insertion of GRIN2D can be seen in Figure 4.5. When generating the construct for human and mouse GRIN2D, the pre-engineered restriction sites *Bam*HI and *Eco*RI were utilised. GRIN2D was digested from amplified, purified DNA from competent *E.coli* using a double digest technique. The ends were then dephosphorylated with antarctic phosphatase, and then ligated into the pIgG vector using the same restriction sites at both 1:3 and 1:5 vector to insert ratios using T4 ligase. Both ratios were successful, and presence of the insert was confirmed on an agarose gel following re-digest of plasmid DNA from re-transformed *E.coli* (Figure 4.6), and was also sequence verified by the functional genomics facility at the University of Birmingham. Data was analysed using Sequencher software (Gene Codes Corporation, Ann Arbor, USA).

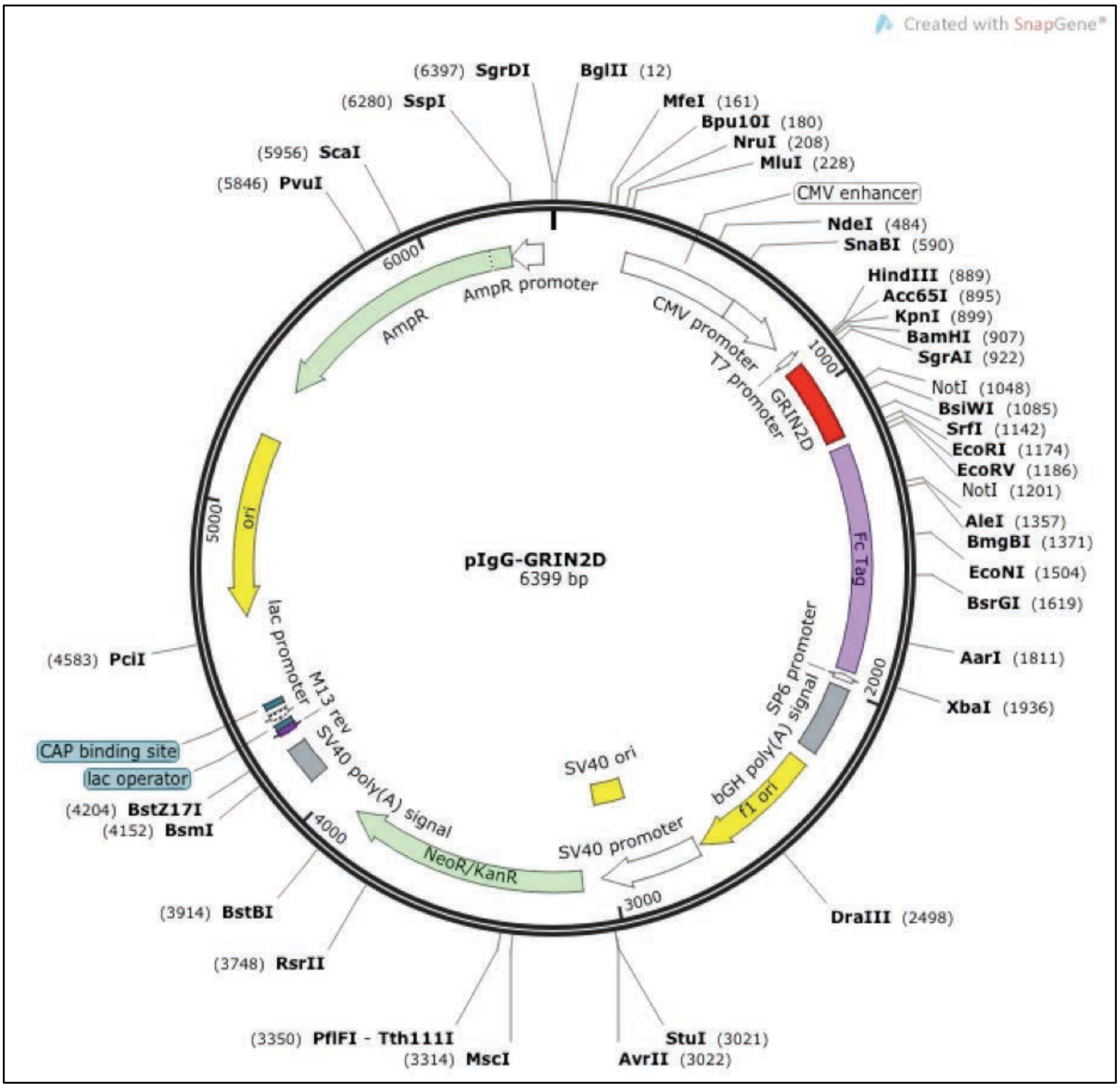
Created with SnapGene®
(6397) SgrDI
BglII (12)
(6280) SspI
MfeI (161)
Bpu10I (180)
NruI (208)
MluI (228)
(5956) ScaI
(5846) PvuI
CMV enhancer
NdeI (484)
SnaBI (590)
HindIII (889)
Acc65I (895)
KpnI (899)
BamHI (907)
SgrAI (922)
NotI (1048)
BsiWI (1085)
SrfI (1142)
EcoRI (1174)
EcoRV (1186)
NotI (1201)
AleI (1357)
BmgBI (1371)
EcoNI (1504)
BsrGI (1619)
AarI (1811)
XbaI (1936)
DraIII (2498)
StuI (3021)
AvrII (3022)
(3350) PflFI - Tth111I
(3314) MscI
(3748) RsrII
(3914) BstBI
(4204) BstZ17I
(4152) BsmI
lac operator
CAP binding site
(4583) PciI
AmpR promoter
AmpR
CMV promoter
T7 promoter
GRIN2D
Fc Tag
SP6 promoter
bGH poly(A) signal
f1 ori
SV40 promoter
SV40 ori
NeoR/KanR
SV40 poly(A) signal
M13 rev
lac promoter
ori
pIgG-GRIN2D
6399 bp
1000
2000
3000
4000
5000
6000

Figure 4.5 – Representative Vector Map of the pIgG-GRIN2D Vector. Separate constructs were made for human and mouse GRIN2D-Fc by the same process. The resulting construct was a GRIN2D-Fc fusion protein with the Fc tag at the C-terminal end of the target GRIN2D sequence.

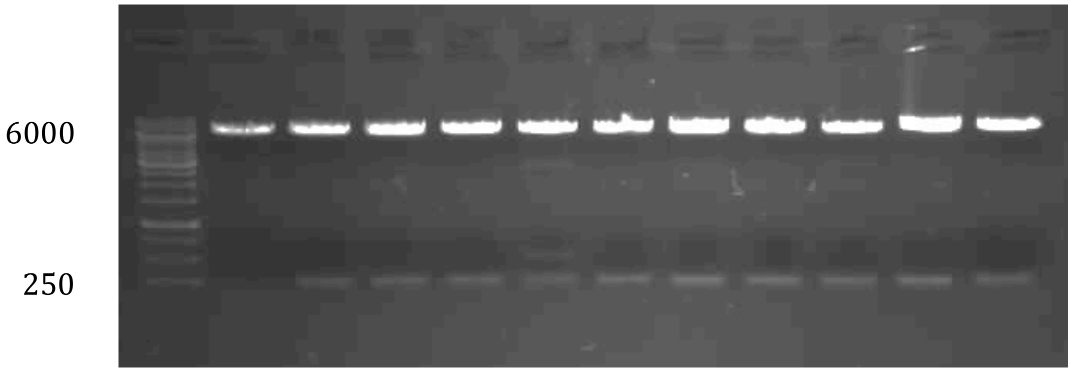

Figure 4.6 – Restriction digest of pIgG-GRIN2D. 1% Agarose gel of digested transformant bacterial colony DNA. The ladder used is a GeneRuler™ 1kb ladder. Lane 1 – 1kb Ladder. Lane 2 – undigested vector. Lanes 3-7 - 1:3 vector to insert ratio. Lanes 8-12 - 1:5 vector to insert ratio. 6kb bands correspond to the vector, with the digested insert corresponding to the expected size of 243 bases in lanes 3-12.

Following verification of the respective human and mouse GRIN2D sequences, PEI transfection of HEK293 cells was performed to induce protein expression. Care had been taken in the design of the target sequence to ensure that a signal peptide was present, to facilitate secretion of the fusion protein from the cells. The presence of the signal peptide was confirmed using SignalP-4.1 prediction software(139).

HEK293 cells are derived from the human embryological kidney, transfected with fragmented adenovirus 5 DNA. This provides the cells with the ability to synthesise large quantities of peptide when transfected with a suitable vector, such as pcDNA3 and its derivatives(140).

Trial transfection was performed on a small scale. Trial pull-down of hGRIN2D-Fc was also performed using 100 µl Protein A beads. This process was analysed by western blot for the presence of Fc-fusion protein of the appropriate size. In the absence of specific anti-GRIN2D antibodies, an anti-Fc blot was used to confirm expression by proxy:

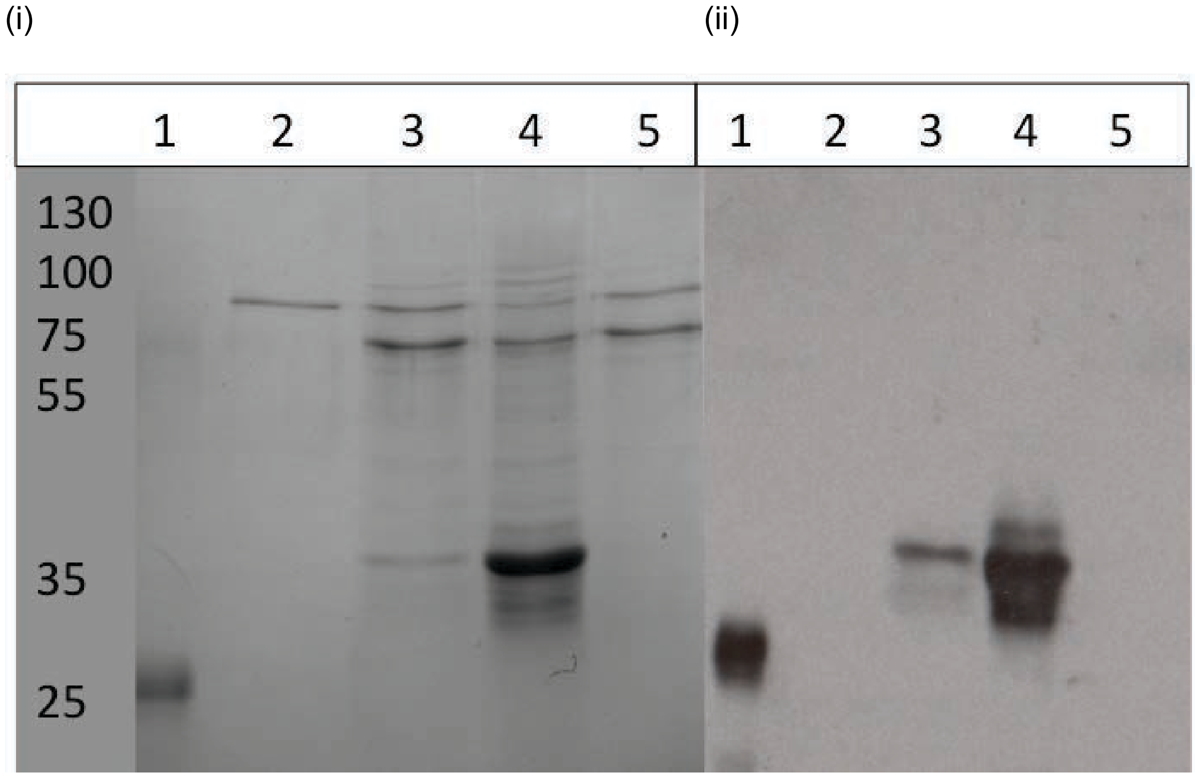

Figure 4.7 – Trial GRIN2D-Fc Production and Purification.

Corresponding Coomassie Stain (i) and anti-Fc Western Blot (ii) of 12% SDS-PAGE Gel. Lane 1 – Purified Human Fc. Lane 2 – Optimem. Lane 3 – Secreted Media. Lane 4 – Purified GRIN2D-Fc. Lane 5 – Depleted Media. Predicted size of hGRIND-Fc = 34 kDa; Fc = 26 kDa

Once the process had been successful on a small scale, twenty 15 cm plates of HEK293 cells were transfected, and incubated with low serum media. Media was collected every other day for 21 days, and the resultant volume passed through a Protein A column. Protein A has a high affinity for the Fc fragment of human IgG, enabling an Fc fusion protein to be effectively purified by exposure to sepharose bound to protein A(141). Elution from the column was carried out at pH 3.0, so the resulting eluate was pH adjusted using TRIS-HCl pH 8.5 to pH 6.5, a point which is both unlikely to denature the protein, and at which the protein is unlikely to precipitate out of solution, as it is away from the predicted isoelectric point (pI) of the GRIN2D-Fc fusion protein as calculated by the Expasy ‘compute pI/Mw tool’(142). For both hGRIN2D-Fc and mGRIN2D-Fc, the pI was predicted to be pH 8.53. The sample was sterile filtered, and stored at 4^{o}C. The concentration of the purified protein was calculated by Pierce BCA Protein Assay, and the identity of the protein again verified by SDS PAGE followed by Coomassie stain and western blot.

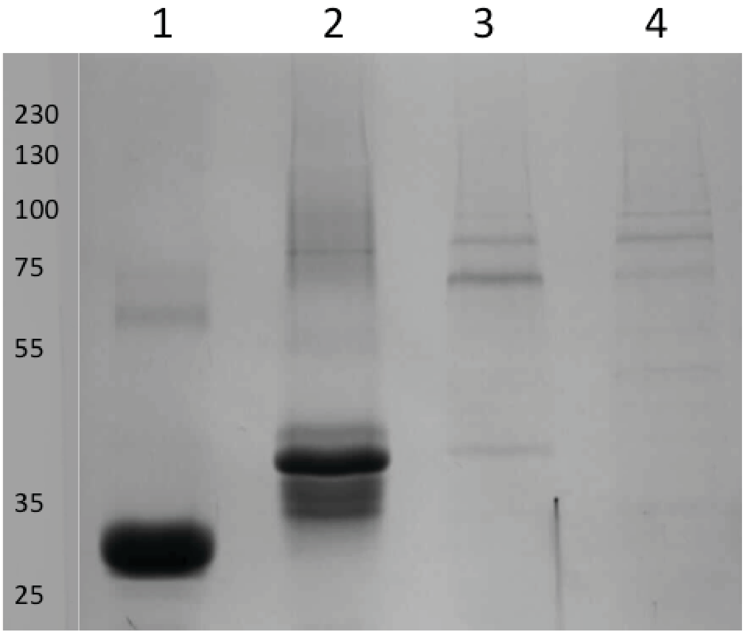

Figure 4.8 – Large-scale Purification of hGRIN2D. Coomassie stain of 12% SDS PAGE Gel. Lane 1 – Purified Human Fc. Lane 2 – Affinity purified GRIN2D-Fc. Lane 3 – Secreted Media. Lane 4 – Depleted Media. Predicted size of hGRIN2D-Fc = 34 kDa; Fc = 26 kDa.

Following Protein A column purification of mGRIN2D, it was noted that there was a contaminant Fc-fusion protein in the final eluate, which had not been represented in the secreted media:

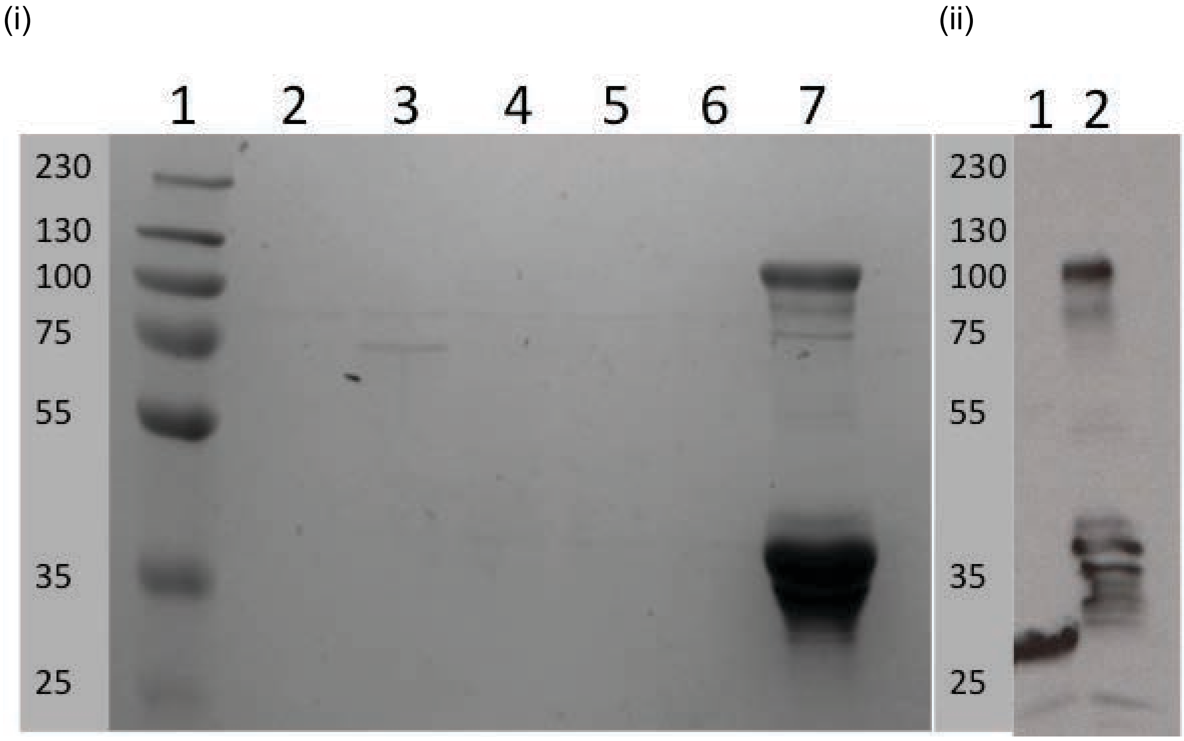

Figure 4.9 – Contaminant Fc-fusion Protein. (i) Coomassie Stain. Lane 1 – PageRuler Plus Ladder, Lane 2 – Optimem, Lanes 3-6 – secreted media, Lane 7 – ‘Purified’ mGRIN2D-Fc. (ii) anti-Fc Western Blot of Lane 1 – Fc, Lane 2 - column eluate Contaminant band >100 kDa on Coomassie corresponds to upper band on anti-Fc blot. 12% SDS-PAGE Gel.

As this protein was confirmed as an Fc-fusion protein on western blot, and would potentially confound any future assays performed with the protein, the sample underwent size exclusion chromatography (SEC). SEC is a method by which proteins of different molecular weights can be separated by the use of a column, which allows passage at different rates depending on size. The column consists of Dextran bound to highly cross-linked porous agarose beads, which permits passage of larger proteins more easily than small proteins, which are hindered by the smaller pores in beads. This allows the collection of differential fractions of column-flow-through, enabling purification of mGRIN2D-Fc, and exclusion of the contaminant protein. The flow through is analysed by UV absorbance, allowing quantification of protein in each fraction (Figure 4.10).

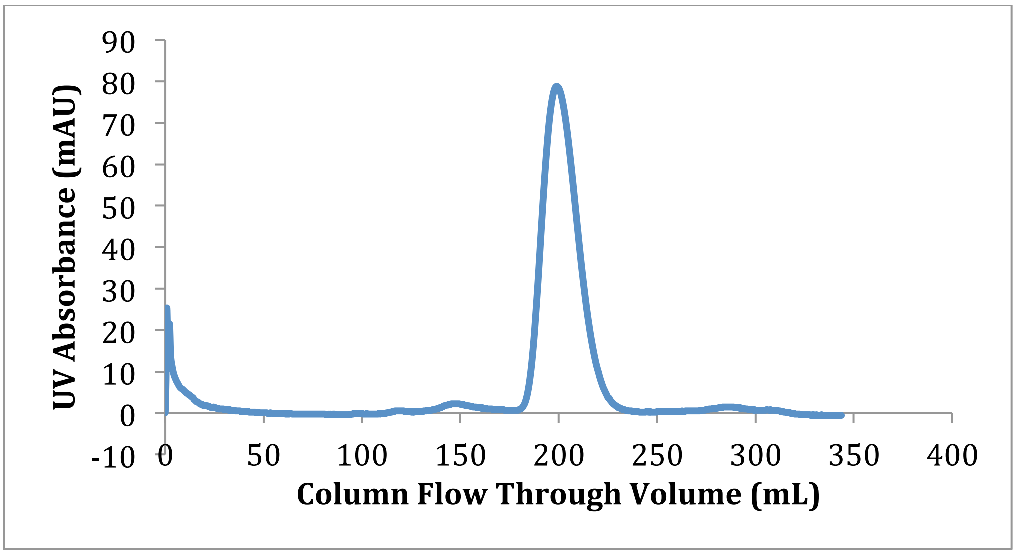

Figure 4.10 – UV Absorbance analysis of SEC for mGRIN2D-Fc. The deflection at 150 ml represents the larger, contaminant protein, with the major deflection from 180 ml to 230 ml representing mGRIN2D. The volume within this major deflection was collected in 5 ml fractions

All fractions expected to contain mGRIN2D-Fc were analysed by SDS-PAGE (Figure 4.11), then those confirmed to contain mGRIN2D were pooled and concentrated using a VivaSpin® column. Protein concentration was then confirmed by BCA Protein Assay, and the sample was sterile filtered and stored at 4^{o}C.

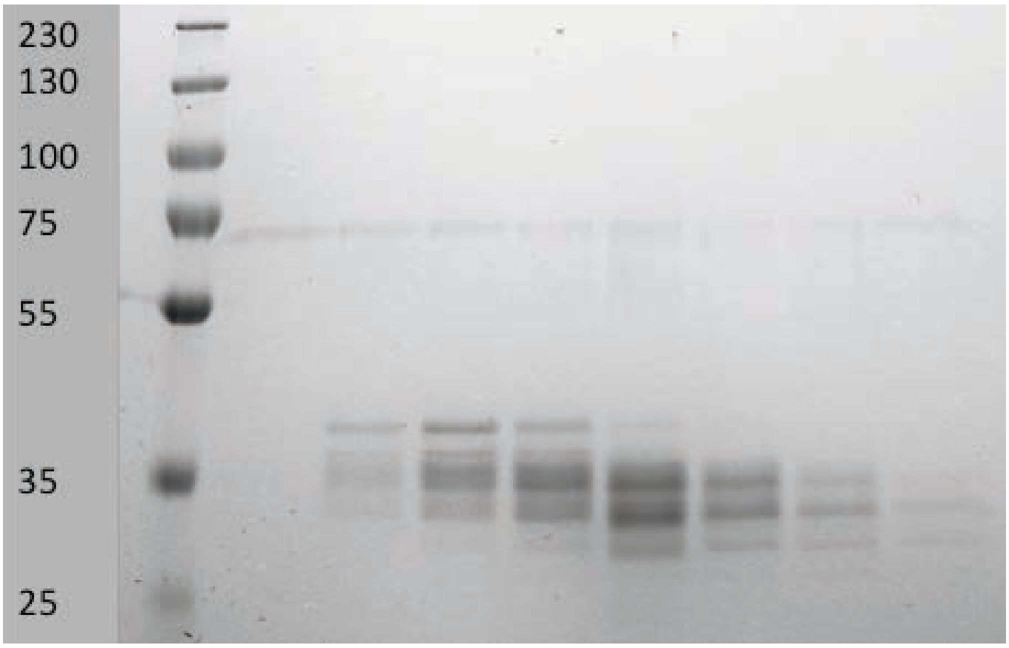

Figure 4.11 – Fractions Collected from SEC for mGRIN2D-Fc.

12% SDS-PAGE Gel, Coomassie Stain. Expected size for mGRIN2D-Fc = 33 kDa

4.2.3 – Expression of GST-hGRIN2D and GST-mGRIN2D Fusion Protein

While Fc-conjugate protein was desirable for some applications, the presence of the Fc-tag would also complicate production of polyclonal antisera against the N-terminus of GRIN2D, as large quantities of human Fc-specific immunoglobulins would result, and confound future immunohistochemistry. Efforts were made to cleave off the Fc-tag by the use of Papain, but this was unsuccessful. Therefore, the Glutathione S-Transferase (GST) Gene Fusion System (GE Healthcare, Little Chalfont, UK) was utilised to provide a fusion protein with an alternate tag, which would not confound IHC in the same way. The pGEX expression vectors available within this system code for GST from *Schistosoma japonicum*. As GST is a bacterial enzyme, it would not be present on human histological slides, and so a polyclonal serum derived from this protein could be used without purification.

The pGEX vector family is large, but pGEX-2T was chosen for subsequent expression because of the presence of both *Bam*HI and *Eco*RI sites within the multiple cloning site, and the close proximity of the STOP codon to *Eco*RI, thereby minimising the extra amino acids appended to GST-GRIN2D during subsequent expression. The pGEX vectors possess the *tac* promoter, and as such are active in bacteria, rather than in mammalian cells as is the case with the pIgG vector. A bacterial expression system has the advantage of relatively high yield over a shorter period of time than a mammalian system(143), but bacteria lack the ability to perform post translational modification of generated peptides, which can potentially affect their secondary, tertiary and quaternary structures(144). Bioinformatic prediction did not identify any glycosylation sites or potential disulphide bonds within the target sequence of mouse or human GRIN2D, so bacterial expression was considered appropriate. The *tac* promoter system exists in a repressed state due to the presence of the *lac* repressor, and therefore requires induction by isopropyl-β-galactosidase (IPTG) to achieve protein expression(145). IPTG is a molecular mimic of allolactose, a lactose metabolite, which triggers transcription of the *lac* operator, and deregulation of the *tac* system.

The human and mouse GRIN2D constructs synthesised by IDT were once again utilised, and ligated into the pGEX2T vector utilising the *Bam*HI and *Eco*RI restriction sites, verified by Agarose Gel analysis, and sequence verified as previously described.

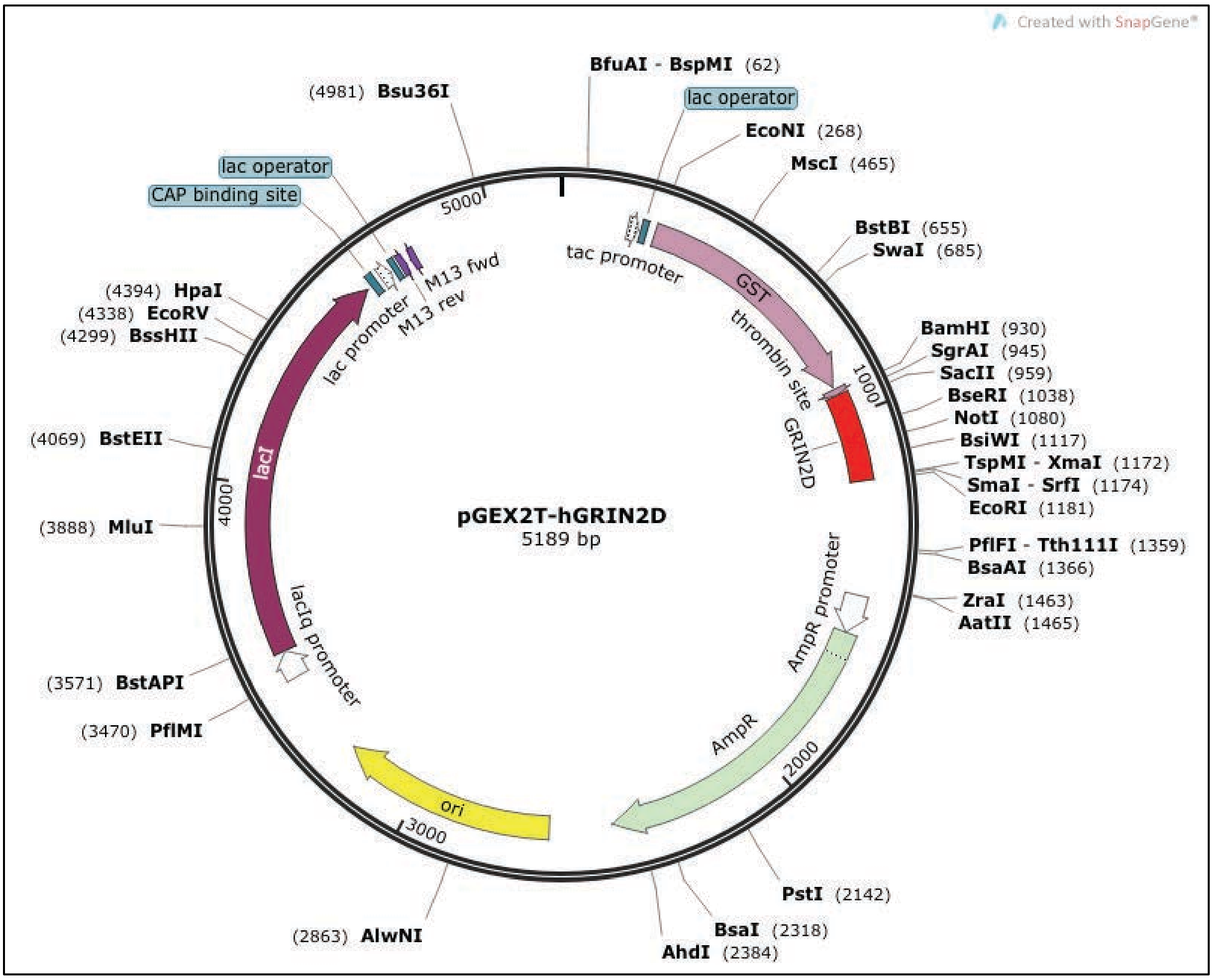
Created with SnapGene®
BfuAI - BspMI (62)
lac operator
EcoNI (268)
MscI (465)
BstBI (655)
SwaI (685)
BamHI (930)
SgrAI (945)
SacII (959)
BseRI (1038)
NotI (1080)
BsiWI (1117)
TspMI - XmaI (1172)
SmaI - SrfI (1174)
EcoRI (1181)
PflFI - Tth111I (1359)
BsaAI (1366)
ZraI (1463)
AatII (1465)
PstI (2142)
BsaI (2318)
AhdI (2384)
(2863) AlwNI
(3470) PflMI
(3571) BstAPI
(3888) MluI
(4069) BstEII
(4299) BssHII
(4338) EcoRV
(4394) HpaI
CAP binding site
lac operator
(4981) Bsu36I
tac promoter
GST
thrombin site
GRIN2D
AmpR promoter
AmpR
ori
lacIq promoter
lacI
lac promoter
M13 rev
M13 fwd
pGEX2T-hGRIN2D
5189 bp
1000
2000
3000
4000
5000

Figure 4.12 – Vector Map of the pGEX2T-hGRIN2D Vector. Utilised for bacterial expression of GST-fusion protein.

Following sequence verification, BL21 *E.coli* were transformed with the pGEX2T-GRIN2D vector. BL21 *E.coli* are highly efficient, competent cells, which allow routine expression of non-T7 promoter based plasmids(146). Following transformation, trial induction and culture was performed on a small scale. 10 ml samples of cultured bacteria were collected at various time points, and analysed by SDS-PAGE. Upregulated production of a protein band between 25 and 35 kDa was maximal at 4 hrs post-induction. Pull-down of this protein utilising glutathione sepharose beads was also successful (Figure 4.13).

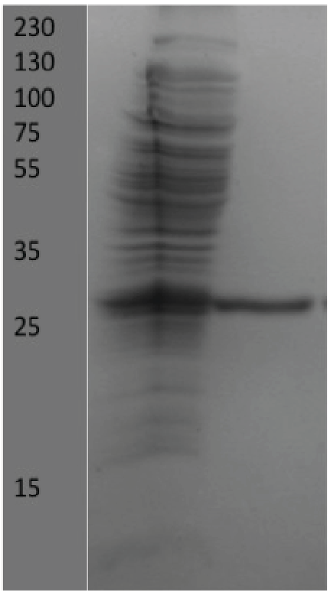

Figure 4.13 – Isolation of GST-GRIN2D from Bacterial Lysate. 12% SDS PAGE Gel, Coomassie Stain.

Lane 1 – Bacterial Cell Lysate

Lane 2 – Purified GRIN2D-GST Protein following incubation with glutathione sepharose beads.

Predicted size GST-GRIN2D = 34 kDa

Reserved, uninduced transformant bacteria from this process were cultured and stored as a stock culture for subsequent expressions. Following optimisation, large-scale protein production was performed utilising 2 litres of bacterial culture. Stock culture was incubated for 2 hrs, until an OD_{600} of 0.6 was reached. Then induction with 1 mM IPTG was performed and the culture further incubated for 4 hrs. The culture was then collected, spun down, and the bacterial pellet lysed using a sequential freeze/thaw cycle at -80^{o}C, and mild sonication in a lysis buffer containing DTT and protease inhibitors to reduce the chances of protein denaturation or aggregation. The bacterial lysate was then incubated with 1 ml of glutathione sepharose beads for 2 hrs. Elution was performed with 1 ml of 30 mM glutathione sepharose at pH 8.5. The predicted pI of GST-GRIN2D is 7.53, but fortunately, protein aggregation was not an issue at pH 8.5. However, interestingly, any greater volume of elution buffer resulted in aggregation of the protein within the eluate, independent of pH. Eluate from this process contained glutathione, which interfered with all attempted protein quantification assays. The eluate was therefore buffer exchanged using a PD10 column and quantified. The sample was placed into storage buffer consisting of 50mM MES at pH 5.5, with 150 nM NaCl, a point further from the pI of the produced protein, thereby decreasing the risk of aggregation during storage.

Bands apparent on SDS-PAGE gel fall below not only the expected size of GRIN2D-GST, but was also not the size of the GST tag alone. To ensure that this band represented the expected product, plasmid DNA was extracted from the transformed BL21 bacteria and sent for sequencing. This confirmed the presence of both the GST tag and the DNA for mouse or human GRIN2D within the plasmid, increasing the likelihood of this protein being the expected compound. Mass spectroscopy was then performed, which indicated that the GRIN2D component of the fusion protein was being cleaved early within the sequence, presumably by a bacterial peptidase, with only a short fragment remaining as the fusion protein. Further validation work has shown this short fragment as sufficient to act as an antigen in both ELISA and IHC.

CHAPTER FIVE

INVESTIGATING GRIN2D AS A TUMOUR ENDOTHELIAL MARKER IN A MURINE COLORECTAL CANCER MODEL

5.1 GRIN2D AS A TEM IN MURINE COLORECTAL TUMOURS

While GRIN2D represented a potential endothelial marker in colorectal cancer, with anti-angiogenic effects demonstrated *in vitro,* translation of this potential required *in vivo* studies. This chapter describes the establishment of a murine vaccine model utilising recombinant GRIN2D as the basis for a vaccine. Then, the effects of this novel vaccine upon *in vivo* angiogenesis and colorectal cancer growth are also described, utilising the subcutaneous sponge and subcutaneous tumour models. All protocols were performed at [redacted] [redacted] under the Project License 40/3339 held by Roy Bicknell. A personal license (number 70/25131 - subsequently transferred to the electronic license system, with the designation I350D34BB) was gained to allow personal performance of animal work.

To ensure transferability of GRIN2D into murine experiments, a pilot study was performed utilising subcutaneous growth of CT26 colorectal cancer cells in Balb/c mice. A previous protocol performed within the Bicknell laboratory by Joseph Wragg had established the optimum cell number to be implanted within a subcutaneous tumour model in 4T1 cells was $1x10^5$. This number was based on the length of time required for tumour establishment, and also the rate of subsequent tumour growth to allow adequate observation before the protocol end-point was reached. Therefore, $1x10^5$ CT26 cells were injected into the flank of balb/c mice, allowed to establish for one week, then observed for a further two weeks, until the maximum permissible size of 2 cm^3, or tumour ulceration was observed. Tumours from treated mice and tissues from normal control mice were isolated and analysed for presence of GRIN2D.

5.1.1 – The CT26 Cell Line

The CT26 cell line was originally generated in 1975 through chemical induction of rectal malignancy by intrarectal injection of N-nitroso-N-methylurethane(147). It was characterised as an undifferentiated, grade IV malignancy in its original host, a female balb/c mouse. It subsequently underwent repeated subcutaneous transplantation, with 70-100% of subsequent tumour transplant recipients developing metastases, most frequently within the lungs. It has become an established cell line in colorectal cancer research with metastases corroborated in both subsequent subcutaneous models(148), and in an orthotopic model(149). Due to its reliability, rapid growth, and the potential for metastases, it was taken forward as the cell line of choice.

5.1.2 – Isolation of Murine Endothelial Cells

To determine the endothelial specificity of GRIN2D in normal balb/c murine tissues, and in subcutaneous CT26 tumours, it was necessary to isolate endothelium from tissue bulk. This was performed using magnetic Dynabeads® which had been conjugated to anti-mouse-PECAM-1 antibodies. Following tissue homogenation using collagenase type 1, the sample was incubated with the antibody-conjugated Dynabeads®, and separated from the tissue bulk using a magnet within a 15 ml centrifuge tube. Isolation efficiency was assessed using RTqPCR, measuring differential expression of PECAM levels between the endothelial cell fraction and tissue bulk fraction, normalised to beta-actin.

5.1.3 – The Expression Profile of GRIN2D in Murine Tissues and Colorectal Cancer

For further murine experimentation to be considered safe, an expression profile of GRIN2D within the normal murine tissues was established to ensure off-target effects of therapy could be predicted. Further RTqPCR was performed to ascertain relative expression of GRIN2D in gross terms, using beta-actin as a housekeeper gene, and in terms of endothelial specificity by using PECAM-1 as housekeeper, then adjusting for isolation efficiency. When considered in the endothelial compartment, GRIN2D was highly overexpressed in multiple biological replicates of CT26 colorectal carcinoma, when compared to normal body tissues. When tissue bulk was analysed, this specificity was lost, with high levels of expression within the brain, as would be expected, but also to a degree in the lung (Figure 5.1).

(i)

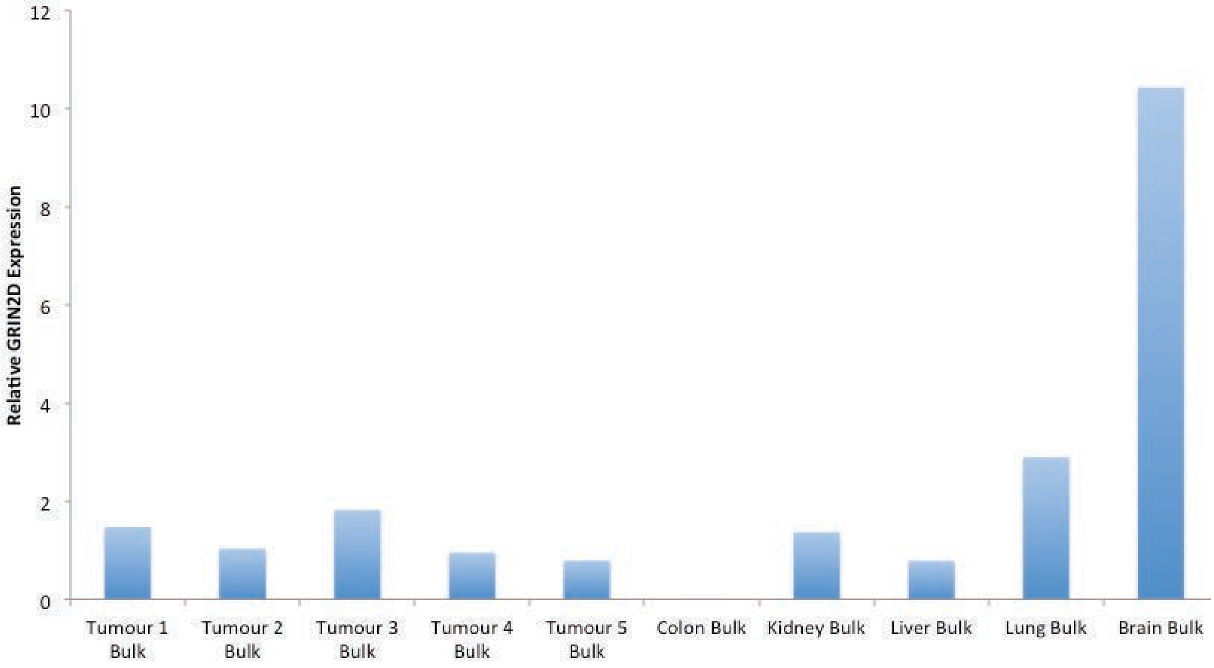

(ii)

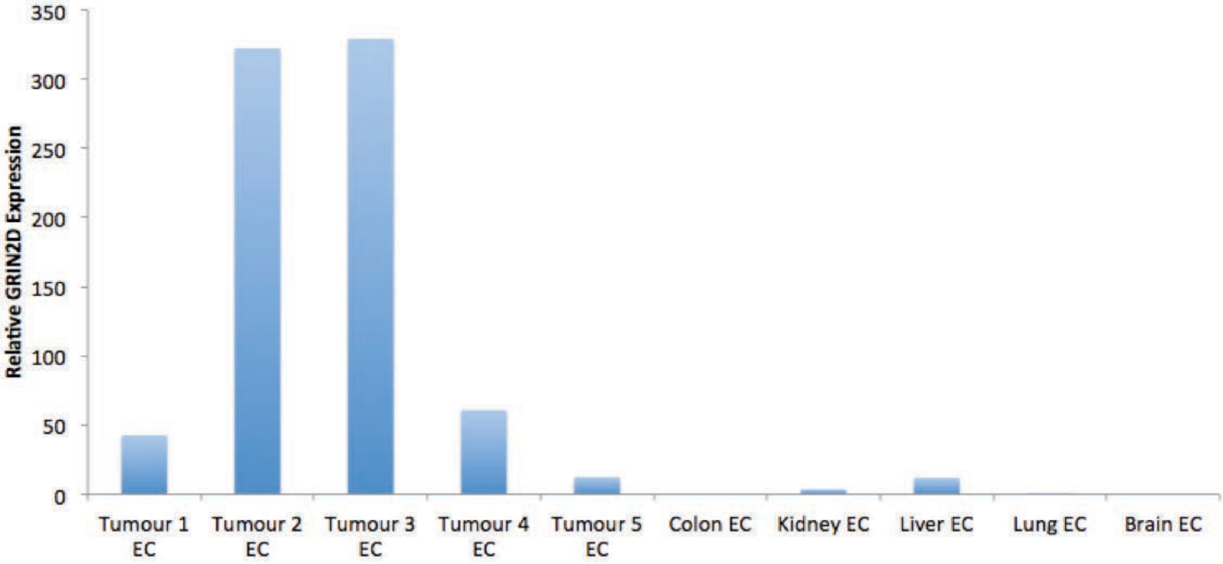

Figure 5.1 – Expression of GRIN2D in Murine Tumours and Tissues.

(i) Expression in the non-endothelial cell fraction of body tissues and tumours, normalised to beta actin; (ii) Relative GRIN2D expression in endothelial cell isolates, normalised to Beta actin, and adjusted for endothelial isolation efficiency

5.2 THE EFFECT OF A GRIN2D-FC PROTEIN VACCINE IN MURINE MODELS OF ANGIOGENESIS AND COLORECTAL CANCER

Previous work by the Bicknell group has shown that protein-based vaccination of Robo4, a tumour-specific endothelial cell marker in lung cancer, can lead to impaired tumour growth in a subcutaneous murine Lewis lung carcinoma model(135). Therefore, it was possible that this method may be applicable utilising GRIN2D as an endothelial-specific tumour marker in Colorectal Cancer. This section describes the investigation of such a vaccine model, and its effect on physiological angiogenesis and subcutaneous tumour growth.

5.2.1 – Establishment of a Murine GRIN2D Vaccine Model

To pursue the project goal of investigating a vaccine-based approach to colorectal cancer targeting, a murine protein-based vaccination model was established. Fc-fusion proteins of both human and mouse GRIN2D were taken forward as antigens. By vaccinating with either a non-self (human) and self (antigen), differential immune responses could also potentially be observed. Non-self antigens mirror infectious disease based vaccines, where the antigens are viral or bacteria components. Vaccination with self-antigens is analogous to products such as OncoVax™, which utilises individual patient tumour cells in a vaccination strategy.

In order to vaccinate against a self-antigen, it is necessary to evade the innate mechanisms for avoidance of auto-immunity, by breaking immune tolerance - a phenomenon controlled by regulatory T-cells(150). Current investigation into mechanisms for breaking of immune tolerance in humans has taken two approaches.

The first is direct infusion of immune antigen-presenting cells, and the second, more established route is co-vaccination with an adjuvant which is highly immunogenic(151).

Freund's adjuvant was selected as a vaccine partner to GRIN2D. It is essentially paraffin oil containing mannide mono-oleate as a surfactant, with dried and inactivated mycobacterial components (Freund's complete adjuvant, FCA) or without mycobacteria (Freund's incomplete adjuvant, FIA)(152). FIA induces the innate immune system, and stimulates cytokine release(153), whereas, in addition, FCA enhances antigen uptake by antigen presenting cells.

Utilising this approach, mice received 50 µg of human or mouse GRIN2D-Fc fusion protein subcutaneously with 100 µl of Freund's adjuvant at two-week intervals. FCA was utilised at Day 0, and FIA at Day 14. Serum was collected via a tail vein bleed on Days 0 and 14, with a terminal cardiac bleed under general anaesthetic performed on day 28 (Figure 5.2). An equivalent control group of mice received 50 µg of human Fc only with adjuvant, in place of the fusion protein. ELISA was performed to quantify GRIN2D-specific antibody titers along the time course of the protocol, and to identify the isotypes of the induced antibodies from each protocol.

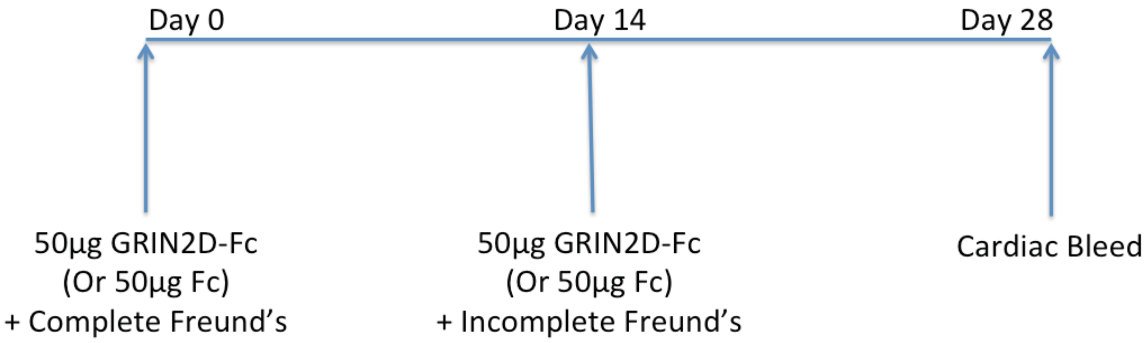
Day 0
Day 14
Day 28
50µg GRIN2D-Fc
(Or 50µg Fc)
+ Complete Freund's
50µg GRIN2D-Fc
(Or 50µg Fc)
+ Incomplete Freund's
Cardiac Bleed

Figure 5.2 – GRIN2D Vaccination Protocol

Following immunisation of mice with human GRIN2D-Fc, a significant increase in specific antibodies to hGRIN2D was detected (P<0.001, Mann-Whitney test), with IgM antibodies predominating (Figure 5.3). When the immunisation was performed with mouse GRIN2D, the immune response was predominated by IgG1 and IgG2b, indicating a Th-2 T-cell response, consistent with immunisation(76). Importantly, there was no evidence of a significant difference in antibody response to the Fc component of the vaccine, when measured by ELISA (p=0.379, Mann Whitney).

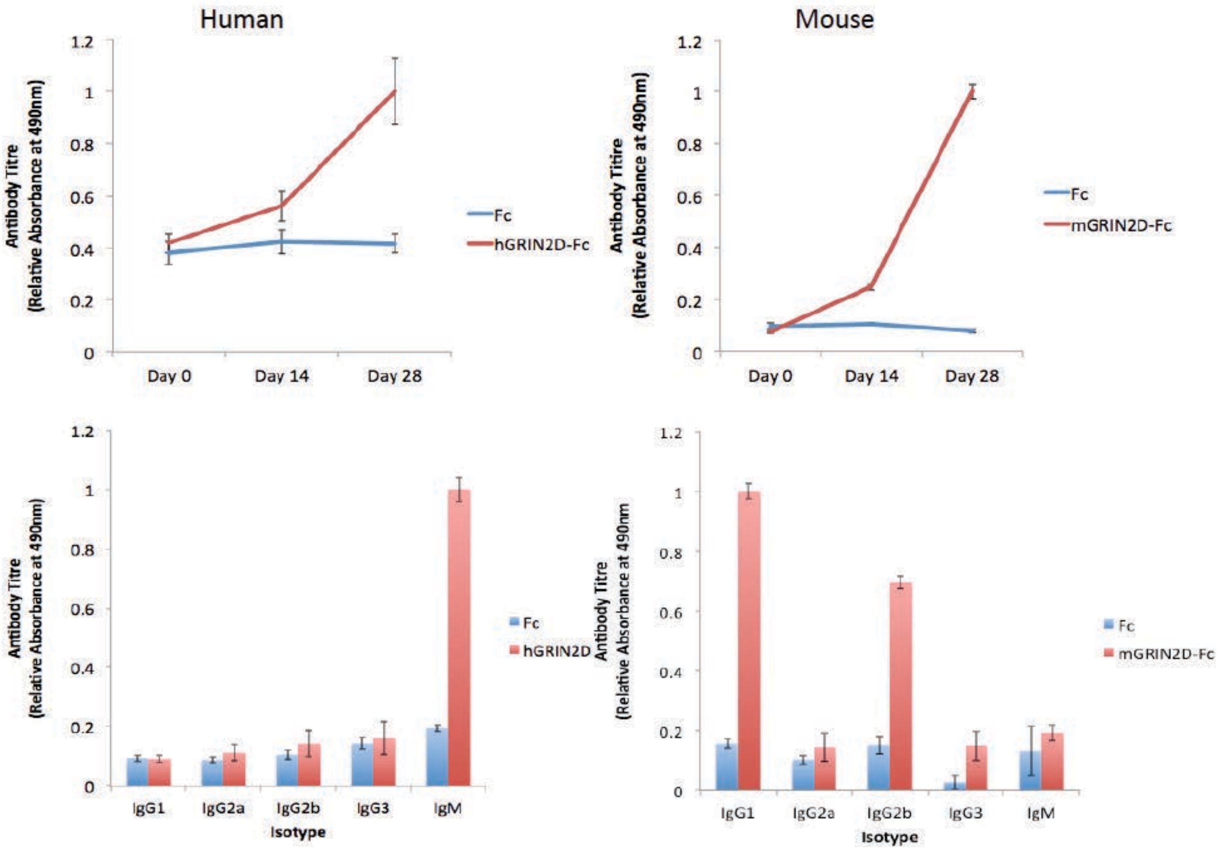

Figure 5.3 – Antibody Response to GRIN2D-Fc Vaccination in Balb/c Mice.

While both immunisation with human and mouse GRIN2D elicits a highly significant, specific antibody response ($p<0.001$ Mann-Whitney), immunisation with hGRIN2D is associated with a predominantly IgM response, with mGRIN2D immunisation resulting in an IgG1 and IgG2b predominant response.

5.2.2 – The Effect of GRIN2D Vaccination on Physiological Angiogenesis

As knockdown of GRIN2D expression in HUVEC had been shown to compromise angiogenesis *in vitro,* these effects were investigated *in vivo* using the murine subcutaneous sponge assay, a validated technique for studying physiological angiogenesis(154). At day 28 of the GRIN2D vaccination protocol, instead of cardiac bleed, treatment and control mice underwent surgical implantation of subcutaneous sponges into the flank. Basic Fibroblast Growth Factor (bFGF) was injected into the sponge on alternate days for 2 weeks (Figure 5.4).

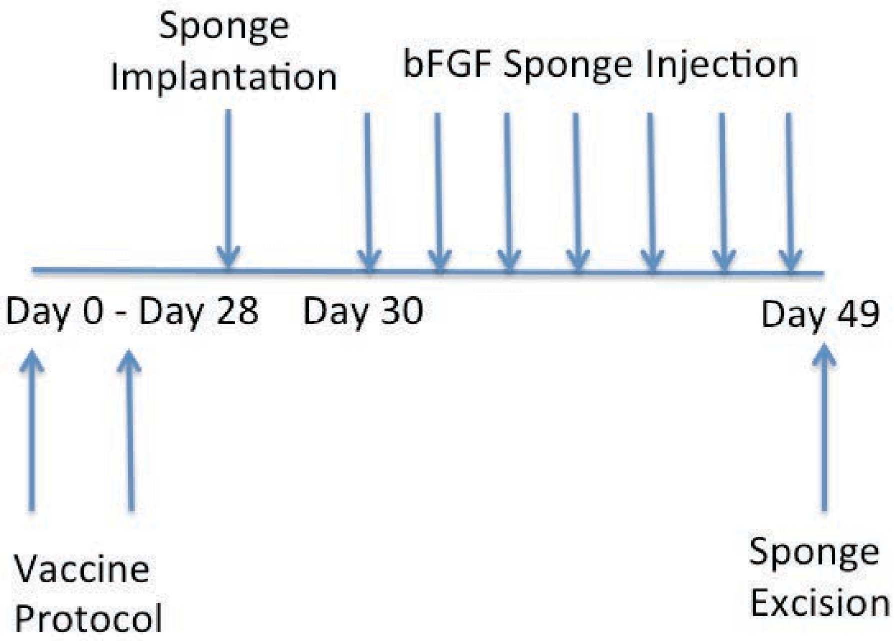

Figure 5.4 – Combined Protocol of Vaccination and Subcutaneous sponge assays

The sponges were then excised, fixed in formalin, embedded in paraffin, sectioned and stained using haematoxylin and eosin. This allowed a gross quantitative analysis of vascular invasion between groups by the analysis of the sponge using ImageJ software (National Institutes of Health, Bethesda, USA). This was achieved by creating a binary mask image of the entire sectioned sponge, and quantifying the invaded proportion relative to the blank, uninvaded portion. Random microscopic fields at 10x magnification were then assessed, and vessels further quantified at this cellular level.

Following vaccination with hGRIN2D-Fc, there was no significant change in the vascular invasion or number of visible vessels per field of sponge. However, following vaccination with mGRIN2D-Fc, a significant decrease in both sponge invasion ($p=0.0026$) and vessel density ($p<0.0001$) was observed (Figures 5.5 and 5.6).

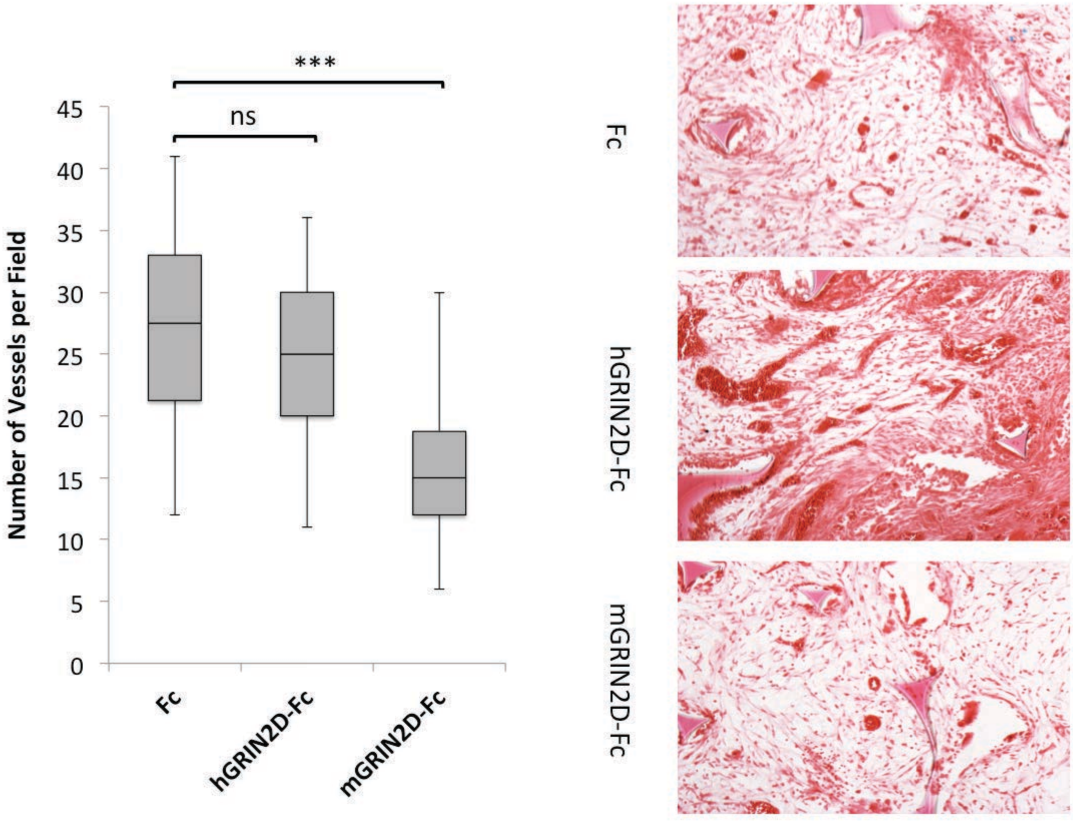

Figure 5.5 – Sponge Vascular Density. A significant decrease in sponge vascular density was observed following mGRIN2D-Fc Vaccination compared to Fc control ($p<0.001$, Mann Whitney), but not following hGRIN2D-Fc Vaccination. n = 6 sponges per group, and 5 random fields per sponge. Haematoxylin and Eosin Staining.

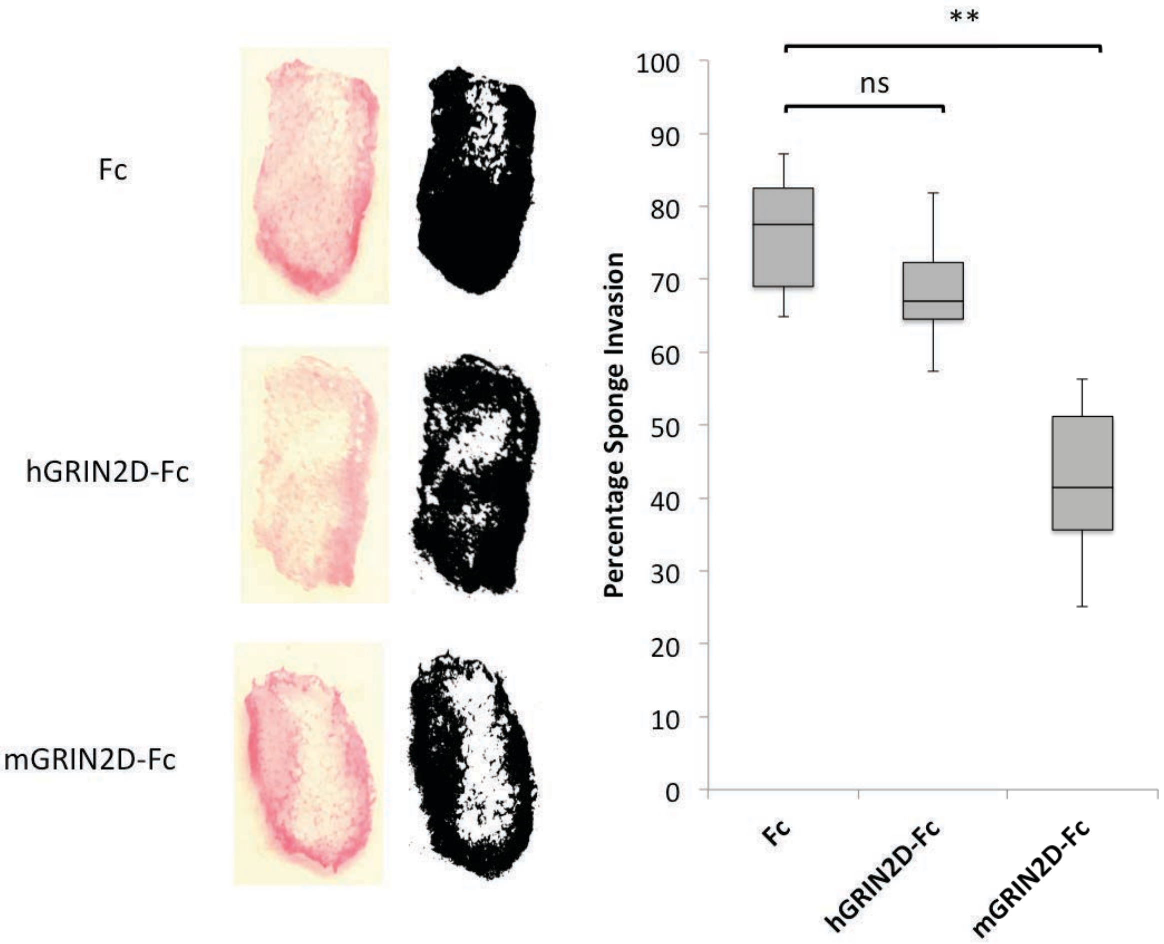

Figure 5.6 – Macroscopic Evaluation of Sponge Assay. Paraffin embedded sponges were stained with Haematoxylin and Eosin, imaged, and reduced to a binary mask using ImageJ software, followed by quantification. Vaccination with mGRIN2D-Fc resulted in a significant decrease in sponge invasion compared to Fc controls (p=0.0026, Mann-Whitney), where no significant decrease was observed following vaccination with hGRIN2D-Fc (p=0.347, Mann-Whitney)

5.2.3 Establishment of a Murine Subcutaneous Colorectal Cancer Model

The CT26 murine colorectal cancer cell line was selected for ongoing study. To enable real-time *in vivo* monitoring of tumour growth and potential metastases, the cell line underwent lentiviral transfection with the MSCV-Luc plasmid (88). This protocol had been optimised, and the CT26-Luc cell line validated within the Bicknell Laboratory by Joseph Wragg. The optimum cell number to be utilised within this model based on length of tumour establishment and rate of growth was determined from previous experiments using 4T1 breast cancer cells as $1x10^5$. Over 3 weeks, this cell number had produced a tumour suitable for future histological analysis, without becoming overly burdensome for the experimental animal. Tumour growth was monitored by routine calliper measurement, and by use of the *In Vitro* Imaging System (IVIS) within the BMSU. The IVIS (PerkinElmer, Walton, MA, USA) is an integrated system allowing real-time, non-invasive imaging while maintaining experimental animals under general anaesthetic. It is able to quantify the bioluminescence emitted by CT26-Luc cells, giving an objective measure of growth, although it relies upon viable cells to produce bioluminescence(155), which will not account for a large tumour with a necrotic core. To support absolute quantitation, the system measures the ‘dark charge’ of the platform during downtime and subtracts this from the total bioluminescence. To facilitate visualization, D-luciferin was injected intraperitoneally at a dose of 30 mg/kg body weight. Images were taken every minute for 25 mins following luciferin injection to ensure peak bioluminescence was measured on each day. This is important as the kinetics of luciferase can vary day-to-day, introducing error to results(155). Tumours were monitored until ulceration occurred or the tumour mass exceeded 2 cm^3, whichever was sooner. Tumours followed a standard growth curve, with little inter-tumour variability (Figure 5.7,i). The end points of excessive tumour growth and potential ulceration were increasingly encountered at 21 days post tumour injection. At the end point of the protocol, the experimental animals again underwent intraperitoneal injection of D-luciferin, followed by resection of the primary tumour. The peritoneal and thoracic cavities were opened, and IVIS imaging performed. No evidence of metastasis was noted on bioluminescent imaging (Figure 5.7,ii). Subsequent haematoxylin and eosin staining of multiple body organs also refuted the presence of metastases in this model.

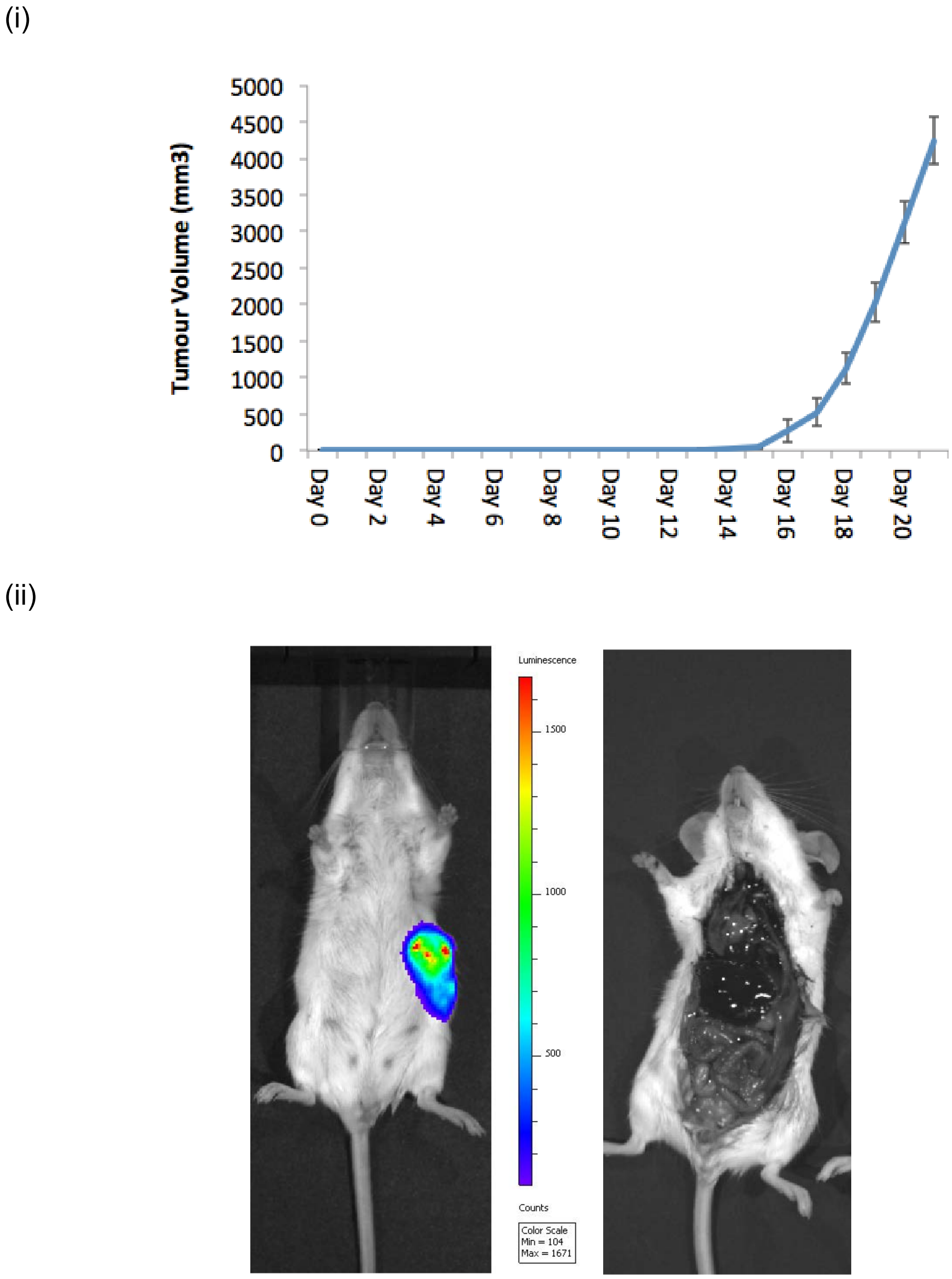

Figure 5.7 – The CT26-Luc Tumour Model. i) A typical growth curve of subcutaneous CT26-Luc colorectal cancer cells in Balb/c mice. ii) Typical IVIS imaging of tumour at day 21 post implantation, and the absence of bioluminescent evidence of metastasis following primary tumour resection.

5.2.4 The Effect of GRIN2D Vaccination on Subcutaneous CT26 Tumour Growth

Once reliable growth of subcutaneous CT26-Luc tumours had been established, and the vaccine method shown to induce a specific immune response to GRIN2D, the protocols were combined (Figure 5.8).

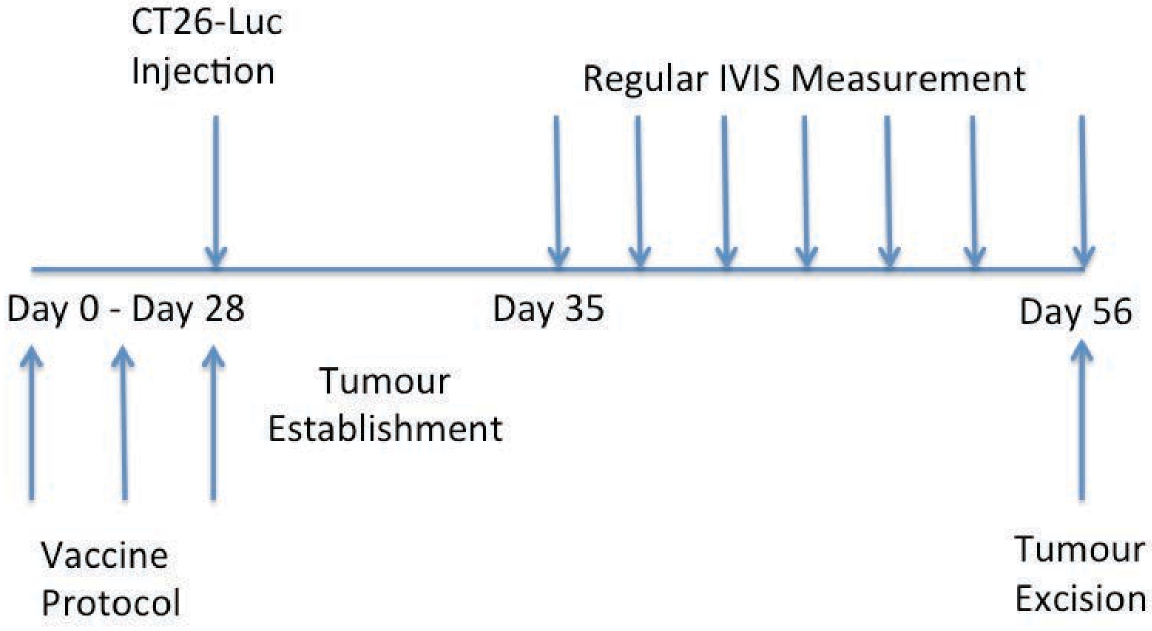
CT26-Luc
Injection
Regular IVIS Measurement
Day 0 - Day 28
Day 35
Day 56
Tumour
Establishment
Vaccine
Protocol
Tumour
Excision

Figure 5.8 – Protocol for GRIN2D Vaccination Followed by Subcutaneous CT26 Tumour Growth Monitoring.

Following immunisation of mice with human GRIN2D-Fc, there was no difference in the growth rate of subcutaneous CT26 tumours to the control group. However, following mouse GRIN2D-Fc vaccination, a significant decrease in tumour growth by calliper measurement was observed (p=0.004, Mann-Whitney) (Figure 5.9). This was corroborated by analysis of excised tumour weight (p=0.0274) and IVIS monitoring of tumour growth. Interestingly, RTqPCR quantification of GRIN2D expression within the endothelial compartment of the excised tumours endothelial cells demonstrated a 5.5-fold upregulation of expression within the mGRIN2D-Fc treated group compared to controls, when adjusted for endothelial isolation efficiency (p=0.0069, Mann-Whitney).

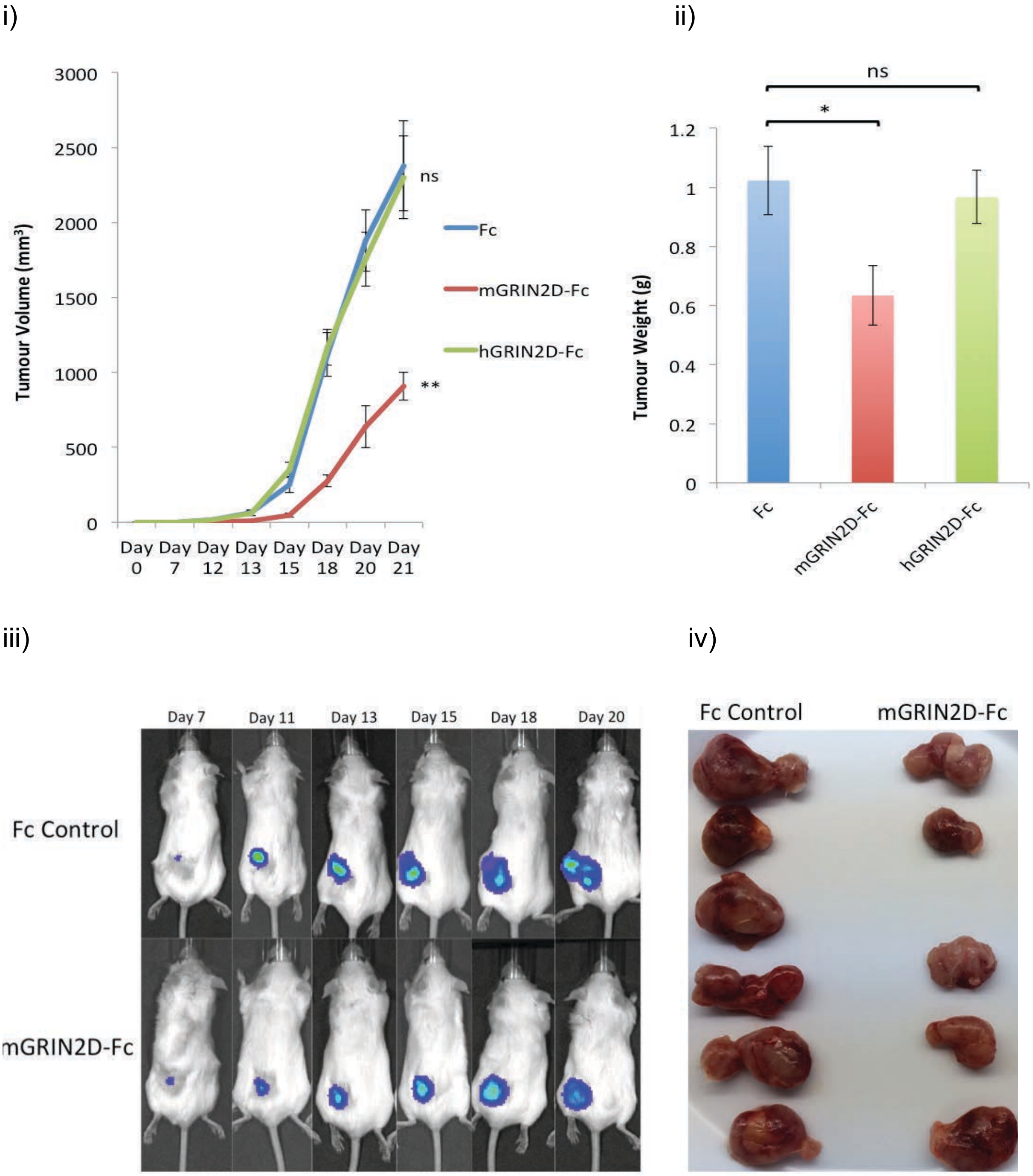

Figure 5.9 – Vaccination with mGRIN2D-Fc Significantly Decreases Subcutaneous CT26 Tumour Growth, but Vaccination with hGRIN2D-Fc Does Not. Reduction in growth with GRIN2D-Fc is confirmed by (i) calliper measurement,

post-resection tumour weight (ii) and size (iv), and throughout the experiment by IVIS imaging (iii). Mann Whitney U-Test to determine significance. n=6 per group. Mouse 3 in the mGRIN2D-Fc treated group died during IVIS imaging, so was not included in statistical analyses.

Vascular density was quantified in excised subcutaneous CT26-Luc tumours, indicating a significant decrease in the numbers of vessels per field in five random microscopic fields per tumour (mean 78 vs. 62 vessels per field, p=0.0367, Mann Whitney) (Figure 5.10)

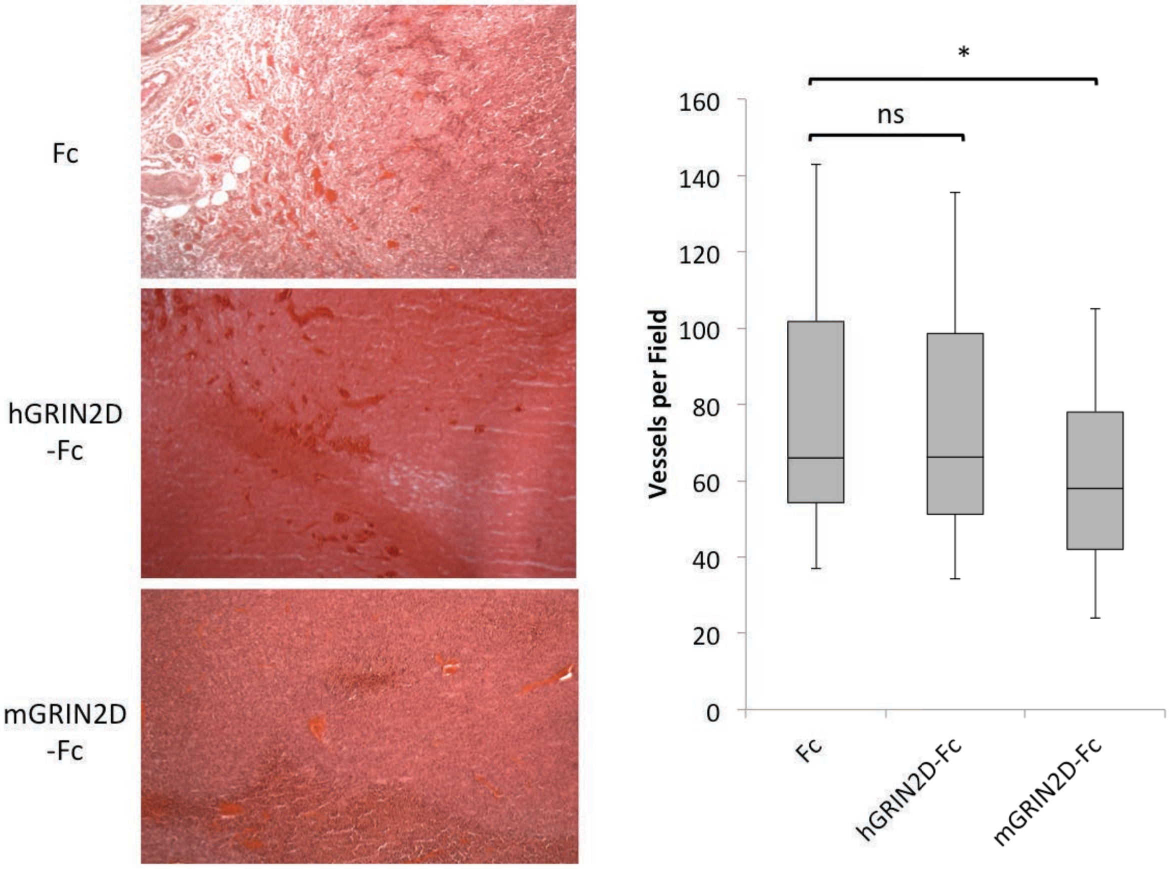

Figure 5.10 – Tumour Vascular Density is Decreased by mGRIN2D-Fc Vaccination, but not by hGRIN2D-Fc Vaccination. Haematoxylin and Eosin staining of excised subcutaneous CT26 tumours.

Chapter Conclusion

Murine vaccination with the human form of GRIN2D precipitated only a minor specific IgM response with no apparent effects on angiogenesis or tumour growth *in vivo*. However, vaccination with endogenous murine GRIN2D stimulates a specific increase in IgG1 and IgG2b titers, indicative of a Th2 T-Cell response. Vaccination significantly impairs physiological angiogenesis as demonstrated by a significant reduction in both sponge invasion and vascular density in the subcutaneous sponge assay. Aside from this physiological effect, vaccination with mGRIN2D-Fc significantly decreases the rate of subcutaneous CT26 tumour growth. Analysis of the resected tumours indicates a small, but statistically significant decrease in vascular density within the mGRIN2D-Fc treated group, adding weight to the likelihood that the observed effect is due to a vascular targeted treatment.

CHAPTER SIX

DISCUSSION

DISCUSSION

The search for novel adjuvant treatments in colorectal cancer has transformed prognosis in a disease that was once uncontrollable if initial surgical resection was not successful. The ability of chemotherapy and, to some extent, radiotherapy to cause a reduction in tumour size has enabled both primary resection in cases previously deemed to be inoperable, and also systemic treatment of potential or observed systemic metastasis. More recently, biological agents have formed the next frontier in agent development, with Cetuximab, Bevacizumab, and a third monoclonal antibody, Panitumumab, currently licenced for use in the treatment of advanced colorectal cancer. However, evidence of benefit in CRC is limited, with response rates below 5% when used as a monotherapy (23). Development of new agents necessitates the identification of cell surface target proteins that are consistently upregulated in malignancy, but not in other body tissues. The tumour endothelium is hypothesised to be an effective target in malignancy, due to its relative genetic stability, and the ease of access from the systemic circulation in contrast to tumour cells(156).

Initial efforts targeted the systemic process of angiogenesis, but this approach risks off-target side effects due to a lack of specificity. A number of approaches have been employed to identify so-called Tumour Endothelial Markers (TEMs) to achieve more accurate tumour vascular targeting, but the most applicable to colorectal cancer was the work of St. Croix et al. in 2000(53), which utilised primary isolation of endothelium from normal colon and colorectal cancer, followed by RNA extraction and serial analysis of gene expression. The original targets identified by this group (TEM1-9) have been open to some criticism, specifically with TEM1, or endosialin, having been shown to be a contaminant from tumour associated fibroblasts and pericytes within the endothelially enriched compartment(157). However, it has also been shown that TEM1 knockout mice exhibit impaired angiogenesis in an orthotopic xenograft model of colorectal cancer(158). Aside from this group of endothelial targets, work following similar methodology within the Bicknell group has identified Robo4(159) and Clec-14A(160) as validated tumour endothelial markers.

In Chapter three, the results of further genomic analysis within the Bicknell group of patient-matched colorectal cancer and normal colon were explored. A systematic approach to validation including exhaustive literature review, subsequent validation on multiple biological replicates, and immunohistochemistry was completed, resulting in GRIN2D being identified as a putative TEM in colorectal cancer. The utilisation of only one further replicate to narrow the shortlist from nine to four candidates may have introduced inaccuracy into this process, as candidates may have been dismissed unfairly at this stage, should the biological replicate that was used have been genetically atypical of CRC. However, this fact does not affect the decision to pursue GRIN2D as a promising target. The lack of a specific antibody against human GRIN2D was severely limiting in validating GRIN2D as a target on a protein level through immunohistochemistry. While an endothelial pattern was observed in CRC with the commercially available, non-specific, antibodies, this pattern had to be confirmed retrospectively once a polyclonal serum was produced as part of this thesis. It would have been scientifically more sound to gain a reliable endothelial pattern before pursuing GRIN2D further. This staining pattern could also be confirmed more convincingly by performing immunofluorescent co-localisation with an appropriate endothelial marker such as CD31.

Glutamate receptors have been previously described within human cancer cell lines(66), and knockdown of some glutamate receptors, but not GRIN2D, has demonstrated variously pro- and anti-tumour effects(161). GRIN2D's specific role in visceral pain perception and colonic inflammation has also been previously defined(64), and raises interest in GRIN2D as a protein of interest within the GI tract. Its predominant neonatal and embryological expression profile(60) also gives a logical reason as to why it may be upregulated in the proliferative microenvironment of a malignancy.

Serum levels of glutamate have been observed to tally with Gleason grade in prostatic cancer(162), and noted to act as a marker of malignant potential in pancreatic cancer precursor lesions(163). The hypothesis linked to this latter observation is especially relevant to colorectal cancer, as what is proposed is that glutamate acts as a genetic switch which decreases the threshold of k-ras-induced oncogenic signalling (164). Mutation of the k-ras oncogene is a well-recognised step in the progression from adenoma to colorectal cancer, as discussed in Chapter one.

The finding of upregulated GRIN2D expression in CRC-associated endothelium in Chapter four adds another level of interest to these previous studies identifying the significance of glutamate and its receptors within tumour cell biology. The shared embryonic stem cell lineage of neuronal and vascular cells is well recognised, with significant cross-expression of conventionally endothelial and conventionally neuronal proteins observed(165). Indeed, the same processes govern modelling of both vascular and neuronal architecture. It is not therefore a great surprise that the neuronal glutamate receptor GRIN2D could also be expressed on endothelial cells. Also within Chapter four, it has been shown that siRNA knockdown of GRIN2D function in HUVEC decreases cellular migration, tube formation and chemotaxis, which may well be due to its role as a calcium channel component. VEGF, a potent and well known stimulator of angiogenesis, propagates endothelial cell migration, tube formation, and proliferation, at least in part, through VEGF-receptor-mediated calcium influx into the endothelial cell(166). It has also been shown that calcium influx into the cell determines VEGF-driven vascular permeability in the frog microvasculature(167). With reference to this point, the function of GRIN2D in neurons holds relevance, in that it induces a prolonged action potential compared to other GRIN2/3 subgroup members(168,169). It is not a great step to transfer this potential for prolonged intracellular calcium influx to CRC-associated endothelial cells, where it may offer a proliferative or survival advantage. Calcium metabolism also accounts for the observed anti-angiogenic effects of GRIN2D knockdown. Specifically, increases in free intracellular calcium concentration have been shown to promote cellular migration, and formation of vascular tubules in a Matrigel assay(170). This has been translated to assays involving the migration and tubulogenesis of tumor-derived endothelium, in which arachidonic acid, a potent inducer of intracellular calcium flux, again increased cellular migration and tube formation(171). There has been a call for interference in calcium metabolism to be utilized in targeting tumour angiogenesis(172), and it may be that targeting of GRIN2D is a route to achieve this.

Within Chapter three, the sequence and structure of GRIN2D was analysed, and a therapeutic vaccine produced. In order to be targetable by circulating antibodies, the antigen must be extracellular, and unique to the protein of interest, to prevent off-target effects. The N-terminal domain of glutamate dependent NMDA receptors defines their function(59), and is universally considered to be extracellular, in contrast to the C-terminus, which is variably described as extra- or intracellular. This difficulty was demonstrated by the bioinformatic prediction performed to determine transmembrane regions, and hence extracellular regions in GRIN2D. This exercise demonstrated the difficulties associated with relying upon bioinformatics software for target design. Structure prediction sites rely upon calculations of molecular charge and likely intra- and inter-molecular interactions mapped to known existing structures of comparable sequences. They are not a substitute for protein crystallography, but are much more accessible and readily performed(173). These are, however, issues that must be allowed for when dealing with a target of interest about which there is little consensus regarding structure.

Not only does the protein need to be unique and targetable, but it must also possess a secondary and tertiary structure that is likely to stimulate an immune response within the host. Again, bioinformatic software was utilised to determine a secondary structure for the extracellular N-terminus of GRIN2D, demonstrating that there were likely to be coiled and helical elements, increasing its chances of being immunogenic.

The differing immune response precipitated by the human and murine GRIN2D N-terminus sequences are an interesting finding. Logic would dictate that immune reaction to a foreign protein sequence would be more established than that precipitated by breaking tolerance to a highly similar self-antigen. Hypothetically, it is also possible that the ‘foreign’ part of the human protein would be the focus of the immune response, with the equivalent ‘self’ segments stimulating less of a response. This would contrast to the full ‘self’ sequence in the case of mGRIN2D, which would stimulate antibodies to its full length. Psipred bioinformatic prediction of the secondary structure of the human and mouse GRIN2D peptide sequences ostensibly shows conformational homology. However, the difference in the middle section of the peptide sequence is potentially an interesting one:

```
                                                  37
Human : MRGAGGPRGPRGPAKMLLLLALACASPFPEEAPGPGGAGGPGGGLGGARPLNVALVFSGP

Mouse :  MRGAGGPRGPRGPAKMLLLLALACASPFPEEVPGPGAAGG - - - GTGGARPLNVALVFSGP
```

At position 37, there is a deletion within the mouse sequence of PGG - a proline and two glycine residues. While these residues are not particularly immunogenic in their own right, the absence of a proline-glycine sequence within this region may be omitting a ‘helix breaker’(174). Proline is a unique amino acid in that it lacks the amide hydrogen atom, and it is therefore unable to act as a hydrogen bond donor. Consequently, it does not tend to form bonds with the carbonyl group of another residue in the preceding turn of the helix, thereby disrupting its uniform turns(175). While this deletion has not indicated a specific effect in the bioinformatic structure prediction that was performed, this region may well represent the reason for the differential in immune reactivity of the human and mouse GRIN2D components of the Fc-fusion proteins. The consequent lack of physiological effect observed on either angiogenesis or tumour growth with immunisation with hGRIN2D-Fc is likely due to this difference in immunogenic potential between the sequences.

The creation of an Fc-fusion protein was chosen as a method to increase immunogenicity of the GRIN2D target sequence. This has previously been shown to be a successful strategy both as a result of an increased half-life of the fusion protein(176) and also through Fc receptor-mediated uptake by antigen-presenting cells such as dendritic cells(177).

Completion of the vaccine strategy required selection of an appropriate adjuvant to stimulate the host immune system. Freund's adjuvant was selected for its proven record, and its ability to stimulate both a Th1 and Th2 response to the co-administered antigen, and stimulate lasting immune memory(178). This vaccine formulation would not be appropriate for human vaccination due to its severe local toxicity, and a different adjuvant strategy, such as the use of an aluminium salt, which is the most commonly used strategy in human vaccination. This approach has been successfully utilised in Robo4-Fc vaccination in the context of subcutaneous Lewis Lung Carcinoma tumours(135), and would represent a logical next step for GRIN2D, and would give increased translational impact to this work.

The IgM predominant response triggered by hGRIN2D-Fc immunisation indicates an immature immune response, and results only from early differentiation of B-cells into plasma cells(75). Isotype switching would normally be expected if a significant immune response had been elicited, as was the case with mGRIN2D-Fc vaccination. This fact alone could explain the difference observed between the physiological effects of the vaccinations on both angiogenesis and tumour growth. The IgG1 response elicited by mGRIN2D-Fc vaccination more accurately reflects a mature immune response, and is consistent with the presence of persisting circulating immune molecules to the target. This is associated with a T-helper 2-type (Th2) immune reaction(179), which is typical of vaccination with a protein-based construct(180). The concurrent IgG2b response to mGRIN2D-Fc vaccination is somewhat atypical, and generally is seen in vaccinations involving polysaccharide vaccine components(181). In this context it is more likely to represent non-specific activation secondary to the activation of Freund's complete and incomplete adjuvant, which has been previously described(182).

In this immune context, the *in vivo* observations of decreased physiological angiogenesis and decreased tumour growth described in Chapter five, alongside the *in vitro* effects of siRNA knockdown of GRIN2D in HUVEC, described in Chapter three, point to an antibody-mediated treatment effect on CRC endothelial cell function. The specific intracellular effects of GRIN2D-Fc vaccination on endothelial cells has not been studied, but the upregulation of GRIN2D expression within treated CT26 tumour versus control Fc vaccinated mice could hold the key. This upregulation is likely to point to a functional impairment of GRIN2D function as opposed to a targeted killing effect on endothelial calls expressing GRIN2D, in which one might expect to see absent GRIN2D expression in treated mice. If indeed there is a targeted anti-angiogenic effect from GRIN2D vaccination, it is likely that this effect would be systemic, and potentially persistent. It is unfortunate that the subcutaneous CT26 model has not been shown to be a metastatic model, as the anti-angiogenic effects of GRIN2D-targeting may well be relevant to metastatic spread, or indeed in the prevention of growth in micrometastases. Imminent future work within the group will translate the subcutaneous experience to an orthotopic model, and address these hypotheses.

The murine expression profile of GRIN2D summarised in Chapter five indicates that in terms of endothelial expression, GRIN2D appears to be highly tumour specific. This specificity does not extend to bulk tissues, and treatment strategy must be guided by this fact. The selection of an immune strategy has been highly fortuitous for GRIN2D as a target, as while bulk expression in the brain is high, the blood-brain-barrier (BBB) anatomically and physiologically prevents passage of antibodies from circulating microvessels into the abutting astrocytes(183). Thus, the demonstrable immune response against GRIN2D is limited to the endothelial compartment, guarding against potentially serious side-effects of brain cell death. The BBB can be disrupted in patients with advanced malignancy, exhibited particularly by those who develop brain metastases. However, spread to this site is uncommon in CRC, occurring in only 2-3% of cases(184). Disruption of the BBB might make targeting of GRIN2D in patients with known brain metastases unwise. This will prove a hurdle to overcome in phase two and three clinical trials, which universally focus on patients with metastatic CRC, as it is here which benefit is easiest to demonstrate. Pre-clinical data could be presented if the brains of GRIN2D-Fc vaccinated and Fc-only vaccinated mice were histologically analysed to assess for the presence or otherwise of inflammatory infiltrates in neuronal tissues surrounding the blood vessels within the brain.

If the GRIN2D expression profile in humans can be considered analogous to that of mice, then the most important factor to consider would be the potential for neurological or psychiatric side effects. It has been shown that despite the widespread expression of GRIN2D within the developing diencephalon, a selective knockout mouse is able to develop normally both pre- and post-natally, including normal mating behaviour(185). Indeed, these mice exhibited no differences compared to wild-type mice in motor activity and anxiety tests, but did show reduced spontaneous activity measured in an open-field test. Further characterization performed more recently indicated less sensitivity to stress induced by forced swimming tests and light-dark box models. It was therefore hypothesised that GRIN2D knockout mice have dysfunctional NMDA receptors and altered emotional behavior(186). These observations draw analogies with the glutaminergic theory of schizophrenia, which has been the focus of much research, summarized in Moghaddam and Javitt, 2012(187). This theory is based on the observations that agents which block NMDA-receptors, such as ketamine and phencyclidine (PCP) can precipitate schizoid symptomatology(188,189). However, due to the lack of expression in adult rodent brains(190), it has been hypothesised that GRIN2D is unlikely to play a major part in the pathophysiology of schizophrenia(191). Indeed, recent investigations into circulating antibodies to NMDA receptor in schizophrenia have focused away from GRIN2D as a candidate(192), following demonstration of comparable expression of GRIN2D in the thalamic nuclei of schizophrenic and normal control human brains(193).

Beyond the brain, expression of GRIN2D has been confirmed in the autonomic and enteric nervous systems(64), and unforeseen effects may occur in these sites. Based upon the murine expression profile, there may also be effects upon the hepatic or renal endothelial compartments, and any translational work should bear the possibility of toxicity in mind. There is clearly more translational work to be performed in this respect, with immunohistochemistry of human tissue arrays being the first step to corroborate the murine expression profile.

Immune therapy is an established, but still rapidly expanding field within anti-cancer therapy, with monoclonal antibody therapy forming the bulk of approved immune therapies in colorectal cancer, as previously discussed. The field is constantly evolving, and novel applications have been described, including the use of a photosensitiser conjugated to an antibody specific to the Extra Domain B (EDB) of fibronectin, which demonstrated complete tumour ablation in a murine xenograft model of embryological tumour growth(194). Other groups have focused on the generation of chimeric antigen receptor regulatory T-cells to selectively target the vasculature, for instance through the targeting of VEGFR2 in multiple murine cell lines, including the CT26 line(195). Work has been performed to this end in colitis-associated colorectal cancer using CEA-specific Chimeric Antigen Receptor (CAR) regulatory T-cells(196).

Vaccination based targeting of endothelial cell function offers certain benefits over these other novel approaches to tumour targeting, not least its potential for a relative lack of cost, due to the persistence of the immune response, and the avoidance of regular drug infusions. Having said this, evidence has also suggested that vaccination against a self-antigen does not result in a persistent immune response, with circulating antibodies returning to baseline after seven months(197), in a murine, Freund’s based vaccination strategy, which is not transferable to humans. It is also important to note that for vaccination to be a successful strategy, it requires the host to possess an intact immune system. This is often compromised in patients with malignancy, either from their malignancy itself(198), or from the effects of exogenous steroids(199), chemotherapeutic agents(200), opioids(201) and even the emotional stress brought on by a cancer diagnosis and treatment(202). Mechanisms are highly varied, but include T-cell mediated immunity, which may impact on the potential success of a pure vaccine-based treatment in this context.

In terms of future work, this thesis presents just the beginning of a potentially exciting journey for GRIN2D. A human expression profile by means of IHC tissue array analysis alongside studies of potential toxicity within the murine model are prerequisites for moving GRIN2D forward towards clinical trials. There is also much work to be done to characterize the exact mode of tumour growth suppression demonstrated here, with exploration of whether targeting GRIN2D is interfering with calcium influx, leading to decreased angiogenesis and tumour growth. The animal models represented within this work should be taken forward not only to formulate a GRIN2D-based vaccine, which could be potentially usable in humans, but also to apply this vaccine within an orthotopic colorectal cancer model, whereby the potential anti-metastatic effects of this treatment can be investigated. There is also potential for the use of antibody-drug conjugates in augmenting the efficacy of targeting GRIN2D(203), and future work could also focus upon collaborating with industry to this end.

APPENDIX

Relevant Authored Publications

Available online at www.sciencedirect.com
ScienceDirect
ELSEVIER
EJSO 40 (2014) 133–136
EJSO the Journal of Cancer Surgery
www.ejso.com

For debate

Vaccination against tumour blood vessels in colorectal cancer

H.J.M. Ferguson [a,b,*], J. Wragg [a], T. Ismail [b], R. Bicknell, Prof.[a]

[a] *School of Immunity and Infection and Cancer Studies, Institute for Biomedical Research, College of Medical and Dental Sciences, University of Birmingham, Edgbaston, Birmingham B15 2TT, UK*
[b] *Department of Colorectal Surgery, Queen Elizabeth Hospital, Mindelsohn Way, Birmingham B15 2TH, UK*

Accepted 25 November 2013
Available online 13 December 2013

Angiogenesis
DOI 10.1007/s10456-014-9448-z

ORIGINAL PAPER

Robo4 vaccines induce antibodies that retard tumor growth

Xiaodong Zhuang · Forhad Ahmed · Yang Zhang · Henry J. Ferguson · Jane C. Steele · Neil M. Steven · Zsuzsanna Nagy · Victoria L. Heath · Kai-Michael Toellner · Roy Bicknell

Received: 27 January 2014 / Accepted: 13 October 2014
© Springer Science+Business Media Dordrecht 2014

REFERENCES

1. Office for National Statistics. Cancer Statistics Registrations England (Series MB1), No 41, 2010 [cited 2013 May 28]. pp. 1–18. Available from: http://www.ons.gov.uk/ons/dcp171778_267154.pdf

2. Quirke P, Durdey P, Dixon MF, Williams NS. Local recurrence of rectal adenocarcinoma due to inadequate surgical resection. Histopathological study of lateral tumour spread and surgical excision. Lancet. 1986 Nov 1;2(8514):996–9.

3. Tebbutt NC, Cattell E, Midgley R, Cunningham D, Kerr D. Systemic treatment of colorectal cancer. Eur J Cancer. 2002 May;38(7):1000–15.

4. Lokich J. Infusional 5-FU: historical evolution, rationale, and clinical experience. Oncology (Williston Park, NY). 1998 Oct;12(10 Suppl 7):19–22.

5. Kelly H, Goldberg RM. Systemic therapy for metastatic colorectal cancer: current options, current evidence. J Clin Oncol. 2005 Jul 10;23(20):4553–60.

6. Ferguson HJM, Wragg J, Ismail T, Bicknell R. Vaccination against tumour blood vessels in colorectal cancer. Eur J Surg Oncol. 2013 Dec 13.

7. Ponz de Leon M, Di Gregorio C. Pathology of colorectal cancer. Digestive and Liver Disease. 2001 May;33(4):372–88.

8. Hardy RG, Meltzer SJ, Jankowski JA. ABC of colorectal cancer. Molecular basis for risk factors. BMJ. 2000 Oct 7;321(7265):886–9.

9. DUKES CE, BUSSEY HJ. The spread of rectal cancer and its effect on prognosis. Br J Cancer. 1958 Sep;12(3):309–20.

10. Cancer Research UK. Bowel cancer survival statistics. [cited 2013 May 28] Available from: http://www.cancerresearchuk.org/cancer-info/cancerstats/types/bowel/

11. Bleday R, Babineau T, Forse RA. Laparoscopic surgery for colon and rectal cancer. Semin Surg Oncol. 1993 Jan;9(1):59–64.

12. Spinoglio G, Summa M, Priora F, Quarati R, Testa S. Robotic colorectal surgery: first 50 cases experience. Dis Colon Rectum. 2008 Nov;51(11):1627–32.

13. Hodgson S. Mechanisms of inherited cancer susceptibility. J Zhejiang Univ Sci B. 2008 Jan;9(1):1–4.

14. Nordic Gastrointestinal Tumor Adjuvant Therapy Group. Expectancy or primary chemotherapy in patients with advanced asymptomatic colorectal cancer: a randomized trial. J Clin Oncol. 1992 Jun;10(6):904–11.

15. Zhou Z, Nimeiri HS, Benson AB III. Preoperative chemotherapy for locally advanced resectable colon cancer - a new treatment paradigm in colon cancer? Annals of Translational Medicine. 2013 Jul 3;1(2).

16. Morris EJA, Maughan NJ, Forman D, Quirke P. Who to treat with adjuvant therapy in Dukes B/stage II colorectal cancer? The need for high quality pathology. Gut. 2007 Oct 1;56(10):1419–25.

17. NICE. Colorectal cancer: The diagnosis and management of colorectal cancer [Internet]. nice.org.uk. 2011 [cited 2014 Jul 23]. Available from: http://www.nice.org.uk/guidance/CG131

18. Longley DB, Harkin DP, Johnston PG. 5-Fluorouracil: mechanisms of action and clinical strategies. Nat Rev Cancer. 2003 May;3(5):330–8.

19. O'Connell MJ. Oxaliplatin or irinotecan as adjuvant therapy for colon cancer: the results are in. J Clin Oncol. 2009 Jul 1;27(19):3082–4.

20. Willett CG. Cancer of the Lower Gastrointestinal Tract [Internet]. American Cancer Society. 2001 [cited 2014 Jul 23]. Available from: http://books.google.co.uk/books/about/Cancer_of_the_Lower_Gastrointestinal_Tra.html?id=0Q5Ej9t7PHUC&redir_esc=y

21. Mosolits S, Ullenhag G, Mellstedt H. Therapeutic vaccination in patients with gastrointestinal malignancies. A review of immunological and clinical results. Ann Oncol. 2005 Jun;16(6):847–62.

22. Nagorsen D, Thiel E. Clinical and immunologic responses to active specific cancer vaccines in human colorectal cancer. Clin Cancer Res. 2006 May 15;12(10):3064–9.

23. Cersosimo RJ. Management of advanced colorectal cancer, part 2. Am J Health Syst Pharm. 2013 Mar 15;70(6):491–506.

24. Casanovas O, Hickey R, Bergers G, Hanahan D. Drug resistance by evasion of antiangiogenic targeting of VEGF signaling in late-stage pancreatic islet tumors. Cancer Cell. 2005 Oct;8(4):299–309.

25. McDermott FD, Heeney A, Kelly ME, Steele RJ, Carlson GL, Winter DC. Systematic review of preoperative, intraoperative and postoperative risk factors for colorectal anastomotic leaks. Br J Surg. 2015 Apr;102(5):462-79

26. Risau W. Mechanisms of angiogenesis. Nature. 1997 Apr 17;386(6626):671–4.

27. Zhao Y, Bao Q, Renner A, Camaj P, Eichhorn M, Ischenko I, et al. Cancer stem cells and angiogenesis. Int J Dev Biol. 2011;55(4-5):477–82.

28. Breier G, Risau W. The role of vascular endothelial growth factor in blood vessel formation. Trends Cell Biol. 1996 Dec;6(12):454–6.

29. Caduff JH, Fischer LC, Burri PH. Scanning electron microscope study of the developing microvasculature in the postnatal rat lung. Anat Rec. 1986 Oct;216(2):154–64.

30. Makanya AN, Hlushchuk R, Djonov VG. Intussusceptive angiogenesis and its role in vascular morphogenesis, patterning, and remodeling. Angiogenesis. 2009;12(2):113–23.

31. Djonov V, Schmid M, Tschanz SA, Burri PH. Intussusceptive angiogenesis: its role in embryonic vascular network formation. Circ Res. 2000 Feb 18;86(3):286–92.

32. Hobson B, Denekamp J. Endothelial proliferation in tumours and normal tissues: continuous labelling studies. Br J Cancer. 1984 Apr;49(4):405–13.

33. Yancopoulos GD, Davis S, Gale NW, Rudge JS, Wiegand SJ, Holash J. Vascular-specific growth factors and blood vessel formation. Nature. 2000 Sep 14;407(6801):242–8.

34. Folkman J, Cole P, Zimmerman S. Tumor behavior in isolated perfused organs: in vitro growth and metastases of biopsy material in rabbit thyroid and canine intestinal segment. Ann Surg. 1966 Sep;164(3):491–502.

35. Folkman J. Tumor angiogenesis: therapeutic implications. N Engl J Med. 1971 Nov 18;285(21):1182–6.

36. de Castro Junior G, Puglisi F, de Azambuja E, Saghir El NS, Awada A. Angiogenesis and cancer: A cross-talk between basic science and clinical trials (the “do ut des” paradigm). Crit Rev Oncol Hematol. 2006 Jul;59(1):40–50.

37. Boehm T, Folkman J, Browder T, O'Reilly MS. Antiangiogenic therapy of experimental cancer does not induce acquired drug resistance. Nature. 1997 Nov 27;390(6658):404–7.

38. Cristofanilli M, Charnsangavej C, Hortobagyi GN. Angiogenesis modulation in cancer research: novel clinical approaches. Nat Rev Drug Discov. 2002 Jun;1(6):415–26.

39. Eichhorn ME, Strieth S, Dellian M. Anti-vascular tumor therapy: recent advances, pitfalls and clinical perspectives. Drug Resist Updat. 2004 Apr;7(2):125–38.

40. Gasparini G, Longo R, Fanelli M, Teicher BA. Combination of antiangiogenic therapy with other anticancer therapies: results, challenges, and open questions. J Clin Oncol. 2005 Feb 20;23(6):1295–311.

41. Denekamp J. The tumour microcirculation as a target in cancer therapy: a clearer perspective. Eur J Clin Invest. 1999 Sep;29(9):733–6.

42. Liu L-X, Zhang W-H, Jiang H-C. Current treatment for liver metastases from colorectal cancer. World J Gastroenterol. 2003 Feb;9(2):193–200.

43. Thorpe PE, Chaplin DJ, Blakey DC. The first international conference on vascular targeting: meeting overview. Cancer Res. 2003 Mar 1;63(5):1144–7.

44. Tozer GM, Kanthou C, Parkins CS, Hill SA. The biology of the combretastatins as tumour vascular targeting agents. Int J Exp Pathol. 2002 Feb;83(1):21–38.

45. Thurston G, McLean JW, Rizen M, Baluk P, Haskell A, Murphy TJ, et al. Cationic liposomes target angiogenic endothelial cells in tumors and chronic inflammation in mice. J Clin Invest. 1998 Apr 1;101(7):1401–13.

46. Moncada S, Higgs A (eds.). The vascular endothelium. 2006. Springer.

47. Vandenbroucke E, Mehta D, Minshall R, Malik AB. Regulation of endothelial junctional permeability. Ann N Y Acad Sci. 2008 Mar;1123:134–45.

48. Chung AS, Ferrara N. Developmental and pathological angiogenesis. Annu Rev Cell Dev Biol. 2011;27:563–84.

49. Red-Horse K, Crawford Y, Shojaei F, Ferrara N. Endothelium-microenvironment interactions in the developing embryo and in the adult. Dev Cell. 2007 Feb;12(2):181–94.

50. Gimbrone MA, Cotran RS, Folkman J. Human vascular endothelial cells in culture. Growth and DNA synthesis. J Cell Biol. 1974 Mar;60(3):673–84.

51. Jaffe EA, Nachman RL, Becker CG, Minick CR. Culture of human endothelial cells derived from umbilical veins. Identification by morphologic and immunologic criteria. J Clin Invest. 1973 Nov;52(11):2745–56.

52. Durr E, Yu J, Krasinska KM, Carver LA, Yates JR, Testa JE, et al. Direct proteomic mapping of the lung microvascular endothelial cell surface in vivo and in cell culture. Nat Biotechnol. 2004 Aug;22(8):985–92.

53. St Croix B, Rago C, Velculescu V, Traverso G, Romans KE, Montgomery E, et al. Genes expressed in human tumor endothelium. Science. 2000 Aug 18;289(5482):1197–202.

54. Chung AS, Lee J, Ferrara N. Targeting the tumour vasculature: insights from physiological angiogenesis. Nat Rev Cancer. 2010 Jul;10(7):505–14.

55. Kalsi G, Whiting P, Bourdelles BL, Callen D, Barnard EA, Gurling H. Localization of the human NMDAR2D receptor subunit gene (GRIN2D) to 19q13.1-qter, the NMDAR2A subunit gene to 16p13.2 (GRIN2A), and the NMDAR2C subunit gene (GRIN2C) to 17q24-q25 using somatic cell hybrid and radiation hybrid mapping panels. Genomics. 1998 Feb 1;47(3):423–5.

56. Laube B, Hirai H, Sturgess M, Betz H, Kuhse J. Molecular determinants of agonist discrimination by NMDA receptor subunits: analysis of the glutamate binding site on the NR2B subunit. Neuron. 1997 Mar;18(3):493–503.

57. Monyer H, Sprengel R, Schoepfer R, Herb A, Higuchi M, Lomeli H, et al. Heteromeric NMDA receptors: molecular and functional distinction of subtypes. Science. 1992 May 22;256(5060):1217–21.

58. Stern P, Béhé P, Schoepfer R, Colquhoun D. Single-channel conductances of NMDA receptors expressed from cloned cDNAs: comparison with native receptors. Proc Biol Sci. 1992 Dec 22;250(1329):271–7.

59. Siegler Retchless B, Gao W, Johnson JW. A single GluN2 subunit residue controls NMDA receptor channel properties via intersubunit interaction. Nat Neurosci. 2012 Mar;15(3):406–13–S1–2.

60. Masu M, Nakajima Y, Moriyoshi K, Ishii T, Akazawa C, Nakanashi S. Molecular characterization of NMDA and metabotropic glutamate receptors. Ann N Y Acad Sci. 1993 Dec 20;707:153–64.

61. Bliss TV, Collingridge GL. A synaptic model of memory: long-term potentiation in the hippocampus. Nature. 1993 Jan 7;361(6407):31–9.

62. Choi KH, Zepp ME, Higgs BW, Weickert CS, Webster MJ. Expression profiles of schizophrenia susceptibility genes during human prefrontal cortical development. J Psychiatry Neurosci. 2009 Nov;34(6):450–8.

63. McRoberts JA, Coutinho SV, Marvizón JC, Grady EF, Tognetto M, Sengupta JN, et al. Role of peripheral N-methyl-D-aspartate (NMDA) receptors in visceral nociception in rats. Gastroenterology. 2001 Jun;120(7):1737–48.

64. Zhou Q, NICE. NMDA Receptors and Colitis: Basic Science and Clinical Implications. Rev Analg. 2008 Nov 1;10(1):33–43.

65. Yano S, Tokumitsu H, Soderling TR. Calcium promotes cell survival through CaM-K kinase activation of the protein-kinase-B pathway. Nature. 1998 Dec 10;396(6711):584–7.

66. Stepulak A, Luksch H, Gebhardt C, Uckermann O, Marzahn J, Sifringer M, et al. Expression of glutamate receptor subunits in human cancers. Histochem Cell Biol. 2009 Jun 14;132(4):435–45.

67. Dinc G, Ulman YI. The introduction of variolation “A La Turca” to the West by Lady Mary Montagu and Turkey's contribution to this. Vaccine. 2007 May;25(21):4261–5.

68. Jenner E. An Inquiry Into the Causes and Effects of the Variolae Vaccinae, Or Cow-Pox. [Internet]. Sampson Low, Soho, London, UK. 1798 [cited 2014 Jul 28]. Available from: http://www.bartleby.com/38/4/1.html

69. Group TFIS. Quadrivalent Vaccine against Human Papillomavirus to Prevent High-Grade Cervical Lesions. N Engl J Med. 2007 May 10;356(19):1915–27.

70. Rueckert C, Guzmán CA. Vaccines: from empirical development to rational design. PLoS Pathog. 2012;8(11):e1003001.

71. Adkins I, Holubova J, Kosova M, Sadilkova L. Bacteria and their toxins tamed for immunotherapy. Curr Pharm Biotechnol. 2012 Jun;13(8):1446–73.

72. Caminschi I, Shortman K. Boosting antibody responses by targeting antigens to dendritic cells. Trends Immunol. 2012 Feb;33(2):71–7.

73. Hoebe K, Janssen E, Beutler B. The interface between innate and adaptive immunity. Nat Immunol. 2004 Oct;5(10):971–4.

74. Iwasaki A, Medzhitov R. Toll-like receptor control of the adaptive immune responses. Nat Immunol. 2004 Oct;5(10):987–95.

75. Siegrist CA. Vaccine Immunology. In: Vaccines. Plotkin SA, Orenstein WA, Offit PA (eds). Elsevier Health Sciences; 2008. p17-36.

76. Deenick EK, Hasbold J, Hodgkin PD. Decision criteria for resolving isotype switching conflicts by B cells. Eur J Immunol. 2005 Oct;35(10):2949–55.

77. Goldblatt D, Vaz AR, Miller E. Antibody avidity as a surrogate marker of successful priming by Haemophilus influenzae type b conjugate vaccines following infant immunization. J Infect Dis. 1998 Apr;177(4):1112–5.

78. O'Garra A, Robinson D. Development and function of T helper 1 cells. Adv Immunol. 2004;83:133–62.

79. Stetson DB, Voehringer D, Grogan JL, Xu M, Reinhardt RL, Scheu S, et al. Th2 cells: orchestrating barrier immunity. Adv Immunol. 2004;83:163–89.

80. Wherry EJ, Puorro KA, Porgador A, Eisenlohr LC. The induction of virus-specific CTL as a function of increasing epitope expression: responses rise steadily until excessively high levels of epitope are attained. J Immunol. 1999 Oct 1;163(7):3735–45.

81. Huehn J, Siegmund K, Hamann A. Migration rules: functional properties of naive and effector/memory-like regulatory T cell subsets. Curr Top Microbiol Immunol. 2005;293:89–114.

82. Okaji Y, Tsuno NH, Kitayama J, Saito S, Takahashi T, Kawai K, et al. Vaccination with autologous endothelium inhibits angiogenesis and metastasis of colon cancer through autoimmunity. Cancer Sci. 2004 Jan;95(1):85–90.

83. Vermorken JB, Claessen AM, van Tinteren H, Gall HE, Ezinga R, Meijer S, et al. Active specific immunotherapy for stage II and stage III human colon cancer: a randomised trial. Lancet. 1999 Jan 30;353(9150):345–50.

84. Hanna MG, Hoover HC, Vermorken JB, Harris JE, Pinedo HM. Adjuvant active specific immunotherapy of stage II and stage III colon cancer with an autologous tumor cell vaccine: first randomized phase III trials show promise. Vaccine. 2001 Mar 21;19(17-19):2576–82.

85. Okaji Y, Tsuno NH, Tanaka M, Yoneyama S, Matsuhashi M, Kitayama J, et al. Pilot study of anti-angiogenic vaccine using fixed whole endothelium in patients with progressive malignancy after failure of conventional therapy. Eur J Cancer. 2008 Feb;44(3):383–90.

86. Kaufman HL, Lenz H-J, Marshall J, Singh D, Garett C, Cripps C, et al. Combination chemotherapy and ALVAC-CEA/B7.1 vaccine in patients with metastatic colorectal cancer. Clin Cancer Res. 2008 Aug 1;14(15):4843–9.

87. Harrop R, Connolly N, Redchenko I, Valle J, Saunders M, Ryan MG, et al. Vaccination of colorectal cancer patients with modified vaccinia Ankara delivering the tumor antigen 5T4 (TroVax) induces immune responses which correlate with disease control: a phase I/II trial. Clin Cancer Res. 2006 Jun 1;12(11 Pt 1):3416–24.

88. Fang L, Lee VC, Cha E, Zhang H, Hwang ST. CCR7 regulates B16 murine melanoma cell tumorigenesis in skin. J Leukoc Biol. 2008 Oct;84(4):965–72.

89. Schroeder A, Mueller O, Stocker S, Salowsky R, Leiber M, Gassmann M, et al. The RIN: an RNA integrity number for assigning integrity values to RNA measurements. BMC Mol Biol. 2006;7:3.

90. Miettinen M, Lindenmayer AE, Chaubal A. Endothelial cell markers CD31, CD34, and BNH9 antibody to H- and Y-antigens--evaluation of their specificity and sensitivity in the diagnosis of vascular tumors and comparison with von Willebrand factor. Mod Pathol. 1994 Jan;7(1):82–90.

91. Livak KJ, Schmittgen TD. Analysis of relative gene expression data using real-time quantitative PCR and the 2(-Delta Delta C(T)) Method. Methods. 2001 Dec;25(4):402–8.

92. Buckanovich RJ, Sasaroli D, O'Brien-Jenkins A, Botbyl J, Hammond R, Katsaros D, et al. Tumor vascular proteins as biomarkers in ovarian cancer. J Clin Oncol. 2007 Mar 1;25(7):852–61.

93. Buchner G, Broccoli V, Bulfone A, Orfanelli U, Gattuso C, Ballabio A, et al. MAEG, an EGF-repeat containing gene, is a new marker associated with dermatome specification and morphogenesis of its derivatives. Mech Dev. 2000 Nov;98(1-2):179–82.

94. Yeung G, Mulero JJ, Berntsen RP, Loeb DB, Drmanac R, Ford JE. Cloning of a novel epidermal growth factor repeat containing gene EGFL6: expressed in tumor and fetal tissues. Genomics. 1999 Dec 1;62(2):304–7.

95. Oberauer R, Rist W, Lenter MC, Hamilton BS, Neubauer H. EGFL6 is increasingly expressed in human obesity and promotes proliferation of adipose tissue-derived stromal vascular cells. Mol Cell Biochem. 2010 Oct;343(1-2):257–69.

96. Lawler J, Detmar M. Tumor progression: the effects of thrombospondin-1 and -2. Int J Biochem Cell Biol. 2004 Jun;36(6):1038–45.

97. Simantov R, Febbraio M, Silverstein RL. The antiangiogenic effect of thrombospondin-2 is mediated by CD36 and modulated by histidine-rich glycoprotein. Matrix Biol. 2005 Feb;24(1):27–34.

98. Miyoshi N, Ishii H, Mimori K, Takatsuno Y, Kim H, Hirose H, et al. Abnormal expression of TRIB3 in colorectal cancer: a novel marker for prognosis. Br J Cancer. 2009 Nov 17;101(10):1664–70.

99. Wennemers M, Bussink J, van den Beucken T, Sweep FCGJ, Span PN. Regulation of TRIB3 mRNA and protein in breast cancer. PLoS ONE. 2012;7(11):e49439.

100. Slattery ML, Wolff RK, Herrick JS, Caan BJ, Potter JD. IL6 genotypes and colon and rectal cancer. Cancer Causes Control. 2007 Dec;18(10):1095–105.

101. Ozawa T, Kazama S, Akiyoshi T, Murono K, Yoneyama S, Tanaka T, et al. Nuclear Notch3 Expression is Associated with Tumor Recurrence in Patients with Stage II and III Colorectal Cancer. Ann Surg Oncol. 2014 Aug;21(8):2650–8.

102. Beaty RM, Edwards JB, Boon K, Siu I-M, Conway JE, Riggins GJ. PLXDC1 (TEM7) is identified in a genome-wide expression screen of glioblastoma endothelium. J Neurooncol. 2007 Feb;81(3):241–8.

103. Jiao X, Wood LD, Lindman M, Jones S, Buckhaults P, Polyak K, et al. Somatic mutations in the Notch, NF-KB, PIK3CA, and Hedgehog pathways in human breast cancers. Genes Chromosomes Cancer. 2012 May;51(5):480–9.

104. Terasaki H, Saitoh T, Shiokawa K, Katoh M. Frizzled-10, up-regulated in primary colorectal cancer, is a positive regulator of the WNT - beta-catenin - TCF signaling pathway. Int J Mol Med. 2002 Feb;9(2):107–12.

105. Morel S, Burnier L, Roatti A, Chassot A, Roth I, Sutter E, et al. Unexpected role for the human Cx37 C1019T polymorphism in tumour cell proliferation. Carcinogenesis. 2010 Nov;31(11):1922–31.

106. Klaus A, Birchmeier W. Wnt signalling and its impact on development and cancer. Nat Rev Cancer. 2008 May;8(5):387–98.

107. Zhang Y, Lu N, Xue Y, Zhang M, Li Y, Si Y, et al. Expression of immunoglobulin-like transcript (ILT)2 and ILT3 in human gastric cancer and its clinical significance. Mol Med Rep. 2012 Apr;5(4):910–6.

108. Suciu-Foca N, Feirt N, Zhang Q-Y, Vlad G, Liu Z, Lin H, et al. Soluble Ig-like transcript 3 inhibits tumor allograft rejection in humanized SCID mice and T cell responses in cancer patients. J Immunol. 2007 Jun 1;178(11):7432–41.

109. Ikeda Y, Imai Y, Kumagai H, Nosaka T, Morikawa Y, Hisaoka T, et al. Vasorin, a transforming growth factor beta-binding protein expressed in vascular smooth muscle cells, modulates the arterial response to injury in vivo. Proc Natl Acad Sci USA. 2004 Jul 20;101(29):10732–7.

110. Lin TS. Ofatumumab: a novel monoclonal anti-CD20 antibody. Pharmgenomics Pers Med. 2010;3:51–9.

111. Daino K, Ugolin N, Altmeyer-Morel S, Guilly M-N, Chevillard S. Gene expression profiling of alpha-radiation-induced rat osteosarcomas: identification of dysregulated genes involved in radiation-induced tumorigenesis of bone. Int J Cancer. 2009 Aug 1;125(3):612–20.

112. Kropp M, Wilson SI. The expression profile of the tumor suppressor gene Lzts1 suggests a role in neuronal development. Dev Dyn. 2012 Mar 30;241(5):984–94.

113. Delaney JT, Muhammad R, Blair MA, Kor K, Fish FA, Roden DM, et al. A KCNJ8 mutation associated with early repolarization and atrial fibrillation. Europace. 2012 Oct;14(10):1428–32.

114. Escudero-Esparza A, Martin TA, Davies ML, Jiang WG. PGF isoforms, PLGF-1 and PGF-2, in colorectal cancer and the prognostic significance. Cancer Genomics Proteomics. 2009 Jul;6(4):239–46.

115. Cui T, Tsolakis AV, Li S-C, Cunningham JL, Lind T, Öberg K, et al. Olfactory receptor 51E1 protein as a potential novel tissue biomarker for small intestine neuroendocrine carcinomas. Eur J Endocrinol. 2013 Feb;168(2):253–61.

116. Weng J, Wang J, Hu X, Wang F, Ittmann M, Liu M. PSGR2, a novel G-protein coupled receptor, is overexpressed in human prostate cancer. Int J Cancer. 2006 Mar 15;118(6):1471–80.

117. Kim JH, Lee JY, Lee KT, Lee JK, Lee KH, Jang K-T, et al. RGS16 and FosB underexpressed in pancreatic cancer with lymph node metastasis promote tumor progression. Tumour Biol. 2010 Oct;31(5):541–8.

118. Pasmant E, Masliah-Planchon J, Lévy P, Laurendeau I, Ortonne N, Parfait B, et al. Identification of genes potentially involved in the increased risk of malignancy in NF1-microdeleted patients. Mol Med. 2011 Jan;17(1-2):79–87.

119. Heid CA, Stevens J, Livak KJ, Williams PM. Real time quantitative PCR. Genome Res. 1996 Oct;6(10):986–94.

120. Slamon DJ, Clark GM, Wong SG, Levin WJ, Ullrich A, McGuire WL. Human breast cancer: correlation of relapse and survival with amplification of the HER-2/neu oncogene. Science. 1987 Jan 9;235(4785):177–82.

121. Raeymaekers L. A commentary on the practical applications of competitive PCR. Genome Res. 1995 Aug;5(1):91–4.

122. Cao H, Shockey JM. Comparison of TaqMan and SYBR Green qPCR Methods for Quantitative Gene Expression in Tung Tree Tissues. J Agric Food Chem. 2012 Dec 19;60(50):12296–303.

123. Higuchi R, Dollinger G, Walsh PS, Griffith R. Simultaneous amplification and detection of specific DNA sequences. Biotechnology (NY). 1992 Apr;10(4):413–7.

124. Emani S, Zhang J, Guo L, Guo H, Kuo PC. RNA stability regulates differentialexpression of the metastasis protein, osteopontin, in hepatocellular cancer. Surgery. 2008 Jun;143(6):803–12.

125. Zhuang X, Cross D, Heath VL, Bicknell R. Shear stress, tip cells and regulators of endothelial migration. Biochem Soc Trans. 2011 Dec;39(6):1571–5.

126. Verissimo AR, Herbert JMJ, Heath VL, Legg JA, Sheldon H, Andre M, et al. Functionally defining the endothelial transcriptome, from Robo4 to ECSCR. Biochem Soc Trans. 2009 Dec;37(Pt 6):1214–7.

127. Liang C-C, Park AY, Guan J-L. In vitro scratch assay: a convenient and inexpensive method for analysis of cell migration in vitro. Nat Protoc. 2007;2(2):329–33.

128. Hughes CS, Postovit LM, Lajoie GA. Matrigel: a complex protein mixture required for optimal growth of cell culture. Proteomics. 2010 May;10(9):1886–90.

129. Vukicevic S, Kleinman HK, Luyten FP, Roberts AB, Roche NS, Reddi AH. Identification of multiple active growth factors in basement membrane Matrigel suggests caution in interpretation of cellular activity related to extracellular matrix components. Exp Cell Res. 1992 Sep;202(1):1–8.

130. Senger DR, Perruzzi CA, Streit M, Koteliansky VE, de Fougerolles AR, Detmar M. The alpha(1)beta(1) and alpha(2)beta(1) integrins provide critical support for vascular endothelial growth factor signaling, endothelial cell migration, and tumor angiogenesis. Am J Pathol. 2002 Jan;160(1):195–204.

131. Labtech T. Acumen hci Application Note [Internet]. discover.ttplabtech.com. [cited 2014 Sep 11]. Available from: http://discover.ttplabtech.com/rs/ttplabtech/images/acumen-hci_cell-cycle_TTPLabtech-appNote-2013.pdf?mkt_tok=3RkMMJWWfF9wsRokuKnOZKXonjHpfsX56%2BklWKazlMI%2F0ER3fOvrPUfGjI4ERcd0aPyQAgobGp5I5FEPS7fYSLh3t6wEWQ%3D%3D

132. Sobolevsky AI, Rosconi MP, Gouaux E. X-ray structure, symmetry and mechanism of an AMPA-subtype glutamate receptor. Nature. 2009 Dec 10;462(7274):745–56.

133. Chester KA, Hawkins RE. Clinical issues in antibody design. Trends in Biotechnology. 1995 Aug;13(8):294–300.

134. Teng H, Cai W, Zhou L, Zhang J, Liu Q, Wang Y, et al. Evolutionary mode and functional divergence of vertebrate NMDA receptor subunit 2 genes. PLoS ONE. 2010;5(10):e13342.

135. Zhuang X, Ahmed F, Zhang Y, Ferguson HJ, Steele JC, Steven NM, et al. Robo4 vaccines induce antibodies that retard tumor growth. Angiogenesis. 2014 Oct 28;:1–13.

136. Carter PJ. Introduction to current and future protein therapeutics: a protein engineering perspective. Exp Cell Res. 2011 May;317(9):1261–9.

137. Czajkowsky DM, Hu J, Shao Z, Pleass RJ. Fc-fusion proteins: new developments and future perspectives. EMBO Molecular Medicine. 2012 Oct 1;4(10):1015–28.

138. Nimmerjahn F, Ravetch JV. Fc|[gamma]| receptors as regulators of immune responses. Nature Reviews Immunology. 2008 Jan 1;8(1):34–47.

139. Petersen TN, Brunak S, Heijne von G, Nielsen H. SignalP 4.0: discriminating signal peptides from transmembrane regions. Nat Methods. 2011 Oct 1;8(10):785–6.

140. Graham FL, Smiley J, Russell WC, Nairn R. Characteristics of a Human Cell Line Transformed by DNA from Human Adenovirus Type 5. J Gen Virol. 1977 Jul 1;36(1):59–72.

141. Cannon JP, O'Driscoll M, Litman GW. Construction, Expression, and Purification of Chimeric Protein Reagents Based on Immunoglobulin Fc Regions. In: Jonathan P. Rast and James W.D. Booth (eds.), Immune Receptors: Methods and Protocols, Methods in Molecular Biology, vol. 748, p51-67

142. Bjellqvist B, Hughes GJ, Pasquali C, Paquet N, Ravier F, Sanchez JC, et al. The focusing positions of polypeptides in immobilized pH gradients can be predicted from their amino acid sequences. Electrophoresis. 1993 Oct;14(10):1023–31.

143. Verma R, Boleti E, George AJ. Antibody engineering: comparison of bacterial, yeast, insect and mammalian expression systems. J Immunol Methods. 1998 Jul 1;216(1-2):165–81.

144. Yin J, Li G, Ren X, Herrler G. Select what you need: A comparative evaluation of the advantages and limitations of frequently used expression systems for foreign genes. Journal of Biotechnology. 2007 Jan;127(3):335–47.

145. de Boer HA, Comstock LJ, Vasser M. The tac promoter: a functional hybrid derived from the trp and lac promoters. Proc Natl Acad Sci USA. 1983 Jan;80(1):21–5.

146. Bioline. Competent Cells [Internet]. bioline.com. [cited 2014 Dec 4]. Available from: http://www.bioline.com/uk/downloads/dl/file/id/1126/bl21_fact_sheet.pdf

147. Griswold DP, Corbett TH. A colon tumor model for anticancer agent evaluation. Cancer. 1975 Dec;36(6 Suppl):2441–4.

148. Ikubo A, Aoki Y, Nagai E, Suzuki T. Highly metastatic variant of a mouse colon carcinoma cell line, LM17 and its response to GM-CSF gene therapy. Clin Exp Metastasis. 1999 Oct 1;17(10):849–55.

149. Endo T, Toda M, Watanabe M, Iizuka Y, Kubota T, Kitajima M, et al. In situ cancer vaccination with a replication-conditional HSV for the treatment of liver metastasis of colon cancer. Cancer Gene Ther. 2002 Feb;9(2):142–8.

150. Sakaguchi S, Yamaguchi T, Nomura T, Ono M. Regulatory T cells andimmune tolerance. Cell. 2008 May 30;133(5):775–87.

151. Mapara MY, Sykes M. Tolerance and cancer: mechanisms of tumor evasion and strategies for breaking tolerance. J Clin Oncol. 2004 Mar 15; 22(6): 1136-1151

152. Billiau A, Matthys P. Modes of action of Freund's adjuvants in experimental models of autoimmune diseases. J Leukoc Biol. 2001 Dec;70(6):849–60.

153. Castro AP, Aguas AP, Silva MT. Adjuvant treatment increases the resistance to Mycobacterium avium infection of mycobacteria-susceptible BALB/c mice. Clin Exp Immunol. 1993 Jun;92(3):466–72.

154. Andrade S. Sponge-Induced Angiogenesis in Mice and the Pharmacological Reactivity of the Neovasculature Quantitated by a Fluorimetric Method. Microvascular Research. 1997 Nov;54(3):253–61.

155. Lim E, Modi KD, Kim J. In vivo Bioluminescent Imaging of Mammary Tumors Using IVIS Spectrum. J Vis Exp. 2009 Apr 29;(26):e1210–0.

156. Nanda A, St Croix B. Tumor endothelial markers: new targets for cancer therapy. Curr Opin Oncol. 2004 Jan;16(1):44–9.

157. MacFadyen JR, Haworth O, Roberston D, Hardie D, Webster M-T, Morris HR, et al. Endosialin (TEM1, CD248) is a marker of stromal fibroblasts and is not selectively expressed on tumour endothelium. FEBS Lett. 2005 May 9;579(12):2569–75.

158. Nanda A, Karim B, Peng Z, Liu G, Qiu W, Gan C, et al. Tumor endothelial marker 1 (Tem1) functions in the growth and progression of abdominal tumors. Proc Natl Acad Sci USA. 2006 Feb 28;103(9):3351–6.

159. Huminiecki L, Gorn M, Suchting S, Poulsom R, Bicknell R. Magic roundabout is a new member of the roundabout receptor family that is endothelial specific and expressed at sites of active angiogenesis. Genomics. 2002 Apr;79(4):547–52.

160. Mura M, Swain RK, Zhuang X, Vorschmitt H, Reynolds G, Durant S, et al. Identification and angiogenic role of the novel tumor endothelial marker CLEC14A. Oncogene. 2012 Jan 19;31(3):293–305.

161. Luksch H, Uckermann O, Stepulak A, Hendruschk S, Marzahn J, Bastian S, et al. Silencing of selected glutamate receptor subunits modulates cancer growth. Anticancer Res. 2011 Oct;31(10):3181–92.

162. Koochekpour S. Glutamate, a metabolic biomarker of aggressiveness and a potential therapeutic target for prostate cancer. Asian J Androl. 2013 Mar;15(2):212–3.

163. Herner A, Sauliunaite D, Michalski CW, Erkan M, De Oliveira T, Abiatari I, et al. Glutamate increases pancreatic cancer cell invasion and migration via AMPA receptor activation and Kras-MAPK signaling. Int J Cancer. 2011 Nov 15;129(10):2349–59.

164. Stepulak A, Rola R, Polberg K, Ikonomidou C. Glutamate and its receptors in cancer. J Neural Transm. 2014 Aug;121(8):933–44.

165. Gualandris A, Noghero A, Geuna M, Arese M, Valdembri D, Serini G, et al. Microenvironment drives the endothelial or neural fate of differentiating embryonic stem cells coexpressing neuropilin-1 and Flk-1. FASEB J. 2009 Jan;23(1):68–78.

166. Zadeh MAH, Glass CA, Magnussen A, Hancox JC, Bates DO. VEGF-Mediated Elevated Intracellular Calcium and Angiogenesis in Human Microvascular Endothelial Cells In Vitro are Inhibited by Dominant Negative TRPC6. Microcirculation. 2008 Oct 1;15(7):605–14.

167. Bates DO, Curry FE. Vascular endothelial growth factor increases microvascular permeability via a Ca(2+)-dependent pathway. Am J Physiol. 1997 Aug;273(2 Pt 2):H687–94.

168. Wyllie DJ, Béhé P, Colquhoun D. Single-channel activations and concentration jumps: comparison of recombinant NR1a/NR2A and NR1a/NR2D NMDA receptors. J Physiol (Lond). 1998 Jul 1;510 (Pt 1):1–18.

169. Cull-Candy S, Brickley S, Farrant M. NMDA receptor subunits: diversity, development and disease. Curr Opin Neurobiol. 2001 Jun;11(3):327–35.

170. Fiorio Pla A, Grange C, Antoniotti S, Tomatis C, Merlino A, Bussolati B, et al. Arachidonic acid-induced Ca2+ entry is involved in early steps of tumor angiogenesis. Mol Cancer Res. 2008 Apr;6(4):535–45.

171. Luca Munaron MS. Multilevel complexity of calcium signaling: Modeling angiogenesis. World Journal of Biological Chemistry. 2012 Jun 26;3(6):121–6.

172. Munaron L, Tomatis C, Fiorio Pla A. The secret marriage between calcium and tumor angiogenesis. Technol Cancer Res Treat. 2008 Aug;7(4):335–9.

173. Giorgetti A, Piccoli S. Knowledge Based Membrane Protein Structure Prediction. From: X-Ray Crystallography to Bioinformatics and Back to Molecular Biology. 2011.

174. Chou PY, Fasman GD. Prediction of the secondary structure of proteins from their amino acid sequence. Adv Enzymol Relat Areas Mol Biol. 1978;47:45–148.

175. Chakrabarti P, Chakrabarti S. C--H...O hydrogen bond involving proline residues in alpha-helices. J Mol Biol. 1998 Dec 11;284(4):867–73.

176. Schmidt SR. Fusion-proteins as biopharmaceuticals--applications and challenges. Curr Opin Drug Discov Devel. 2009 Mar;12(2):284–95.

177. Pleass RJ. Fc-receptors and immunity to malaria: from models to vaccines. Parasite Immunol. 2009 Sep;31(9):529–38.

178. Petrovsky N, Aguilar JC. Vaccine adjuvants: Current state and future trends. Immunology and Cell Biology. 2004 Oct 1;82(5):488–96.

179. Toellner KM, Luther SA, Sze DM, Choy RK, Taylor DR, MacLennan IC, et al. T helper 1 (Th1) and Th2 characteristics start to develop during T cell priming and are associated with an immediate ability to induce immunoglobulin class switching. J Exp Med. 1998 Apr 20;187(8):1193–204.

180. Esser C, Radbruch A. Immunoglobulin class switching: molecular and cellular analysis. Annu Rev Immunol. 1990;8:717–35.

181. Lefeber DJ, Benaissa-Trouw B, Vliegenthart JFG, Kamerling JP, Jansen WTM, Kraaijeveld K, et al. Th1-directing adjuvants increase the immunogenicity of oligosaccharide-protein conjugate vaccines related to Streptococcus pneumoniae type 3. Infect Immun. 2003 Dec;71(12):6915–20.

182. Avramidis N, Victoratos P, Yiangou M, Hadjipetrou-Kourounakis L. Adjuvant regulation of cytokine profile and antibody isotype of immune responses to Mycoplasma agalactiae in mice. Veterinary Microbiology. 2002 Sep;88(4):325–38.

183. Lampson LA. Monoclonal antibodies in neuro-oncology: Getting past the blood-brain barrier. mAbs. 2014 Oct 27;3(2):153–60.

184. Mege D, Ouaissi M, Fuks D, Metellus P, Peltier J, Dufour H, et al. Patients with brain metastases from colorectal cancer are not condemned. Anticancer Res. 2013 Dec;33(12):5645–8.

185. Ikeda K, Araki K, Takayama C, Inoue Y, Yagi T, Aizawa S, et al. Reduced spontaneous activity of mice defective in the epsilon 4 subunit of the NMDA receptor channel. Brain Res Mol Brain Res. 1995 Oct;33(1):61–71.

186. Miyamoto Y, Yamada K, Noda Y, Mori H, Mishina M, Nabeshima T. Lower sensitivity to stress and altered monoaminergic neuronal function in mice lacking the NMDA receptor epsilon 4 subunit. J Neurosci. 2002 Mar 15;22(6):2335–42.

187. Moghaddam B, Javitt D. From Revolution to Evolution: The Glutamate Hypothesis of Schizophrenia and its Implication for Treatment. Neuropsychopharmacology. 2012 Jan 1;37(1):4–15.

188. Chen GM, Weston JK. The analgesic and anesthetic effect of 1-(1-phenylcyclohexyl) piperidine HCl on the monkey. Anesth Analg. 1960 Mar;39:132–7.

189. Luby ED, Gottlieb JS, Cohen BD, Rosenbaum G, Domino EF. Model psychoses and schizophrenia. Am J Psychiatry. 1962 Jul;119:61–7.

190. Monyer H, Burnashev N, Laurie DJ, Sakmann B, Seeburg PH. Developmental and regional expression in the rat brain and functional properties of four NMDA receptors. Neuron. 1994 Mar;12(3):529–40.

191. Inta D, Monyer H, Sprengel R, Meyer-Lindenberg A, Gass P. Mice with genetically altered glutamate receptors as models of schizophrenia: a comprehensive review. Neurosci Biobehav Rev. 2010 Mar;34(3):285–94.

192. Steiner J, Walter M, Glanz W, Sarnyai Z, Bernstein H-G, Vielhaber S, et al. Increased prevalence of diverse N-methyl-D-aspartate glutamate receptor antibodies in patients with an initial diagnosis of schizophrenia: specific relevance of IgG NR1a antibodies for distinction from N-methyl-D-aspartate glutamate receptor encephalitis. JAMA Psychiatry. 2013 Mar;70(3):271–8.

193. Ibrahim HM, Hogg AJ, Healy DJ, Haroutunian V, Davis KL, Meador-Woodruff JH. Ionotropic glutamate receptor binding and subunit mRNA expression in thalamic nuclei in schizophrenia. Am J Psychiatry. 2000 Nov;157(11):1811–23.

194. Palumbo A, Hauler F, Dziunycz P, Schwager K, Soltermann A, Pretto F, et al. A chemically modified antibody mediates complete eradication of tumours by selective disruption of tumour blood vessels. Br J Cancer. 2011 Mar 29;104(7):1106–15.

195. Chinnasamy D, Yu Z, Theoret MR, Zhao Y, Shrimali RK, Morgan RA, et al. Gene therapy using genetically modified lymphocytes targeting VEGFR-2 inhibits the growth of vascularized syngenic tumors in mice. J Clin Invest. 2010 Nov;120(11):3953–68.

196. Blat D, Zigmond E, Alteber Z, Waks T, Eshhar Z. Suppression of murine colitis and its associated cancer by carcinoembryonic antigen-specific regulatory T cells. Mol Ther. 2014 May;22(5):1018–28.

197. Huijbers EJM, Femel J, Andersson K, Björkelund H, Hellman L, Olsson A-K. The non-toxic and biodegradable adjuvant Montanide ISA 720/CpG can replace Freund's in a cancer vaccine targeting ED-B - a prerequisite for clinical development. Vaccine. 2012 Jan 5;30(2):225–30.

198. I Finn OJ. Immuno-oncology: understanding the function and dysfunction of the immune system in cancer. Ann Oncol. 2012 Sep;23 Suppl 8:6–9.

199. Agnes E Coutinho KEC. The anti-inflammatory and immunosuppressive effects of glucocorticoids, recent developments and mechanistic insights. Molecular and Cellular Endocrinology. 2011 Mar 15;335(1):2–13.

200. Zitvogel L, Apetoh L, Ghiringhelli F, Kroemer G. Immunological aspects of cancer chemotherapy. Nature Reviews Immunology. 2008 Jan 1;8(1):59–73.

201. Brack A, Rittner HL, Stein C. Immunosuppressive Effects of Opioids—Clinical Relevance. J Neuroimmune Pharmacol. 2011 Jul 5;6(4):490–502.

202. Reiche EMV, Nunes SOV, Morimoto HK. Stress, depression, the immune system, and cancer. Lancet Oncol. 2004 Oct;5(10):617–25.

203. Sassoon I, Blanc V. Antibody-drug conjugate (ADC) clinical pipeline: a review. - PubMed - NCBI. Antibody-Drug Conjugates. Totowa, NJ: Humana Press; 2013 Jul 1;1045(Chapter 1):1–27.

Available online at www.sciencedirect.com
ScienceDirect
ELSEVIER
EJSO
the Journal of Cancer Surgery
EJSO xx (2013) 1–4
www.ejso.com

Editorial

Vaccination against tumour blood vessels in colorectal cancer

[redacted]

Please cite this article in press as: Ferguson HJM, Vaccination against tumour blood vessels in colorectal cancer, Eur J Surg Oncol (2013), http://dx.doi.org/10.1016/j.ejso.2013.11.025

Angiogenesis
DOI 10.1007/s10456-014-9448-z

ORIGINAL PAPER

Robo4 vaccines induce antibodies that retard tumor growth

Xiaodong Zhuang · Forhad Ahmed · Yang Zhang · Henry J. Ferguson · Jane C. Steele · Neil M. Steven · Zsuzsanna Nagy · Victoria L. Heath · Kai-Michael Toellner · Roy Bicknell

Received: 27 January 2014 / Accepted: 13 October 2014
© Springer Science+Business Media Dordrecht 2014

Abstract Tumor endothelial specific expression of Robo4 in adults identifies this plasma membrane protein as an anticancer target for immunotherapeutic approaches, such as vaccination. In this report, we describe how vaccination against Robo4 inhibits angiogenesis and tumor growth. To break tolerance to the auto-antigen Robo4, mice were immunised with the extracellular domain of mouse Robo4, fused to the Fc domain of human immunoglobulin within an adjuvant. Vaccinated mice show a strong antibody response to Robo4, with no objectively detectable adverse effects on health. Robo4 vaccinated mice showed impaired fibrovascular invasion and angiogenesis in a rodent sponge implantation assay, as well as a reduced growth of implanted syngeneic Lewis lung carcinoma. The anti-tumor effect of Robo4 vaccination was present in CD8 deficient mice but absent in B cell or IgG1 knockout mice, suggesting antibody dependent cell mediated cytotoxicity as the anti-vascular/anti-tumor mechanism. Finally, we show that an adjuvant free soluble Robo4-carrier conjugate can retard tumor growth in carrier primed mice. These results point to appropriate Robo4 conjugates as potential anti-angiogenic vaccines for cancer patients.

Keywords Immunotherapy · Conjugate vaccines · ADCC · Cancer

Introduction

Electronic supplementary material The online version of this article (doi:10.1007/s10456-014-9448-z) contains supplementary material, which is available to authorized users.

Springer